Why Has Predicting Downstream Capabilities of Frontier AI Models with Scale Remained Elusive?

Rylan Schaeffer[*] Stanford CS
Hailey Schoelkopf EleutherAI
Brando Miranda Stanford CS
Gabriel Mukobi Berkeley EECS
Varun Madan Stanford CS
Adam Ibrahim MILA
Herbie Bradley University of Cambridge
Stella Biderman EleutherAI
Sanmi Koyejo[*] Stanford CS

Abstract

Predictable behavior from scaling advanced AI systems is an extremely desirable property. Although a well-established literature exists on how pretraining performance scales, the literature on how particular downstream capabilities scale is significantly muddier. In this work, we take a step back and ask: *why has predicting specific downstream capabilities with scale remained elusive?* While many factors are certainly responsible, we identify a new factor that makes modeling scaling behavior on widely used multiple-choice question-answering benchmarks challenging. Using five model families and twelve well-established multiple-choice benchmarks, we show that downstream performance is computed from negative log likelihoods via a sequence of transformations that progressively degrade the statistical relationship between performance and scale. We then reveal the mechanism causing this degradation: downstream metrics require comparing the correct choice against a small number of specific incorrect choices, meaning accurately predicting downstream capabilities requires predicting not just how probability mass concentrates on the correct choice with scale, but also how probability mass fluctuates on specific incorrect choices with scale. We empirically study how probability mass on the correct choice co-varies with probability mass on incorrect choices with increasing compute, suggesting that scaling laws for *incorrect* choices might be achievable. Our work also explains why pretraining scaling laws are commonly regarded as more predictable than downstream capabilities and contributes towards establishing scaling-predictable evaluations of frontier AI models.

1 Introduction

Predictable scaling behavior of frontier AI systems such as GPT-4 [61, 62], Claude [5] and Gemini [73, 64] is crucial for anticipating their capabilities and informing key decisions around their development and deployment [4, 60, 22]. While scaling laws describing relationships between parameters, data, compute, and pretraining loss are well-established [37, 65, 34, 44, 30, 35, 42, 77, 38, 16, 59, 36, 52, 69, 58, 7], the literature is less conclusive concerning predicting specific downstream capabilities with scale. For instance, prior work has observed that performance on standard natural language processing (NLP) benchmarks can exhibit *emergent abilities* [14, 26, 72, 74] where performance changes unpredictably with scale, with further work demonstrating that such unpredictable changes

[*]Correspondence to rschaef@cs.stanford.edu and sanmi@cs.stanford.edu.

Preprint. Under review.

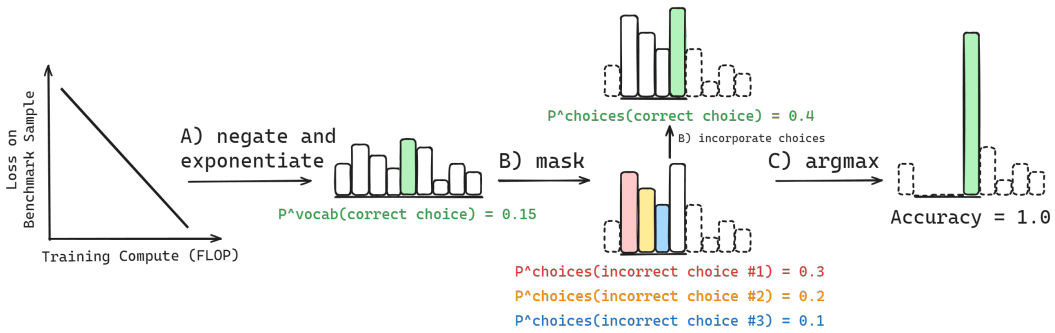

Figure 1: **Multiple-choice benchmark accuracy is computed from negative log-likelihoods via a sequence of transformations that degrades predictability.** Computing Accuracy begins with computing the negative log-likelihoods of each choice, then negating and exponentiating each to obtain the probability of each choice (**A**). Choices are then restricted to a set of available choices by *masking* invalid continuations, and renormalizing to obtain relative probability mass on each choice (**B**). Lastly, the model's choice is defined as $\arg\max_i\{p^{\text{Choices}}(\text{Available Choice}_i)\}$, and `Accuracy` is 1 if and only if the model's choice is the correct choice (**C**).

might at times be artifacts of researchers' analyses, i.e., choices of metrics and lack of resolution [72, 70, 39]. More recently, Du et al. [23] claim that downstream capabilities *can* be predicted, but *only* after the pretraining cross-entropy loss falls below a certain threshold, and Gadre et al. [25] claim that while performance on individual tasks can be difficult to predict, aggregating results across dozens of diverse benchmarks yields clearer scaling trends. In this work, we take a step back and ask: *why has predicting specific downstream capabilities with scale remained elusive?*

While many factors are certainly responsible, we identify a new factor that makes modeling the scaling behavior on widely used multiple-choice question-answering benchmarks challenging. We demonstrate that common multiple-choice metrics like Accuracy, Brier Score, and Probability Correct are computed from raw model outputs (log probabilities) via a sequence of transformations that progressively degrades the statistical relationship between those metrics and the scaling parameters (parameters, data, compute). The cause is that these metrics rely on a direct comparison between the ground truth output and a small set of specific incorrect outputs. As a result, *accurately predicting downstream performance requires modeling not only the concentration of probability mass on the correct output with increasing compute, but also modeling the fluctuations of probability mass on particular incorrect alternatives*, which (to date) is a necessary but unaddressed step. We then empirically study how probability mass on incorrect choices fluctuates with increasing compute. Our findings help explain the apparent unpredictability of individual downstream metrics and the greater robustness of pretraining loss scaling laws, which do not depend on specific incorrect choices. More broadly, we argue that a precise understanding of the factors affecting downstream performance is essential for designing evaluations that can reliably track the progression of frontier AI capabilities.

2 Methodology: Data for Studying Scaling of Downstream Capabilities

To study how downstream capabilities on specific tasks change with scale for different model families, we generated per-sample scores from a large number of model families and multiple-choice NLP benchmarks. To ensure the computed scores were consistent with prior work, we used EleutherAI's Language Model (LM) Evaluation Harness [29] rather than implementing our own evaluations.

Model Families Because our goal was to explore the scaling behavior of evaluations with increasing compute, we chose to evaluate model families with dense combinations of parameter counts and token counts. This includes the following families (additional details in App. D):

1. **Pythia** [9]: The Pythia family contains 8 models from 70M to 12B parameters trained on the Pile [27] for 300B tokens. We use 8 checkpoints per size of the non-deduplicated variants.

2. **Cerebras-GPT** [21]: The Cerebras-GPT family contains 7 models ranging from 111M to 13B parameters. The models were trained on the Pile [27] for different durations as part of a scaling study with $\sim 20\times$ tokens to parameters in a "Chinchilla"-optimal manner [38].
3. **OLMo** [31]: The OLMo family contains a 1B parameter model trained for 3T tokens and two 7B parameter models trained for 2T-2.5T tokens. We selected 7 checkpoints for 1B (spanning 84B[2] to 3T tokens) and 7 checkpoints for 7B (spanning 4B to 2.4T tokens).
4. **INCITE** [2]: The INCITE family contains 3B and 7B parameter models, trained on 0.8T and 1T tokens of RedPajama-v1[18]. The 3B model has only a single checkpoint, so we excluded it. We found this family to be a slight outlier from other families, which we speculate is because its pretraining data were contaminated by benchmarks [24].
5. **LLM360** [50]: LLM360 includes two 7B parameter LLMs trained on 1.3T and 1.4T tokens. We selected 13 checkpoints of Amber spaced approximately logarithmically.

NLP Benchmarks We evaluated the above model families on widely-used multiple-choice benchmarks for assessing comprehension, reasoning, and world knowledge: AI2 Reasoning Challenge (ARC) Easy and Hard [17], HellaSwag [76], MathQA [3], MCTACO [78], MMLU [32], OpenbookQA [55], PIQA [11], RACE [49], SciQ [75], SIQA [67], WinoGrande [45] and XWinoGrad En [57]. For MMLU, we analyzed each of the 57 subjects (e.g., Abstract Algebra) independently. For each benchmark, we used default evaluation settings from the LM Evaluation Harness [29].

Performance Metrics We used three common multiple-choice metrics [72, 70, 23]: `Accuracy`, `Brier Score` [13], and probability mass on the correct choice relative to the available choices.

Compute Budget Calculations Following prior work [44], we approximated[3] the pretraining compute C (in terms of training FLOP) of a given model checkpoint as a function of the parameter count (excluding the embedding layer) N and the amount of training data seen in tokens D:

$$C = C(N, D) \;\approx\; 6\,N\,D$$

3 What Makes Predicting Downstream Performance Difficult?

Performance on multiple choice benchmarks is commonly presented as `Accuracy`, `Brier Score` [70], or probability mass on the correct choice out of the available choices [23]. These quantities are computed via a sequence of transformations that begins with the negative log-likelihood of the correct choice on this particular benchmark sample as some function $f(\cdot, \cdot)$ of compute:

$$\mathcal{L}_\theta^{\text{Vocab}}(\text{Correct Choice}) = f(\text{Compute}, \text{Benchmark Datum}) \tag{1}$$

Two details are critical. Firstly, this negative log-likelihood is not computed in expectation over a corpus; it is specific to this particular singular datum in the benchmark. *All the scores we discuss are per-datum.* Secondly, this negative log-likelihood is computed over the vocabulary of the model. One can then compute the probability mass of the correct choice, again with respect to the vocabulary:

$$p_\theta^{\text{Vocab}}(\text{Correct Choice}) = \exp\big(-\mathcal{L}_\theta^{\text{Vocab}}(\text{Correct Choice})\big) \tag{2}$$

Next, probabilities are restricted to the set of available choices $\{\text{Available Choice}_i\}_i^{|\text{Available Choices}|}$ by masking invalid continuations and normalizing again with respect to this set:

$$p_\theta^{\text{Choices}}(\text{Correct Choice}) \stackrel{\text{def}}{=} \frac{p_\theta^{\text{Vocab}}(\text{Correct Choice})}{\sum_i p_\theta^{\text{Vocab}}(\text{Available Choice}_i)} \tag{3}$$

[2]OLMo 1B checkpoints below 84B tokens were unfortunately accidentally lost by their creators.

[3]This approximation neglects FLOP costs associated with attention calculations over sequence length; however, such operations are negligible so long as $d_{model} >> n_{ctx}/12$, and this approximation is therefore standard in most language model scaling law analyses.

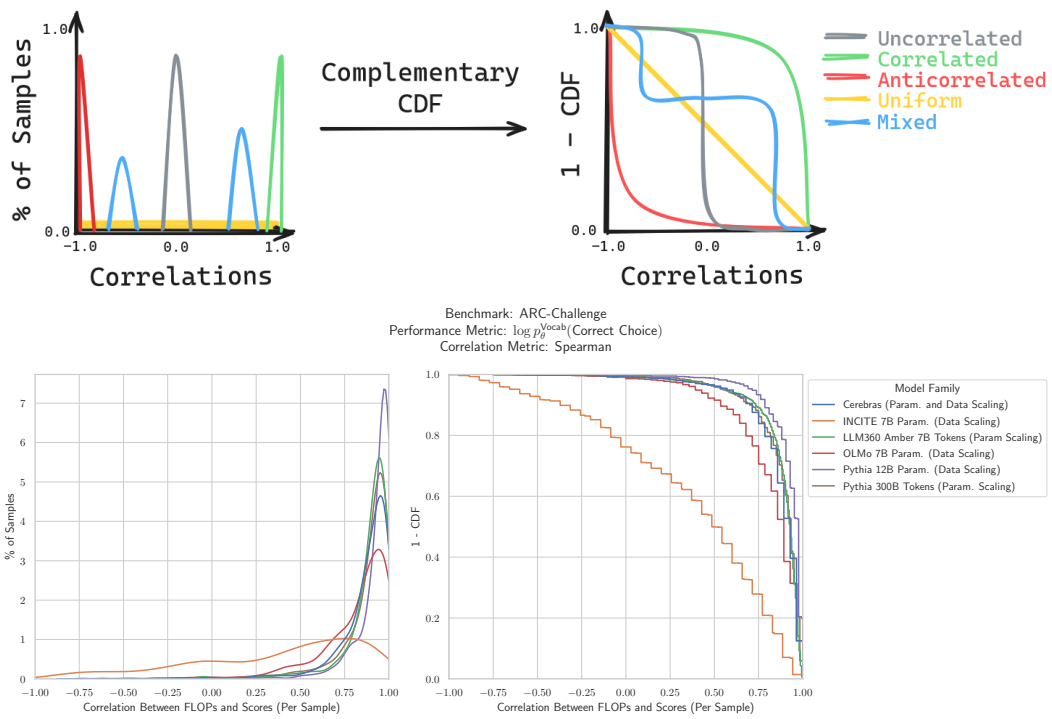

Figure 2: **Distributions of score-compute correlations and their corresponding complementary cumulative distribution functions. Left:** For each benchmark, model family, performance metric, and correlation metric, one can compute how scores correlate with compute. This yields a distribution (over samples) of score-compute correlations. Note: the uniform (yellow) distribution is small but non-zero everywhere. **Right:** To easily extract what fraction of samples in a benchmark have score-compute correlations above any given threshold, we convert the probability distributions to *complementary cumulative distribution functions*, i.e., 1 minus the (empirical) cumulative distribution function (CDF). **Top:** Schematic idealized distributions. **Bottom:** Real data on ARC Challenge [17].

We emphasize the support over the token space of the model versus over the set of available choices in the benchmark's question because, as we will show, this crucially affects predictability. Finally, one uses the choices-normalized probability masses to compute standard downstream metrics:

$$\texttt{Accuracy}_\theta \stackrel{\text{def}}{=} \mathbb{1}\left(\text{Correct Choice} == \arg\max_i \left\{p_\theta^{\text{Choices}}(\text{Available Choice}_i)\right\}\right) \tag{4}$$

$$\texttt{Brier Score}_\theta \stackrel{\text{def}}{=} \sum_i \left(\mathbb{1}(\text{Available Choice}_i == \text{Correct Choice}) - p_\theta^{\text{Choices}}(\text{Available Choice}_i)\right)^2 \tag{5}$$

where $\mathbb{1}(\cdot)$ is an indicator variable. We demonstrate that this sequence of transformations degrades how predictable performance is with scale before identifying the underlying mechanism.

To quantify how this sequence of transformations affects predictability of performance, we measured how per-sample scores correlate with pretraining compute, and then studied how the distribution (over samples) of correlation values shifted as one transitions from loglikelihoods to p_θ^{Vocab}(Correct Choice) to $p_\theta^{\text{Choices}}$(Correct Choice) to `Accuracy` or `Brier Score`. Specifically, for each combination of (*model family, benchmark, performance metric, correlation metric*), we computed a correlation value for each sample in the benchmark between pretraining compute and scores. This yielded a distribution (over samples) of correlation values for the combination (Fig. 2 left). Visualizing the distribution of correlations for the combination told us what fraction of samples in the benchmark yielded scores that are correlated, uncorrelated or anticorrelated with compute (Fig. 2 right). We used three standard correlation metrics - Pearson, Kendall [46] and Spearman [71]) - and found consistent results.

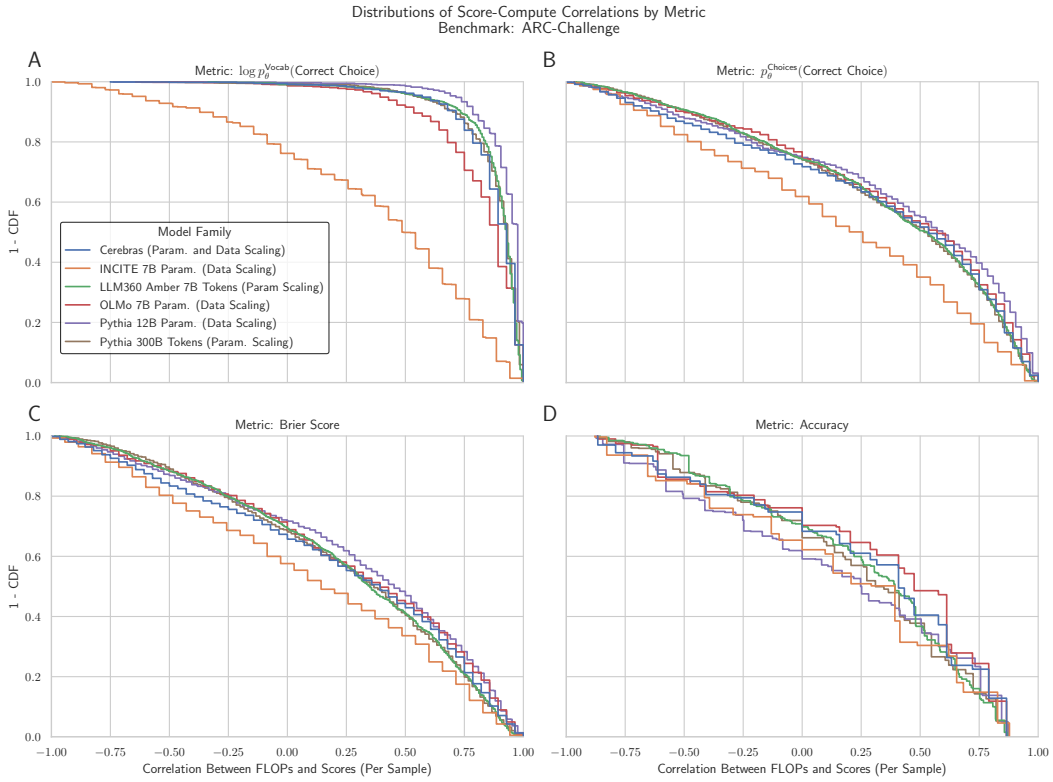

Figure 3: **Multiple-choice metrics like `Accuracy` and `Brier Score` are computed via a sequence of transformations that degrades correlations between performance scores and pretraining compute.** **(A)** Initially, scores under $\log p_\theta^{\text{Vocab}}$(Correct Choice) and compute are highly correlated. Transforming $\log p_\theta^{\text{Vocab}}$(Correct Choice) into p_θ^{Vocab}(Correct Choice) has no effect for rank correlations. **(B)** Transforming p_θ^{Vocab}(Correct Choice) into $p_\theta^{\text{Choices}}$(Correct Choice) decorrelates scores from compute. **(C)** Transforming $p_\theta^{\text{Choices}}$(Correct Choice) into `Brier Score` minorly decreases score-compute correlations. **(D)** Transforming $p_\theta^{\text{Choices}}$(Correct Choice) into `Accuracy` more substantially decorrelates scores from compute. Benchmark: ARC Challenge [17]. Correlation: Spearman. Results are consistent across benchmarks and all three correlation metrics; for more, see App. G.

We present ARC Challenge [17] as an illustrative benchmark to demonstrate how the sequence of transformations affects the distribution of score-compute correlations, but note that all other benchmarks exhibited similar patterns (App. G). We visualized the distributions via their complementary (empirical) cumulative distribution functions (complementary CDFs) (App. B):

$$\hat{S}(c) \overset{\text{def}}{=} \frac{1}{N} \sum_{n=1}^{N} \mathbb{1}\{C_n > c\}, \tag{6}$$

where N is the number of data in the benchmark and C_n is the correlation (over the models in the model family) between compute and scores on the n-th datum in the benchmark. For a given threshold c, the complementary CDF $\hat{S}(c)$ returns the fraction of the benchmark's samples with score-compute correlations greater than the threshold c (Fig. 3A). Beginning with log likelihoods, approximately 90% of samples exhibit score-compute correlations > 0.75, regardless of the model family (Fig. 3A). Transforming negative log-likelihoods into probability masses p_θ^{Vocab}(Correct Choice) does not affect the distribution of score-compute correlations for Spearman and Kendall. However, transforming p_θ^{Vocab}(Correct Choice) into $p_\theta^{\text{Choices}}$(Correct Choice) decreases the distribution of score-compute correlations (Fig. 3B), with only 40% of samples having score-compute correlations > 0.75. Transforming $p_\theta^{\text{Choices}}$(Correct Choice) into `Brier Score` has little-to-no effect (Fig. 3C) but transforming into `Accuracy` (Fig. 3D) furthers decreases score-compute correlations. To quantitatively test whether these transformations indeed decrease the correlation between scores and

Figure 4: **All four statistics of score-compute correlation distributions demonstrate that transforming $\log p_\theta^{\text{Vocab}}(\text{Correct Choice})$ into `Accuracy` causes score-compute correlations to deteriorate.** We find a consistent trend across benchmarks and model families for three correlation metrics (Spearman, Pearson and Kendall) and for four statistics of correlation distributions (mean, median, the area under the survival function, and negative Wasserstein distance from perfect correlation or perfect anti-correlation) that the sequence of transformations degrades score-compute correlations, as shown by the right-to-left $\log p_\theta^{\text{Vocab}}(\text{Correct Choice})$-to-$p_\theta^{\text{Vocab}}(\text{Correct Choice})$-to-$p_\theta^{\text{Choices}}(\text{Correct Choice})$-or-`Brier Score`-to-`Accuracy` vertical stripes. See App. Figs. 7, 8, 9 for other correlation metrics and other score-compute correlation distribution statistics.

compute, we measured four statistics of these score-compute correlation distributions: the mean, the median, the area under the complementary CDF and the negative[4] of the minimum of two Wasserstein distances: between the empirical correlation distribution and an ideal distribution of all correlations $= 1$, and between the empirical distribution and an ideal distribution of all correlations $= -1$. Across the four summary statistics, for most benchmarks and for most model families, we discovered a consistent ordering of metrics of the score-compute correlation distributions (Fig. 4):

$$\begin{aligned}
&\text{Corr}\big(\text{Compute}, \log p_\theta^{\text{Vocab}}(\text{Correct Choice})\big) \\
&\quad \geq \text{Corr}\big(\text{Compute}, p_\theta^{\text{Vocab}}(\text{Correct Choice})\big) \\
&\quad > \text{Corr}\big(\text{Compute}, p_\theta^{\text{Choices}}(\text{Correct Choice})\big) \\
&\quad \geq \text{Corr}\big(\text{Compute}, \texttt{Brier Score}\big) \\
&\quad > \text{Corr}\big(\text{Compute}, \texttt{Accuracy}\big)
\end{aligned}$$

4 Probability Masses on Incorrect Choices Cause Unpredictability

What is the mechanism that degrades how correlated scores are with compute? All three metrics with degraded correlations - $p_\theta^{\text{Choices}}(\text{Correct Choice})$, `Accuracy`, and `Brier Score` - depend not just on how the model's probability mass $p_\theta^{\text{Vocab}}(\text{Correct Choice})$ concentrates on the correct choice

[4]We chose the *negative* Wasserstein distance for consistency with the other statistics: higher values correspond to higher correlations between scores and compute.

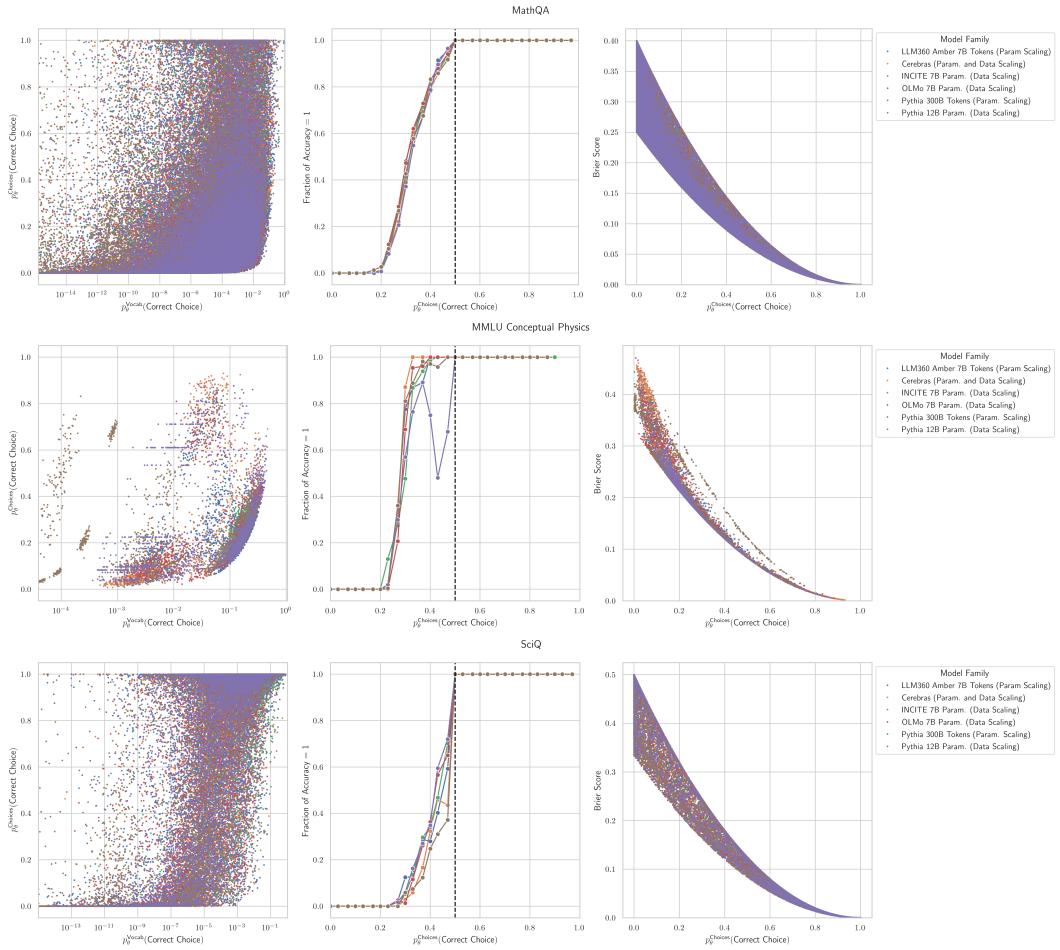

Figure 5: **Predictability deteriorates because of probability mass fluctuating on specific incorrect choices with scale. Left:** Transitioning from $p_\theta^{\text{Vocab}}(\text{Correct Choice})$ to $p_\theta^{\text{Choices}}(\text{Correct Choice})$ demonstrates that $p_\theta^{\text{Vocab}}(\text{Correct Choice})$ contains little information about $p_\theta^{\text{Choices}}(\text{Correct Choice})$ and vice versa; loosely speaking, any value of one can map to any value of the other. **Center:** While $p_\theta^{\text{Choices}}(\text{Correct Choice}) > 0.5$ must yield $\texttt{Accuracy} = 1$, for any $p_\theta^{\text{Choices}}(\text{Correct Choice}) < 0.5$, knowing $p_\theta^{\text{Choices}}(\text{Correct Choice})$ contains little information about $\texttt{Accuracy}$ and vice versa. **Right**: $\texttt{Brier Score}$ is more predictable from $p_\theta^{\text{Choices}}(\text{Correct Choice})$ than $\texttt{Accuracy}$, but still quite variable. Three benchmarks shown: MathQA [3], MMLU Conceptual Physics [32], SciQ [75].

as compute increases, but also depend on how the model's probability mass fluctuates on *incorrect* available choices $\{p_\theta^{\text{Vocab}}(\text{Incorrect Choice})\}_{\text{Incorrect Choices}}$ as compute increases. As an example, suppose $p_\theta^{Vocab}(\text{Correct Choice}) = 0.4$ on a 4-way multiple-choice question; what is the accuracy? Spreading the remaining mass uniformly on the incorrect choices will make $\texttt{Accuracy} = 1$, whereas concentrating mass on a single incorrect choice will make $\texttt{Accuracy} = 0$.

To demonstrate how drastically the probability mass placed on incorrect choices can alter performance, we visualized the relations between pairs of metrics immediately preceding and following a given transformation (Fig. 5). For negative log-likelihood of the correct choice and $p_\theta^{Vocab}(\text{Correct Choice})$ (not pictured), we observed a clean correspondence between performance under the metric and compute: one can reliably map a given value of these metrics to compute, and vice versa. In contrast, once performance is evaluated using a metric that is a function of the incorrect choices - $p_\theta^{\text{Choices}}(\text{Correct Choice})$, $\texttt{Accuracy}$ or $\texttt{Brier Score}$ - nearly any value of a score under one metric can map to any value of $p_\theta^{\text{Vocab}}(\text{Correct Choice})$ or $p_\theta^{\text{Choices}}(\text{Correct Choice})$ respectively (Fig. 5), breaking the chain along which one can cleanly infer compute from an observed metric. We can see that $\texttt{Brier Score}$, a metric meant to produce more continuous scores [70],

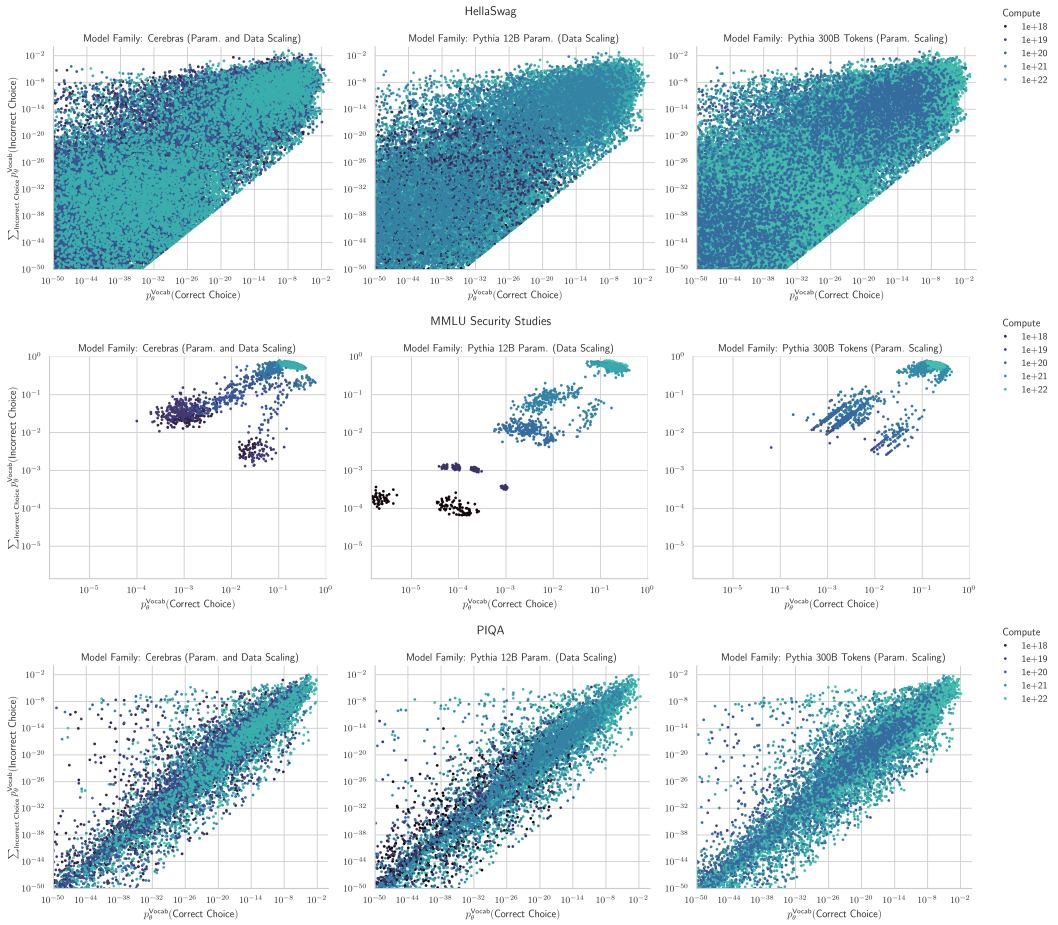

Figure 6: **Probability mass on the correct choices and the incorrect choices are correlated, but can fluctuate substantially.** Probability mass on correct choices and incorrect choices positively covaries and typically increases with compute. However, the spread is large: for any given value of $p_\theta^{\text{Vocab}}(\text{Correct Choice})$, the mass on incorrect choices can vary by many orders of magnitude.

is less variable than `Accuracy` provided a known $p_\theta^{\text{Choices}}(\text{Correct Choice})$, but it cannot recover information about $p_\theta^{\text{Vocab}}(\text{Correct Choice})$ that is lost when shifting to $p_\theta^{\text{Choices}}(\text{Correct Choice})$. We next show that this is because of the additional information regarding the underdetermined values of $p_\theta^{\text{Choices}}(\text{Incorrect Choice})$ for each incorrect choice.

5 Scaling Behavior of Probability Mass on Incorrect Choices

In order to accurately predict performance on multiple-choice question-answering benchmarks, one must predict not just how probability mass concentrates on correct choices with scale, but *also* how probability mass fluctuates on incorrect choices with scale. For metrics like `Accuracy`, these predictions *must* be made for each sample because knowing the average mass (across many data) placed on incorrect choices says little about how much mass is placed on any single incorrect choice for a single sample. We conclude by providing preliminary evidence that achieving such a feat might be possible. Specifically, we test how probability masses on correct choices and probability masses on incorrect choices covary with increasing compute (Fig. 6). Multiple benchmarks display strong positive relationships between mass on correct choices and mass on incorrect choices, suggesting that fitting *per-sample scaling trends for each incorrect choice* might be possible; doing so would enable predicting changepoints in metrics like `Accuracy` or `Brier Score`. However, whether per-benchmark per-sample per-choice scaling trends can be fit and accurately extrapolated is unclear since the spread varies by several orders of magnitude. We leave this challenge to future work.

Takeaway #1: Think through your metrics!
If one cares about scaling-predictable evaluations, then one needs to think through how their evaluations transform raw model outputs into useful signals to know what to expect.

Takeaway #2: Continuous metrics are insufficient to guarantee predictable changes.
As shown by $p_\theta^{\text{Choices}}(\text{Correct Choice})$ & `Brier Score`, even "continuous" metrics can be unpredictable, e.g., if the metric weighs correct behavior against specific incorrect behaviors.

Takeaway #3: Recommended scaling-predictable metrics for pretraining practitioners.
Pretraining practitioners seeking scaling-predictable signals for capabilities should perhaps focus on $p_\theta^{Vocab}(\text{Correct Choice})$ on relevant benchmarks. Scores under this metric provide smoother scaling trends and are arguably more interpretable than the pretraining loss.

Takeaway #4: Evaluations should be reshaped based on intended desiderata.
Too often, we take evaluations as frozen static objects, but evaluations should be adapted to pertinent goals. For instance, if the goal is to predict capabilities with scale, evaluations should be designed or adapted to be scaling-predictable.

6 Discussion, Related Work and Future Directions

This work identifies a factor that induces unpredictability in multiple-choice assessments of frontier AI models, as well as the underlying mechanism: probability mass on incorrect choices. Our results have implications for the design of future evaluations for frontier AI models that are reliably predictable with scaling. We hope that our work will be extended to further the science of scaling-predictable evaluation of AI systems, especially for complex and important model capabilities. We note several future directions for extension of our work and we hope that the community also adopts our framing to further improve scaling-predictable evaluations.

Related Work For a comprehensive exposition of related work, please see App. A.

Direction 1: Beyond Multiple Choice Benchmarks Our study is restricted to benchmarks evaluated via loglikelihood-based multiple-choice formats. While we believe this is inherently valuable due to the usefulness and prevalence of such tasks, this limits the application of our findings. We hope that our discoveries and proposed mechanisms may be used to inform the study of predictable and reliable evaluation writ large, and that future work should explore the extent to which our findings can be generalized to more complex capabilities. Our findings corroborate those of Lyu et al. [51], who find that multiple-choice answer scores often diverge from generative evaluations. Consequently, a particularly important direction for further study is to investigate generative evaluations, which may contain similar transformations distancing performance from the observed loss.

Direction 2: Predicting Benchmark Performance A Priori Our work provides an explanation why multiple-choice benchmark performance is not easily predictable for metrics such as `Accuracy` and `Brier Score`, as observed in the literature [23]. However, our analyses assume access to entire model families' scores across several orders of magnitude of pretraining FLOPs, and do not employ backtesting, as sensibly recommended by Owen [63]. A predictive model should be able to identify change points well in advance on standard metrics like `Accuracy` or `Brier Score`.

Acknowledgements

We thank a number of colleagues for their feedback in improving this work: Tamay Besiroglu, Clémentine Fourrier, Geoffrey Irving, David Owen, Lintang Sutawika and Joshua Kazdan. R.S. acknowledges support from Stanford Data Science and from OpenAI's Superalignment Fast Grant Research Fellowship. S.K. is partially supported by NSF III 2046795, IIS 1909577, CCF 1934986, NIH 1R01MH116226-01A, NIFA award 2020-67021-32799, the Alfred P. Sloan Foundation, and Google Inc.

References

[1] J. Achiam, S. Adler, S. Agarwal, L. Ahmad, I. Akkaya, F. L. Aleman, D. Almeida, J. Altenschmidt, S. Altman, S. Anadkat, et al. Gpt-4 technical report. *arXiv preprint arXiv:2303.08774*, 2023.

[2] T. AI. Releasing 3b and 7b redpajama-incite family of models including base, instruction-tuned & chat models. `https://www.together.ai/blog/redpajama-models-v1`, 2023. Accessed: 2024-05-19.

[3] A. Amini, S. Gabriel, S. Lin, R. Koncel-Kedziorski, Y. Choi, and H. Hajishirzi. MathQA: Towards interpretable math word problem solving with operation-based formalisms. In J. Burstein, C. Doran, and T. Solorio, editors, *Proceedings of the 2019 Conference of the North American Chapter of the Association for Computational Linguistics: Human Language Technologies, Volume 1 (Long and Short Papers)*, pages 2357–2367, Minneapolis, Minnesota, June 2019. Association for Computational Linguistics. doi: 10.18653/v1/N19-1245. URL `https://aclanthology.org/N19-1245`.

[4] Anthropic. Anthropic's responsible scaling policy. `https://www.anthropic.com/news/anthropics-responsible-scaling-policy`, 2023. Accessed: 2024-05-19.

[5] Anthropic. Introducing the next generation of claude. `https://www.anthropic.com/news/claude-3-family`, 2024. Accessed: 2024-05-19.

[6] E. Beeching, C. Fourrier, N. Habib, S. Han, N. Lambert, N. Rajani, O. Sanseviero, L. Tunstall, and T. Wolf. Open llm leaderboard. `https://huggingface.co/spaces/HuggingFaceH4/open_llm_leaderboard`, 2023.

[7] T. Besiroglu, E. Erdil, M. Barnett, and J. You. Chinchilla scaling: A replication attempt, 2024.

[8] S. Biderman, U. S. Prashanth, L. Sutawika, H. Schoelkopf, Q. Anthony, S. Purohit, and E. Raff. Emergent and predictable memorization in large language models, 2023.

[9] S. Biderman, H. Schoelkopf, Q. Anthony, H. Bradley, K. O'Brien, E. Hallahan, M. A. Khan, S. Purohit, U. S. Prashanth, E. Raff, A. Skowron, L. Sutawika, and O. van der Wal. Pythia: A suite for analyzing large language models across training and scaling, 2023.

[10] S. Biderman, H. Schoelkopf, L. Sutawika, L. Gao, J. Tow, B. Abbasi, A. F. Aji, P. S. Ammanamanchi, S. Black, J. Clive, A. DiPofi, J. Etxaniz, B. Fattori, J. Z. Forde, C. Foster, M. Jaiswal, W. Y. Lee, H. Li, C. Lovering, N. Muennighoff, E. Pavlick, J. Phang, A. Skowron, S. Tan, X. Tang, K. A. Wang, G. I. Winata, F. Yvon, and A. Zou. Lessons from the trenches on reproducible evaluation of language models. *arXiv preprint*, 2024.

[11] Y. Bisk, R. Zellers, R. L. Bras, J. Gao, and Y. Choi. Piqa: Reasoning about physical commonsense in natural language. 2020.

[12] S. R. Bowman. Eight things to know about large language models, 2023.

[13] G. W. Brier. Verification of forecasts expressed in terms of probability. *Monthly weather review*, 78(1):1–3, 1950.

[14] T. Brown, B. Mann, N. Ryder, M. Subbiah, J. D. Kaplan, P. Dhariwal, A. Neelakantan, P. Shyam, G. Sastry, A. Askell, et al. Language models are few-shot learners. *Advances in neural information processing systems*, 33:1877–1901, 2020.

[15] E. Caballero, K. Gupta, I. Rish, and D. Krueger. Broken neural scaling laws, 2023.

[16] A. Clark, D. De Las Casas, A. Guy, A. Mensch, M. Paganini, J. Hoffmann, B. Damoc, B. Hechtman, T. Cai, S. Borgeaud, et al. Unified scaling laws for routed language models. In *International Conference on Machine Learning*, pages 4057–4086. PMLR, 2022.

[17] P. Clark, I. Cowhey, O. Etzioni, T. Khot, A. Sabharwal, C. Schoenick, and O. Tafjord. Think you have solved question answering? try arc, the ai2 reasoning challenge. *arXiv preprint arXiv:1803.05457*, 2018.

[18] T. Computer. Redpajama: An open source recipe to reproduce llama training dataset, 2023. URL `https://github.com/togethercomputer/RedPajama-Data`.

[19] W. contributors. Survival function, 2023. URL `https://en.wikipedia.org/wiki/Survival_function`. [Online; accessed 22-May-2024].

[20] DeepSeek-AI, :, X. Bi, D. Chen, G. Chen, S. Chen, D. Dai, C. Deng, H. Ding, K. Dong, Q. Du, Z. Fu, H. Gao, K. Gao, W. Gao, R. Ge, K. Guan, D. Guo, J. Guo, G. Hao, Z. Hao, Y. He, W. Hu, P. Huang, E. Li, G. Li, J. Li, Y. Li, Y. K. Li, W. Liang, F. Lin, A. X. Liu, B. Liu, W. Liu, X. Liu, X. Liu, Y. Liu, H. Lu, S. Lu, F. Luo, S. Ma, X. Nie, T. Pei, Y. Piao, J. Qiu, H. Qu, T. Ren, Z. Ren, C. Ruan, Z. Sha, Z. Shao, J. Song, X. Su, J. Sun, Y. Sun, M. Tang, B. Wang, P. Wang, S. Wang, Y. Wang, Y. Wang, T. Wu, Y. Wu, X. Xie, Z. Xie, Z. Xie, Y. Xiong, H. Xu, R. X. Xu, Y. Xu, D. Yang, Y. You, S. Yu, X. Yu, B. Zhang, H. Zhang, L. Zhang, L. Zhang, M. Zhang, M. Zhang, W. Zhang, Y. Zhang, C. Zhao, Y. Zhao, S. Zhou, S. Zhou, Q. Zhu, and Y. Zou. Deepseek llm: Scaling open-source language models with longtermism, 2024.

[21] N. Dey, G. Gosal, Zhiming, Chen, H. Khachane, W. Marshall, R. Pathria, M. Tom, and J. Hestness. Cerebras-gpt: Open compute-optimal language models trained on the cerebras wafer-scale cluster, 2023.

[22] A. Dragan, H. King, and A. Dafoe. Introducing the frontier safety framework. `https://deepmind.google/discover/blog/introducing-the-frontier-safety-framework/`, 2024. Accessed: 2024-05-19.

[23] Z. Du, A. Zeng, Y. Dong, and J. Tang. Understanding emergent abilities of language models from the loss perspective, 2024.

[24] Y. Elazar, A. Bhagia, I. H. Magnusson, A. Ravichander, D. Schwenk, A. Suhr, E. P. Walsh, D. Groeneveld, L. Soldaini, S. Singh, et al. What's in my big data? In *The Twelfth International Conference on Learning Representations*, 2023.

[25] S. Y. Gadre, G. Smyrnis, V. Shankar, S. Gururangan, M. Wortsman, R. Shao, J. Mercat, A. Fang, J. Li, S. Keh, R. Xin, M. Nezhurina, I. Vasiljevic, J. Jitsev, A. G. Dimakis, G. Ilharco, S. Song, T. Kollar, Y. Carmon, A. Dave, R. Heckel, N. Muennighoff, and L. Schmidt. Language models scale reliably with over-training and on downstream tasks, 2024.

[26] D. Ganguli, D. Hernandez, L. Lovitt, A. Askell, Y. Bai, A. Chen, T. Conerly, N. Dassarma, D. Drain, N. Elhage, et al. Predictability and surprise in large generative models. In *2022 ACM Conference on Fairness, Accountability, and Transparency*, pages 1747–1764, 2022.

[27] L. Gao, S. Biderman, S. Black, L. Golding, T. Hoppe, C. Foster, J. Phang, H. He, A. Thite, N. Nabeshima, S. Presser, and C. Leahy. The pile: An 800gb dataset of diverse text for language modeling, 2020.

[28] L. Gao, J. Schulman, and J. Hilton. Scaling laws for reward model overoptimization, 2022.

[29] L. Gao, J. Tow, B. Abbasi, S. Biderman, S. Black, A. DiPofi, C. Foster, L. Golding, J. Hsu, A. Le Noac'h, H. Li, K. McDonell, N. Muennighoff, C. Ociepa, J. Phang, L. Reynolds, H. Schoelkopf, A. Skowron, L. Sutawika, E. Tang, A. Thite, B. Wang, K. Wang, and A. Zou. A framework for few-shot language model evaluation, 12 2023. URL `https://zenodo.org/records/10256836`.

[30] M. A. Gordon, K. Duh, and J. Kaplan. Data and parameter scaling laws for neural machine translation. In *Proceedings of the 2021 Conference on Empirical Methods in Natural Language Processing*, pages 5915–5922, 2021.

[31] D. Groeneveld, I. Beltagy, P. Walsh, A. Bhagia, R. Kinney, O. Tafjord, A. H. Jha, H. Ivison, I. Magnusson, Y. Wang, S. Arora, D. Atkinson, R. Authur, K. R. Chandu, A. Cohan, J. Dumas, Y. Elazar, Y. Gu, J. Hessel, T. Khot, W. Merrill, J. Morrison, N. Muennighoff, A. Naik, C. Nam, M. E. Peters, V. Pyatkin, A. Ravichander, D. Schwenk, S. Shah, W. Smith, E. Strubell, N. Subramani, M. Wortsman, P. Dasigi, N. Lambert, K. Richardson, L. Zettlemoyer, J. Dodge, K. Lo, L. Soldaini, N. A. Smith, and H. Hajishirzi. Olmo: Accelerating the science of language models, 2024.

[32] D. Hendrycks, C. Burns, S. Basart, A. Zou, M. Mazeika, D. Song, and J. Steinhardt. Measuring massive multitask language understanding. *arXiv preprint arXiv:2009.03300*, 2020.

[33] D. Hendrycks, C. Burns, S. Kadavath, A. Arora, S. Basart, E. Tang, D. Song, and J. Steinhardt. Measuring mathematical problem solving with the math dataset. 2021.

[34] T. Henighan, J. Kaplan, M. Katz, M. Chen, C. Hesse, J. Jackson, H. Jun, T. B. Brown, P. Dhariwal, S. Gray, et al. Scaling laws for autoregressive generative modeling. *arXiv preprint arXiv:2010.14701*, 2020.

[35] D. Hernandez, J. Kaplan, T. Henighan, and S. McCandlish. Scaling laws for transfer. *arXiv preprint arXiv:2102.01293*, 2021.

[36] D. Hernandez, T. Brown, T. Conerly, N. DasSarma, D. Drain, S. El-Showk, N. Elhage, Z. Hatfield-Dodds, T. Henighan, T. Hume, et al. Scaling laws and interpretability of learning from repeated data. *arXiv preprint arXiv:2205.10487*, 2022.

[37] J. Hestness, S. Narang, N. Ardalani, G. Diamos, H. Jun, H. Kianinejad, M. Patwary, M. Ali, Y. Yang, and Y. Zhou. Deep learning scaling is predictable, empirically. *arXiv preprint arXiv:1712.00409*, 2017.

[38] J. Hoffmann, S. Borgeaud, A. Mensch, E. Buchatskaya, T. Cai, E. Rutherford, D. d. L. Casas, L. A. Hendricks, J. Welbl, A. Clark, et al. Training compute-optimal large language models. *arXiv preprint arXiv:2203.15556*, 2022.

[39] S. Hu, X. Liu, X. Han, X. Zhang, C. He, W. Zhao, Y. Lin, N. Ding, Z. Ou, G. Zeng, Z. Liu, and M. Sun. Predicting emergent abilities with infinite resolution evaluation, 2024.

[40] Y. Huang, J. Zhang, Z. Shan, and J. He. Compression represents intelligence linearly, 2024.

[41] B. Isik, N. Ponomareva, H. Hazimeh, D. Paparas, S. Vassilvitskii, and S. Koyejo. Scaling laws for downstream task performance of large language models, 2024.

[42] A. L. Jones. Scaling scaling laws with board games. *arXiv preprint arXiv:2104.03113*, 2021.

[43] M. Joshi, E. Choi, D. Weld, and L. Zettlemoyer. triviaqa: A Large Scale Distantly Supervised Challenge Dataset for Reading Comprehension. *arXiv e-prints*, art. arXiv:1705.03551, 2017.

[44] J. Kaplan, S. McCandlish, T. Henighan, T. B. Brown, B. Chess, R. Child, S. Gray, A. Radford, J. Wu, and D. Amodei. Scaling laws for neural language models. *arXiv preprint arXiv:2001.08361*, 2020.

[45] S. Keisuke, L. Ronan, B. Chandra, and C. Yejin. Winogrande: An adversarial winograd schema challenge at scale. 2019.

[46] M. G. Kendall. A new measure of rank correlation. *Biometrika*, 30(1/2):81–93, 1938.

[47] D. G. Kleinbaum and M. Klein. *Survival Analysis: A Self-Learning Text*. Springer, 3 edition, 2012. ISBN 978-1441966452. doi: 10.1007/978-1-4419-6646-9.

[48] T. Kwiatkowski, J. Palomaki, O. Redfield, M. Collins, A. Parikh, C. Alberti, D. Epstein, I. Polosukhin, M. Kelcey, J. Devlin, K. Lee, K. N. Toutanova, L. Jones, M.-W. Chang, A. Dai, J. Uszkoreit, Q. Le, and S. Petrov. Natural questions: a benchmark for question answering research. *Transactions of the Association of Computational Linguistics*, 2019.

[49] G. Lai, Q. Xie, H. Liu, Y. Yang, and E. Hovy. RACE: Large-scale ReAding comprehension dataset from examinations. In *Proceedings of the 2017 Conference on Empirical Methods in Natural Language Processing*, pages 785–794, Copenhagen, Denmark, Sept. 2017. Association for Computational Linguistics. doi: 10.18653/v1/D17-1082. URL `https://aclanthology.org/D17-1082`.

[50] Z. Liu, A. Qiao, W. Neiswanger, H. Wang, B. Tan, T. Tao, J. Li, Y. Wang, S. Sun, O. Pangarkar, R. Fan, Y. Gu, V. Miller, Y. Zhuang, G. He, H. Li, F. Koto, L. Tang, N. Ranjan, Z. Shen, X. Ren, R. Iriondo, C. Mu, Z. Hu, M. Schulze, P. Nakov, T. Baldwin, and E. P. Xing. Llm360: Towards fully transparent open-source llms, 2023.

[51] C. Lyu, M. Wu, and A. F. Aji. Beyond probabilities: Unveiling the misalignment in evaluating large language models. *arXiv preprint arXiv:2402.13887*, 2024.

[52] A. Maloney, D. A. Roberts, and J. Sully. A solvable model of neural scaling laws. *arXiv preprint arXiv:2210.16859*, 2022.

[53] S. McCandlish, J. Kaplan, D. Amodei, and O. D. Team. An empirical model of large-batch training, 2018.

[54] I. McKenzie, A. Lyzhov, A. Parrish, A. Prabhu, A. Mueller, N. Kim, S. Bowman, and E. Perez. The inverse scaling prize, 2022. URL `https://github.com/inverse-scaling/prize`.

[55] T. Mihaylov, P. Clark, T. Khot, and A. Sabharwal. Can a suit of armor conduct electricity? a new dataset for open book question answering. In *EMNLP*, 2018.

[56] S. Muckatira, V. Deshpande, V. Lialin, and A. Rumshisky. Emergent abilities in reduced-scale generative language models, 2024.

[57] N. Muennighoff, T. Wang, L. Sutawika, A. Roberts, S. Biderman, T. L. Scao, M. S. Bari, S. Shen, Z.-X. Yong, H. Schoelkopf, X. Tang, D. Radev, A. F. Aji, K. Almubarak, S. Albanie, Z. Alyafeai, A. Webson, E. Raff, and C. Raffel. Crosslingual generalization through multitask finetuning, 2023.

[58] N. Muennighoff, A. Rush, B. Barak, T. Le Scao, N. Tazi, A. Piktus, S. Pyysalo, T. Wolf, and C. A. Raffel. Scaling data-constrained language models. *Advances in Neural Information Processing Systems*, 36, 2024.

[59] O. Neumann and C. Gros. Scaling laws for a multi-agent reinforcement learning model. *arXiv preprint arXiv:2210.00849*, 2022.

[60] OpenAI. Openai's approach to frontier risk. `https://openai.com/global-affairs/our-approach-to-frontier-risk/`, 2023. Accessed: 2024-05-19.

[61] OpenAI. Hello gpt-4o. `https://openai.com/index/hello-gpt-4o/`, 2024. Accessed: 2024-05-16.

[62] OpenAI, J. Achiam, S. Adler, S. Agarwal, L. Ahmad, I. Akkaya, F. L. Aleman, D. Almeida, J. Altenschmidt, S. Altman, S. Anadkat, R. Avila, I. Babuschkin, S. Balaji, V. Balcom, P. Baltescu, H. Bao, M. Bavarian, J. Belgum, I. Bello, J. Berdine, G. Bernadett-Shapiro, C. Berner, L. Bogdonoff, O. Boiko, M. Boyd, A.-L. Brakman, G. Brockman, T. Brooks, M. Brundage, K. Button, T. Cai, R. Campbell, A. Cann, B. Carey, C. Carlson, R. Carmichael, B. Chan, C. Chang, F. Chantzis, D. Chen, S. Chen, R. Chen, J. Chen, M. Chen, B. Chess, C. Cho, C. Chu, H. W. Chung, D. Cummings, J. Currier, Y. Dai, C. Decareaux, T. Degry, N. Deutsch, D. Deville, A. Dhar, D. Dohan, S. Dowling, S. Dunning, A. Ecoffet, A. Eleti, T. Eloundou, D. Farhi, L. Fedus, N. Felix, S. P. Fishman, J. Forte, I. Fulford, L. Gao, E. Georges, C. Gibson, V. Goel, T. Gogineni, G. Goh, R. Gontijo-Lopes, J. Gordon, M. Grafstein, S. Gray, R. Greene, J. Gross, S. S. Gu, Y. Guo, C. Hallacy, J. Han, J. Harris, Y. He, M. Heaton, J. Heidecke, C. Hesse, A. Hickey, W. Hickey, P. Hoeschele, B. Houghton, K. Hsu, S. Hu, X. Hu, J. Huizinga, S. Jain, S. Jain, J. Jang, A. Jiang, R. Jiang, H. Jin, D. Jin, S. Jomoto, B. Jonn, H. Jun, T. Kaftan, Łukasz Kaiser, A. Kamali, I. Kanitscheider, N. S. Keskar, T. Khan, L. Kilpatrick, J. W. Kim, C. Kim, Y. Kim, J. H. Kirchner, J. Kiros, M. Knight, D. Kokotajlo, Łukasz Kondraciuk, A. Kondrich, A. Konstantinidis, K. Kosic, G. Krueger, V. Kuo, M. Lampe, I. Lan, T. Lee, J. Leike, J. Leung, D. Levy, C. M. Li, R. Lim, M. Lin, S. Lin, M. Litwin, T. Lopez, R. Lowe, P. Lue, A. Makanju, K. Malfacini, S. Manning, T. Markov, Y. Markovski, B. Martin, K. Mayer, A. Mayne, B. McGrew, S. M. McKinney, C. McLeavey, P. McMillan, J. McNeil, D. Medina, A. Mehta, J. Menick, L. Metz, A. Mishchenko, P. Mishkin, V. Monaco, E. Morikawa, D. Mossing, T. Mu, M. Murati, O. Murk, D. Mély, A. Nair, R. Nakano, R. Nayak, A. Neelakantan, R. Ngo, H. Noh, L. Ouyang, C. O'Keefe, J. Pachocki, A. Paino, J. Palermo, A. Pantuliano, G. Parascandolo, J. Parish, E. Parparita, A. Passos, M. Pavlov, A. Peng, A. Perelman, F. de Avila Belbute Peres, M. Petrov, H. P. de Oliveira Pinto, Michael, Pokorny, M. Pokrass, V. H. Pong, T. Powell, A. Power, B. Power, E. Proehl, R. Puri, A. Radford, J. Rae, A. Ramesh, C. Raymond, F. Real, K. Rimbach, C. Ross, B. Rotsted, H. Roussez, N. Ryder, M. Saltarelli, T. Sanders, S. Santurkar, G. Sastry, H. Schmidt, D. Schnurr, J. Schulman, D. Selsam, K. Sheppard, T. Sherbakov, J. Shieh, S. Shoker, P. Shyam, S. Sidor, E. Sigler, M. Simens, J. Sitkin, K. Slama, I. Sohl, B. Sokolowsky, Y. Song, N. Staudacher, F. P. Such, N. Summers, I. Sutskever, J. Tang, N. Tezak, M. B. Thompson, P. Tillet, A. Tootoonchian, E. Tseng, P. Tuggle, N. Turley, J. Tworek, J. F. C. Uribe, A. Vallone, A. Vijayvergiya, C. Voss, C. Wainwright, J. J. Wang, A. Wang, B. Wang, J. Ward, J. Wei, C. Weinmann, A. Welihinda, P. Welinder, J. Weng, L. Weng, M. Wiethoff, D. Willner, C. Winter, S. Wolrich, H. Wong, L. Workman, S. Wu, J. Wu, M. Wu, K. Xiao, T. Xu, S. Yoo, K. Yu, Q. Yuan, W. Zaremba, R. Zellers, C. Zhang, M. Zhang, S. Zhao, T. Zheng, J. Zhuang, W. Zhuk, and B. Zoph. Gpt-4 technical report, 2024.

[63] D. Owen. How predictable is language model benchmark performance?, 2024.

[64] M. Reid, N. Savinov, D. Teplyashin, D. Lepikhin, T. Lillicrap, J.-b. Alayrac, R. Soricut, A. Lazaridou, O. Firat, J. Schrittwieser, et al. Gemini 1.5: Unlocking multimodal understanding across millions of tokens of context. *arXiv preprint arXiv:2403.05530*, 2024.

[65] J. S. Rosenfeld, A. Rosenfeld, Y. Belinkov, and N. Shavit. A constructive prediction of the generalization error across scales. In *International Conference on Learning Representations*, 2019.

[66] Y. Ruan, C. J. Maddison, and T. Hashimoto. Observational scaling laws and the predictability of language model performance, 2024.

[67] M. Sap, H. Rashkin, D. Chen, R. Le Bras, and Y. Choi. Social iqa: Commonsense reasoning about social interactions. In *Proceedings of the 2019 Conference on Empirical Methods in Natural Language Processing and the 9th International Joint Conference on Natural Language Processing (EMNLP-IJCNLP)*, 2019.

[68] M. Sap, H. Rashkin, D. Chen, R. LeBras, and Y. Choi. Socialiqa: Commonsense reasoning about social interactions, 2019.

[69] N. Sardana and J. Frankle. Beyond chinchilla-optimal: Accounting for inference in language model scaling laws, 2023.

[70] R. Schaeffer, B. Miranda, and S. Koyejo. Are emergent abilities of large language models a mirage? In A. Oh, T. Naumann, A. Globerson, K. Saenko, M. Hardt, and S. Levine, editors, *Advances in Neural Information Processing Systems*, volume 36, pages 55565–55581. Curran Associates, Inc., 2023. URL https://proceedings.neurips.cc/paper_files/paper/2023/file/adc98a266f45005c403b8311ca7e8bd7-Paper-Conference.pdf.

[71] C. Spearman. The proof and measurement of association between two things. 1961.

[72] A. Srivastava, A. Rastogi, A. Rao, A. A. M. Shoeb, A. Abid, A. Fisch, A. R. Brown, A. Santoro, A. Gupta, A. Garriga-Alonso, et al. Beyond the imitation game: Quantifying and extrapolating the capabilities of language models. *arXiv preprint arXiv:2206.04615*, 2022.

[73] G. Team, R. Anil, S. Borgeaud, Y. Wu, J.-B. Alayrac, J. Yu, R. Soricut, J. Schalkwyk, A. M. Dai, A. Hauth, et al. Gemini: a family of highly capable multimodal models. *arXiv preprint arXiv:2312.11805*, 2023.

[74] J. Wei, Y. Tay, R. Bommasani, C. Raffel, B. Zoph, S. Borgeaud, D. Yogatama, M. Bosma, D. Zhou, D. Metzler, et al. Emergent abilities of large language models. *arXiv preprint arXiv:2206.07682*, 2022.

[75] J. Welbl, N. F. Liu, and M. Gardner. Crowdsourcing multiple choice science questions. In L. Derczynski, W. Xu, A. Ritter, and T. Baldwin, editors, *Proceedings of the 3rd Workshop on Noisy User-generated Text*, pages 94–106, Copenhagen, Denmark, Sept. 2017. Association for Computational Linguistics. doi: 10.18653/v1/W17-4413. URL https://aclanthology.org/W17-4413.

[76] R. Zellers, A. Holtzman, Y. Bisk, A. Farhadi, and Y. Choi. Hellaswag: Can a machine really finish your sentence? *arXiv preprint arXiv:1905.07830*, 2019.

[77] X. Zhai, A. Kolesnikov, N. Houlsby, and L. Beyer. Scaling vision transformers. In *Proceedings of the IEEE/CVF Conference on Computer Vision and Pattern Recognition*, pages 12104–12113, 2022.

[78] B. Zhou, D. Khashabi, Q. Ning, and D. Roth. "going on a vacation" takes longer than "going for a walk": A study of temporal commonsense understanding. In K. Inui, J. Jiang, V. Ng, and X. Wan, editors, *Proceedings of the 2019 Conference on Empirical Methods in Natural Language Processing and the 9th International Joint Conference on Natural Language Processing (EMNLP-IJCNLP)*, pages 3363–3369, Hong Kong, China, Nov. 2019. Association for Computational Linguistics. doi: 10.18653/v1/D19-1332. URL https://aclanthology.org/D19-1332.

A Related Work

Language Model Evaluation The capabilities of AI models are typically evaluated using constructed datasets to assess performance on a specific task, acting as a proxy for some real-world usage scenario. However, performing robust and reliable evaluations is a challenge, with many potential pitfalls and unsolved problems [10]. For example, we might prefer to ask models open-ended questions and evaluate their answers in natural language, but it then often becomes difficult to robustly score the resulting model outputs, especially for partial correctness. For this reason, it is common practice for evaluation benchmarks to simplify their scoring via approximations, such as extracting a sub-string from free-form outputs heuristically [43, 48, 33] and checking that it matches a specific gold target string, or casting a task to a *multiple-choice* format, in which a closed set of correct and incorrect answers is known, and the model's answer is determined by selecting the most likely option among these strings. For more details on the precise procedures typically used for multiple choice elsewhere in the literature, see Biderman et al. [10]. We believe that the multiple-choice format is valuable, due to its flexibility, popularity and relevance [14, 6, 10], but we discuss its limitations in Section 6.

Scaling Laws Many neural networks exhibit power-law scaling of the pretraining loss as a function of the amount of compute, data, or parameters used for training [37, 14, 38]. These neural scaling laws demonstrate that the pretraining loss can be highly predictable as a function of these fundamental inputs, which has a number of practical applications: Scaling laws fit to smaller training runs can be used to predict the pretraining loss of a much larger training run, and can be used to determine effective hyperparameters [53, 20], or the optimal allocation of dataset and model size for a given compute budget [38, 58, 21, 69, 7]. In some cases, such laws can be used to predict performance of a larger model in a particular domain, such as coding [1]. The existence of scaling laws turns deep learning into a predictable science at the macro level by providing a simple recipe for improving model quality and de-risking returns on increasing investment into scale [26, 12].

Emergent Abilities Language models have been observed to exhibit apparent *emergent abilities*—behaviors on downstream task performance that cannot be predicted from smaller scales [74, 72]. Emergence appears not to be simply a product of training compute or model size, but is also dependent on other factors such as dataset composition [56, 74]. Schaeffer et al. [70] find that some emergent phenomena can be a "mirage" arising due to choices made by researchers such as the use of discontinuous metrics and insufficient resolution. However, Du et al. [23] note that for many tasks, emergence remains despite the use of continuous metrics. Additionally, discontinuous metrics have been argued to often be the most reflective of real-world usefulness, so emergence in these hard metrics is important. Hu et al. [39] found that for generative evaluations, infinite resolution can be achieved but requires significant compute and that generated answer be verifiable.

Predicting Downstream Task Performance Although predicting macroscopic pretraining loss is useful, a far more useful goal is to predict the scaling of model performance on particular downstream tasks or domains. If this was possible, then model developers could tune their datasets and training procedures in a more fine-grained way before launching computationally intensive training runs. Model performance on a particular downstream task is typically correlated with compute, albeit with a few exceptions [54, 40]. However, despite attempts to fit scaling laws to values other than loss, including benchmark scores [25, 41], model memorization [8], or reward [28], these downstream performance metrics are usually more noisy or require more compute to fit accurately. Owen [63] and Gadre et al. [25] both find that while *aggregate* benchmark performance with more compute can be predicted, the scaling behaviour of individual tasks can be noisy. Additionally, Owen [63], Du et al. [23] and Gadre et al. [25] claim that predicting scaling behavior on a task without access to models exhibiting better-than-random performance (i.e., "before emergence occurs") cannot be done reliably. Concurrently to our work, Ruan et al. [66] propose Observational Scaling Laws by mapping model capabilities from compute to a shared low-dimensional space of capabilities across model families before predicting performance on novel tasks. Our goal in this work is to investigate the comparative unpredictability of individual downstream performance scores, and advise how to create more scaling-predictable evaluations that are closely coupled with real-world use-cases.

B Definition of Survival Function

The survival function $S_X(x)$ – also known as the reliability function, the tail distribution, or the complementary cumulative distribution function – gives the probability that a random variable X exceeds a certain value x [47, 19]:

$$S_X(x) \stackrel{\text{def}}{=} Pr[X > x] = \int_x^{\infty} f_X(x')\,dx' = 1 - F_X(x) \tag{7}$$

where $F_X(x) = Pr[X \leq x]$ is the cumulative distribution function (CDF) and $f_X(x)$ is the probability density function (pdf) or probability mass function (pmf) of the random variable X. The CDF $F_X(x)$ gives the probability that the random variable X is at most x, while the survival function $S_X(x)$ gives the probability that X exceeds x.

When the true distribution of X is unknown, we can use the empirical CDF (ECDF) $\hat{F}_X(x)$ and the empirical survival function (ESF) $\hat{S}_X(x)$:

$$\hat{S}_X(x) \stackrel{\text{def}}{=} \frac{1}{n}\sum_{i=1}^{n} 1\{x_i > x\} = 1 - \hat{F}_X(x) \tag{8}$$

where n is the number of observations, x_i is the realized value of the random variable X for observation i, and $1\{x_i > x\}$ is the indicator function. The empirical survival function $\hat{S}_X(x)$ specifies the fraction of observations for which the sampled random variable X exceeds x.

C Compute Resources for Experiments

Experiments were done across a wide family of model families and sizes. The GPUs we used for medium-sized models (7B parameters and above) used a single A100s with 80GB of vRAM. For smaller models ($\leq$8B) we used A100s with 80GB of vRAM, Quadro RTX 8000 with 48GB of vRAM, or RTX A4000 with 16GB of vRAM. For 70B parameter models, we used at least 2 A100 GPUs with 80GB of vRAM.

D Additional Model Family Details

Here we provide further experimental details regarding our selection of model families.

1. **Pythia** [9]: We consider two "families" for Pythia in our experiments. **Pythia (Parameter Scaling)** refers to the use of fully-trained checkpoints from 9 different model sizes (all model sizes documented in Biderman et al. (2023), as well as a 14M parameter model trained later by the authors). **Pythia-12B (Data Scaling)** refers to the use of 8 checkpoints across training for the Pythia-12B model, namely having seen 2M, 64M, 2B, 6B, 20B, 60B, 200B, and 300B tokens in training.
2. **Cerebras-GPT** [21]: **Cerebras (Parameter and Data Scaling)** refers to our use of 1 checkpoint per model in the Cerebras-GPT family, each fully trained for differing quantities of data as documented by the model creators, for 7 checkpoints in total.
3. **OLMo** [31]: **OLMo (7B Data Scaling)** refers to the use of 7 checkpoints for OLMo-7B across training, namely, checkpoints having seen 4B, 44B, 133B, 442B, 885B, 1.5T, and 2.4T tokens.
4. **INCITE** [2]: **INCITE-7B (Data Scaling)** considers 6 checkpoints over training for the 7B parameter model, having seen 240B, 280B, 400B, 500B, 700B, and 1T tokens.
5. **LLM360** [50]: **LLM360 Amber (Data Scaling)** considers 13 checkpoints of the Amber model, having seen 0B, 3.5B, 7B, 10.5B, 17.5B, 31.5B, 49B, 87.5B, 147B, 252B, 430B, 738B, and 1.26T tokens.

E Broader Impact

This paper contributes to a better understanding of the predictability of large language models (LLMs), which can have both positive and negative societal impacts. On the positive side, by making

LLM benchmarks more predictable, this research can help society anticipate and plan for potential challenges associated with their development and deployment. This increased predictability can facilitate proactive measures to mitigate risks and ensure the responsible use of AI technologies.

However, the increased predictability of LLMs could theoretically be exploited by malicious actors to accelerate the development of AI systems designed for malicious purposes. We also stress the importance of proactive risk assessment and the implementation of safeguards to prevent the misuse of AI technologies.

F Score-Compute Correlation Distributions' Statistics

F.1 Pearson Correlations

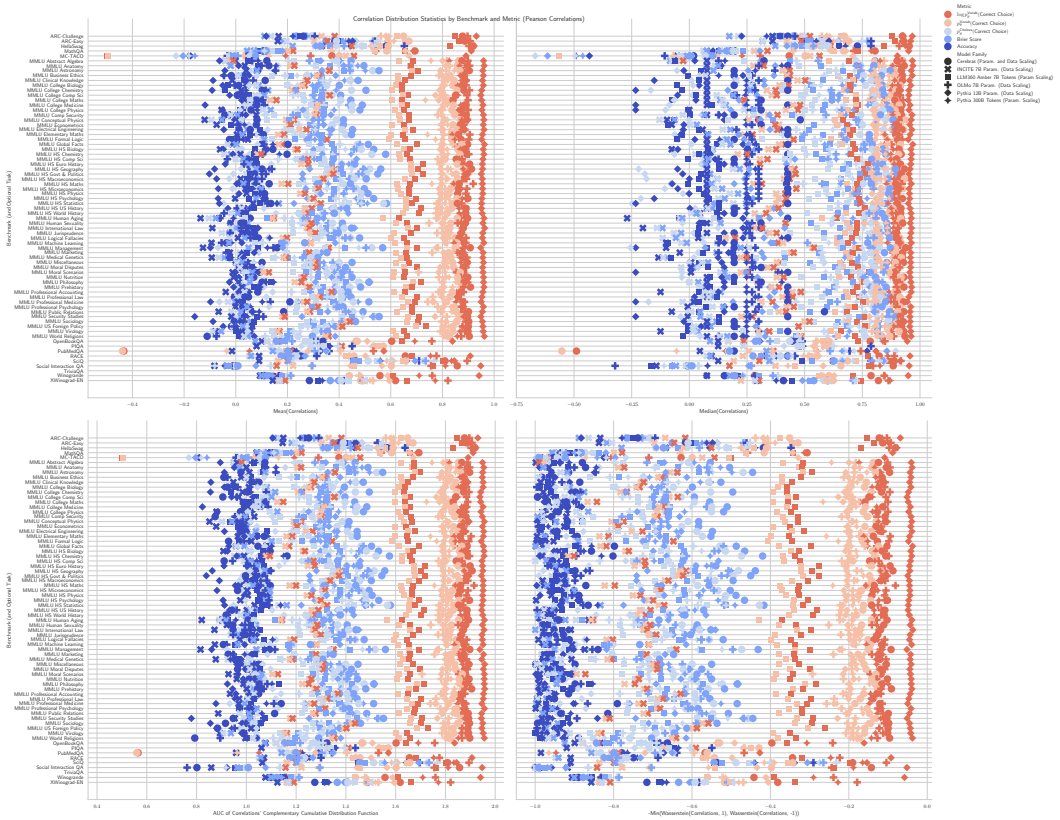

Figure 7: **Statistics for empirical distributions of correlations between scores and compute for all benchmarks and model families.** These correlation values were computed with Pearson correlation and are consistent with the main text's results computed with Spearman correlation (Fig. 4): The sequence of transformations from $\log p_\theta^{\text{Vocab}}(\text{Correct Choice}) \to p_\theta^{\text{Vocab}}(\text{Correct Choice}) \to p_\theta^{\text{Choices}}(\text{Correct Choice}) \to$ Accuracy degrades predictability.

F.2 Spearman Correlations

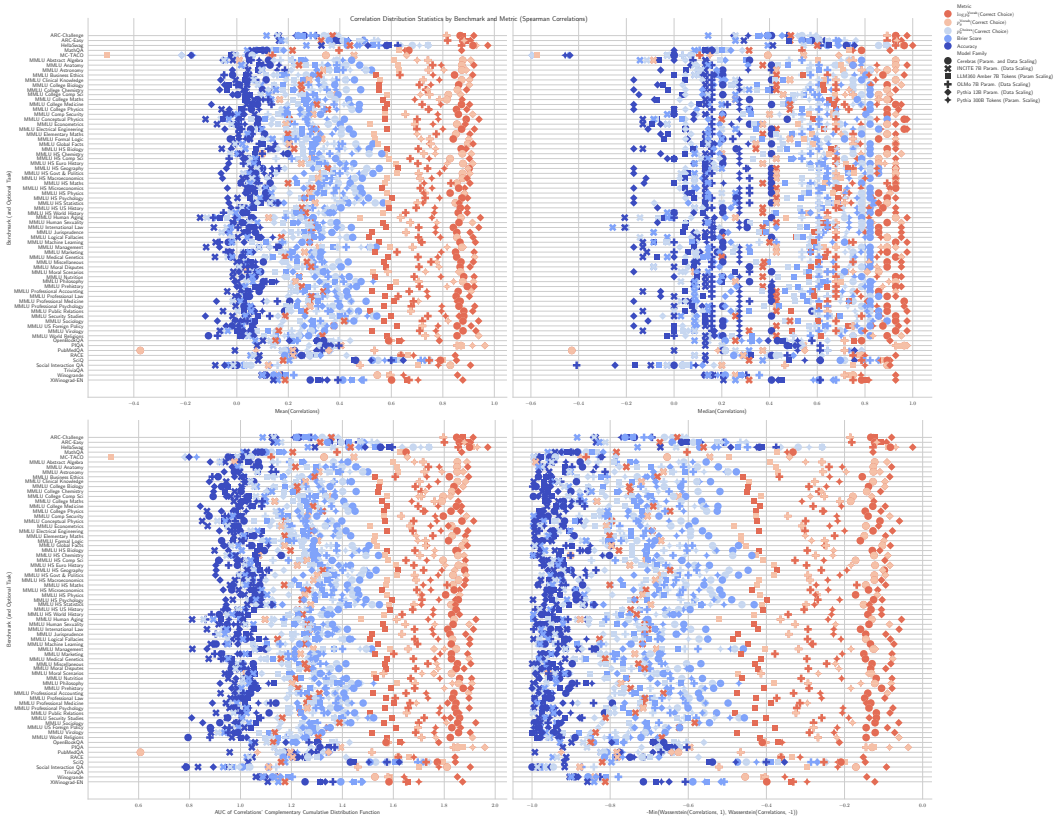

Figure 8: **Statistics for empirical distributions of correlations between scores and compute for all benchmarks and model families.** These correlation values were computed with Spearman correlation. The sequence of transformations from $\log p_\theta^{\text{Vocab}}(\text{Correct Choice}) \to p_\theta^{\text{Vocab}}(\text{Correct Choice}) \to p_\theta^{\text{Choices}}(\text{Correct Choice}) \to$ Accuracy degrades predictability.

F.3 Kendall Correlations

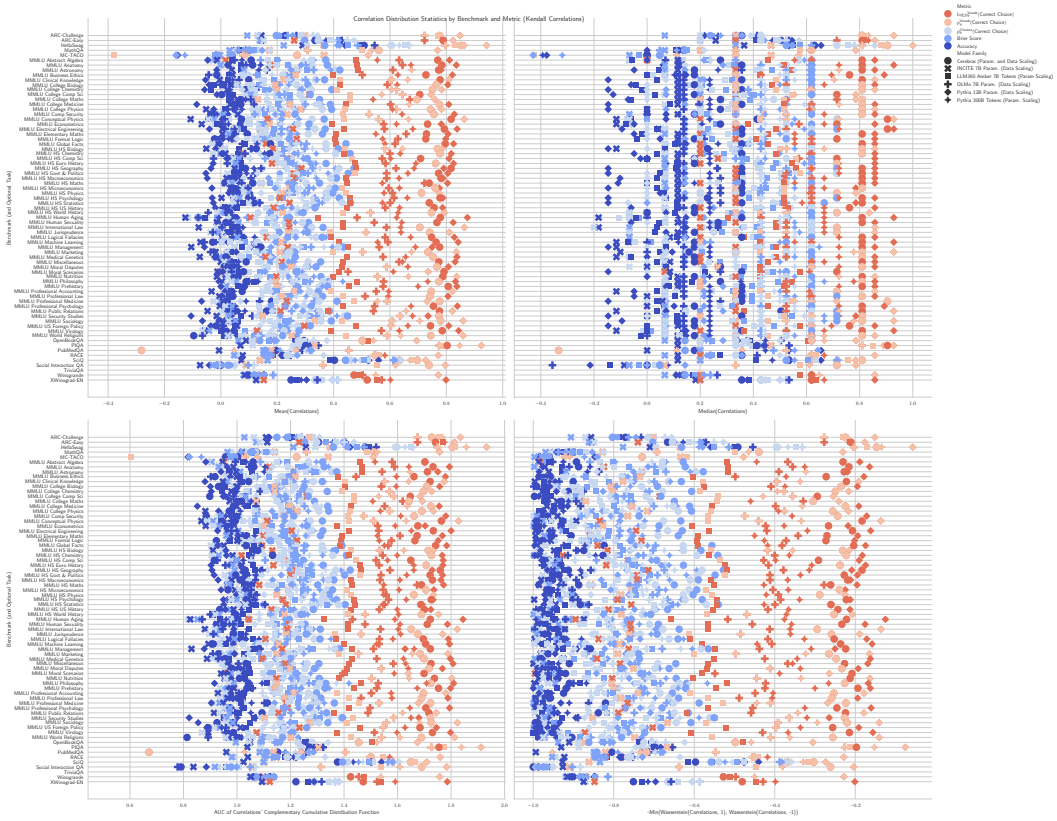

Figure 9: **Statistics for empirical distributions of correlations between scores and compute for all benchmarks and model families.** These correlation values were computed with Kendall correlation and are consistent with the main text's results computed with Spearman correlation (Fig. 4): The sequence of transformations from $\log p_\theta^{\text{Vocab}}(\text{Correct Choice}) \to p_\theta^{\text{Vocab}}(\text{Correct Choice}) \to p_\theta^{\text{Choices}}(\text{Correct Choice}) \to$ Accuracy degrades predictability.

G Per-Benchmark Score-Compute Correlation Distributions

G.1 NLP Benchmark: ARC Challenge [17]

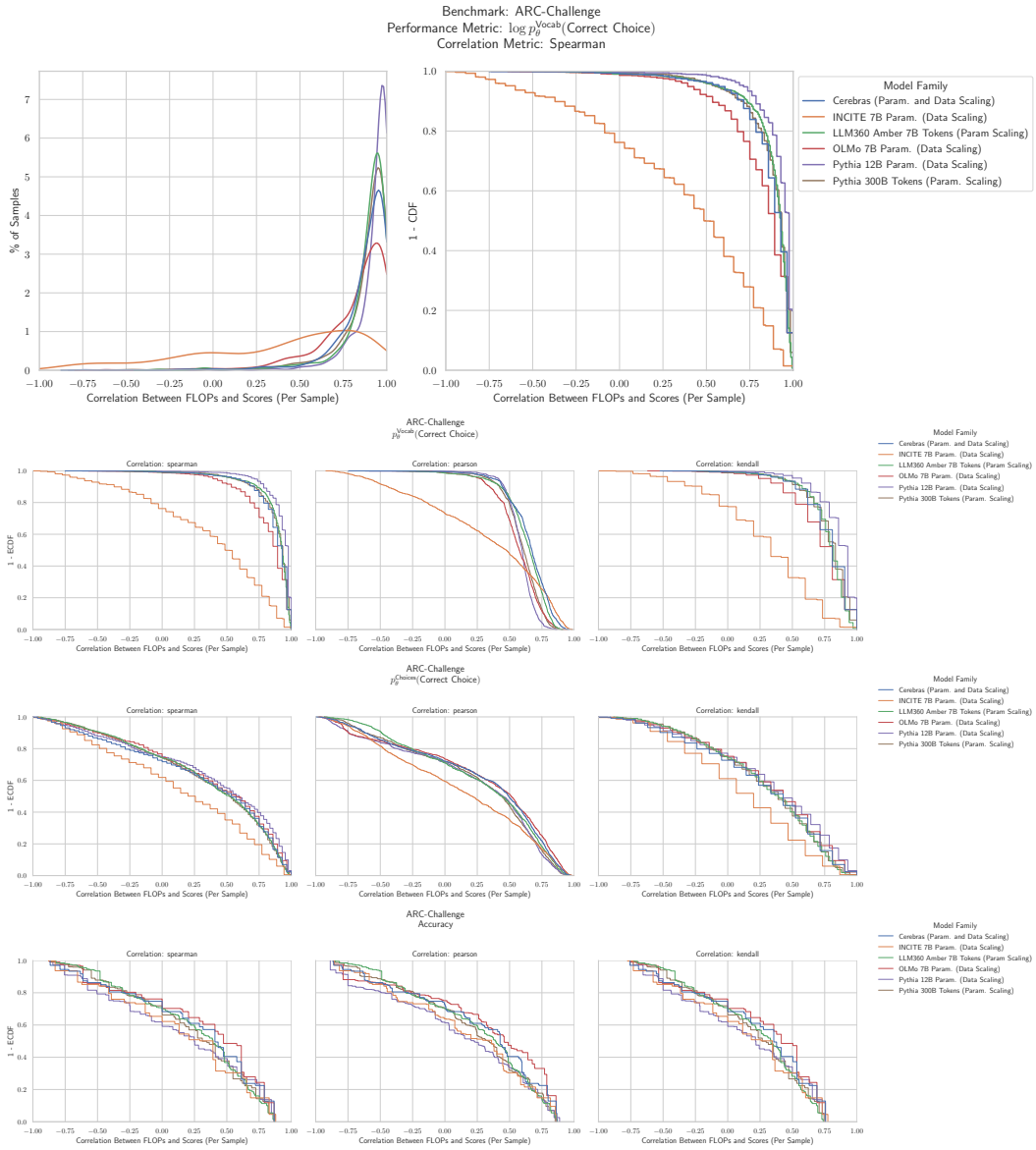

Figure 10: **ARC Challenge: Downstream performance is computed via a sequence of transformations that deteriorate correlations between scores and pretraining compute.**

G.2 NLP Benchmark: ARC Easy [17]

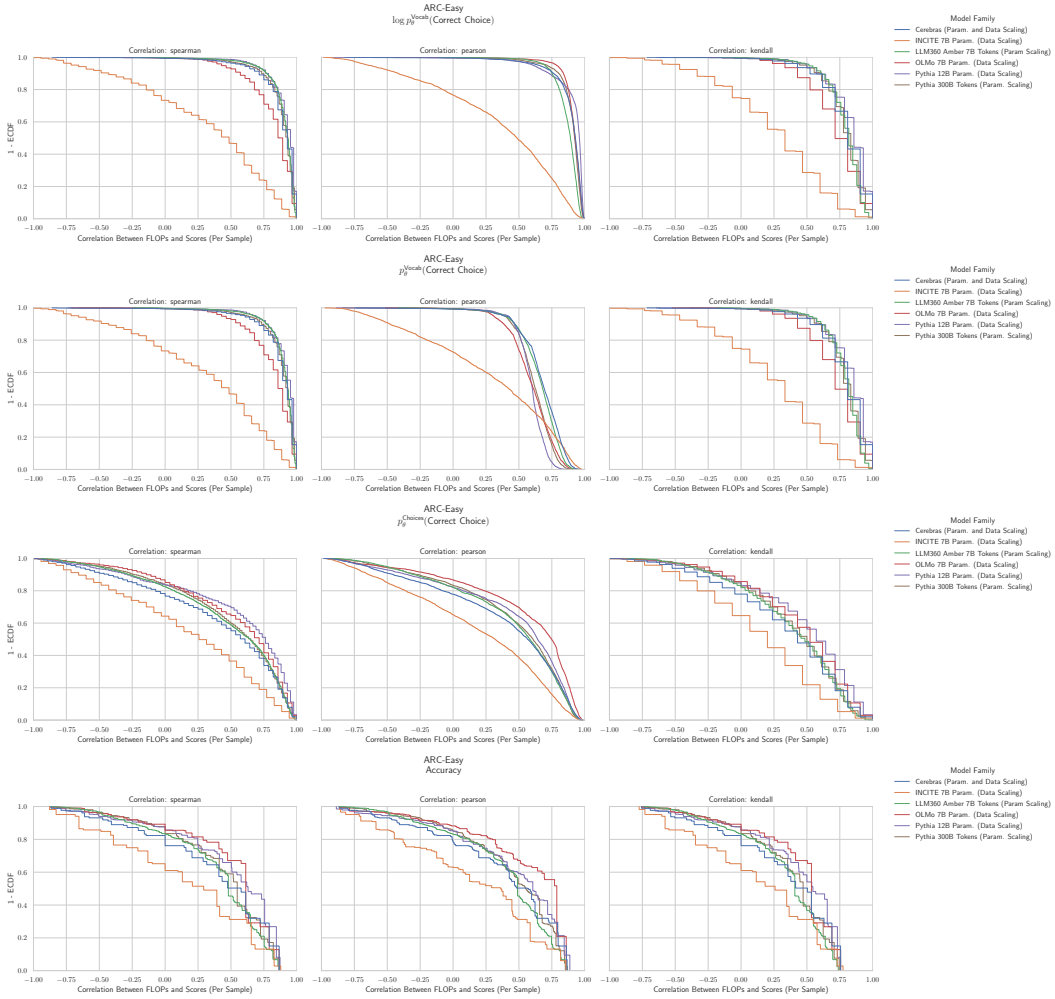

Figure 11: **ARC Easy: Downstream performance is computed via a sequence of transformations that deteriorate correlations between scores and pretraining compute.**

G.3 NLP Benchmark: HellaSwag [76]

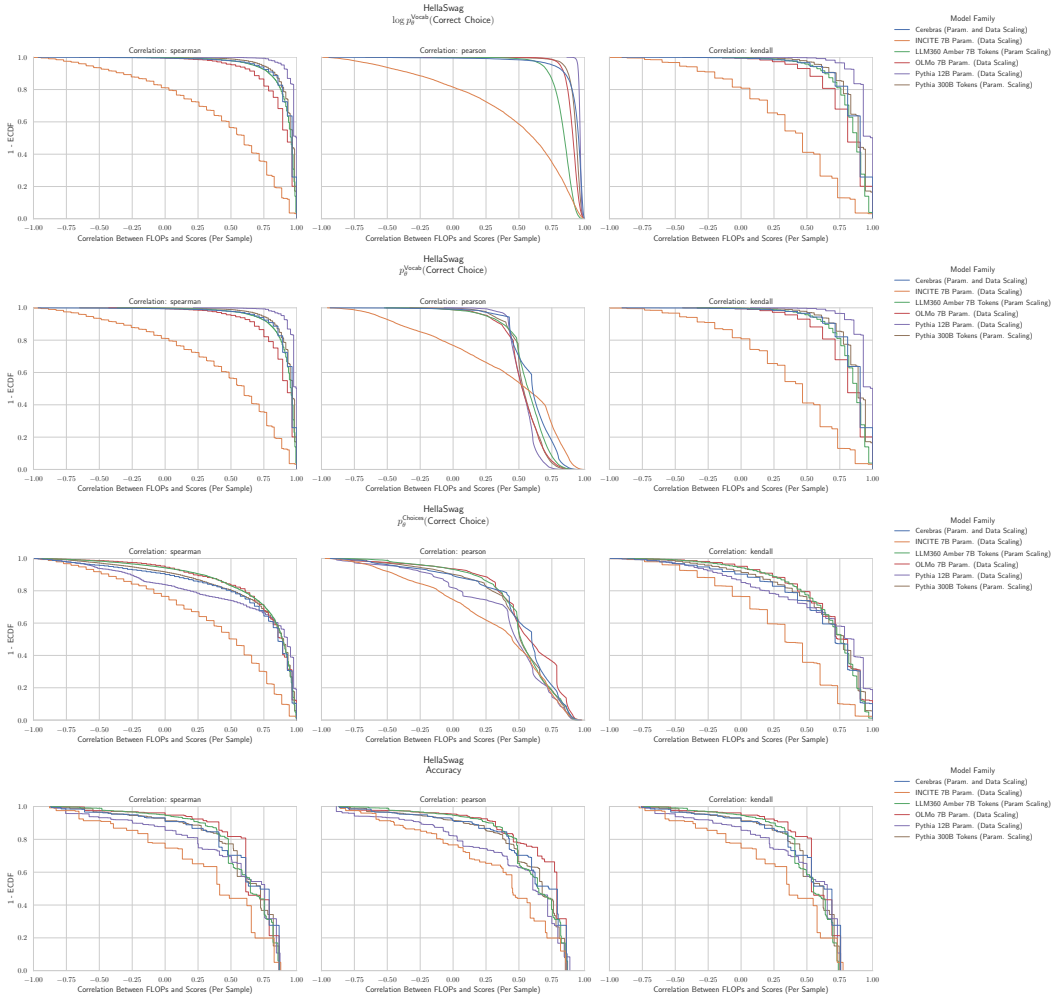

Figure 12: **HellaSwag: Downstream performance is computed via a sequence of transformations that deteriorate correlations between scores and pretraining compute.**

G.4 NLP Benchmark: MathQA [3]

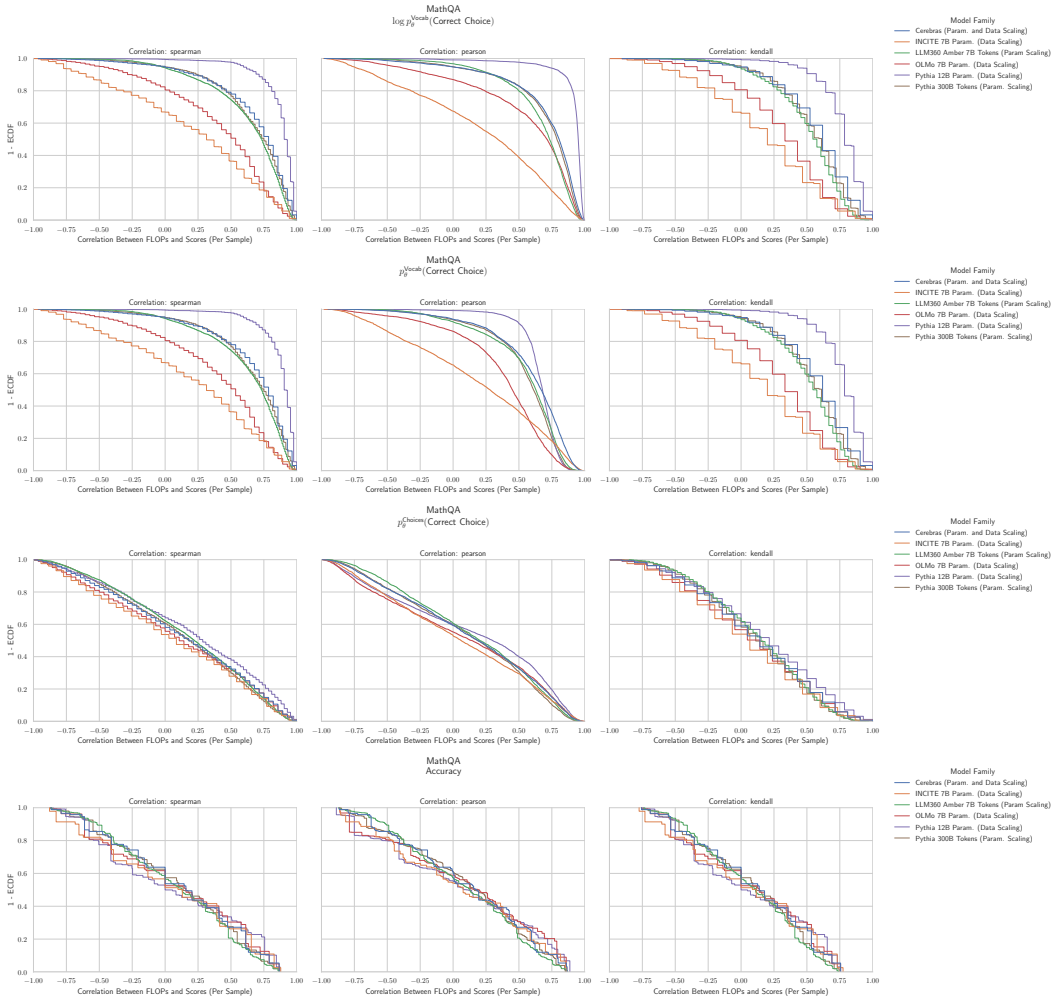

Figure 13: **HellaSwag: Downstream performance is computed via a sequence of transformations that deteriorate correlations between scores and pretraining compute.**

G.5 NLP Benchmark: MC TACO [78]

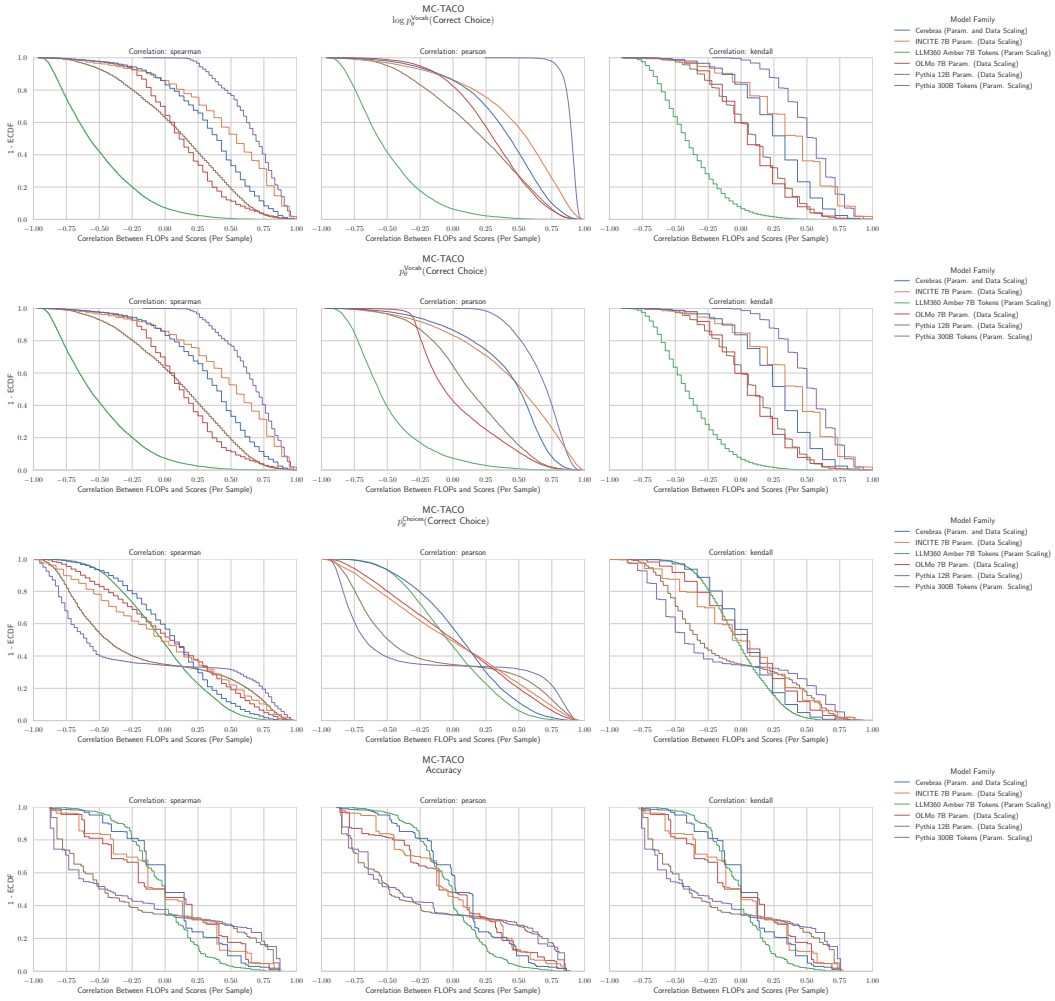

Figure 14: **MC TACO: Downstream performance is computed via a sequence of transformations that deteriorate correlations between scores and pretraining compute.**

G.6 NLP Benchmark: MMLU Abstract Algebra [32]

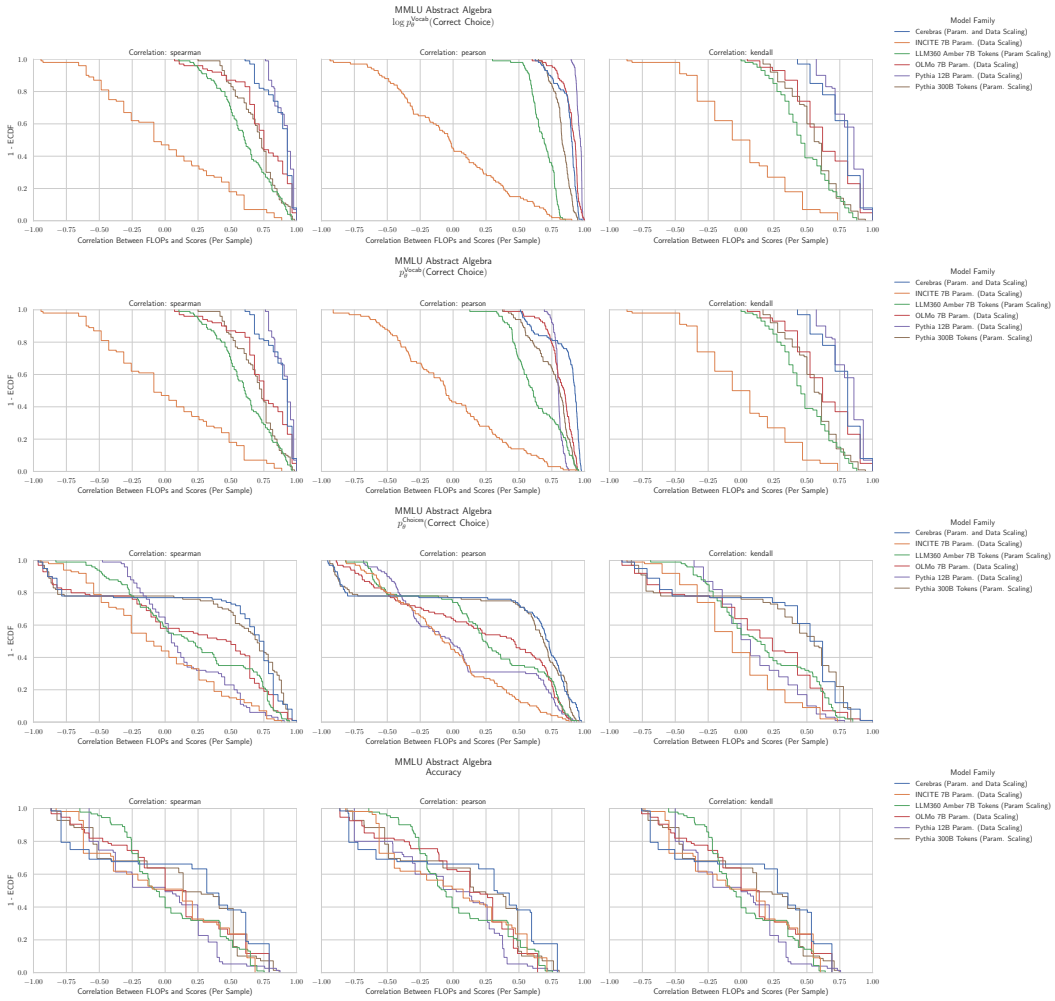

Figure 15: **MMLU Abstract Algebra: Downstream performance is computed via a sequence of transformations that deteriorate correlations between scores and pretraining compute.**

G.7 NLP Benchmark: MMLU Anatomy [32]

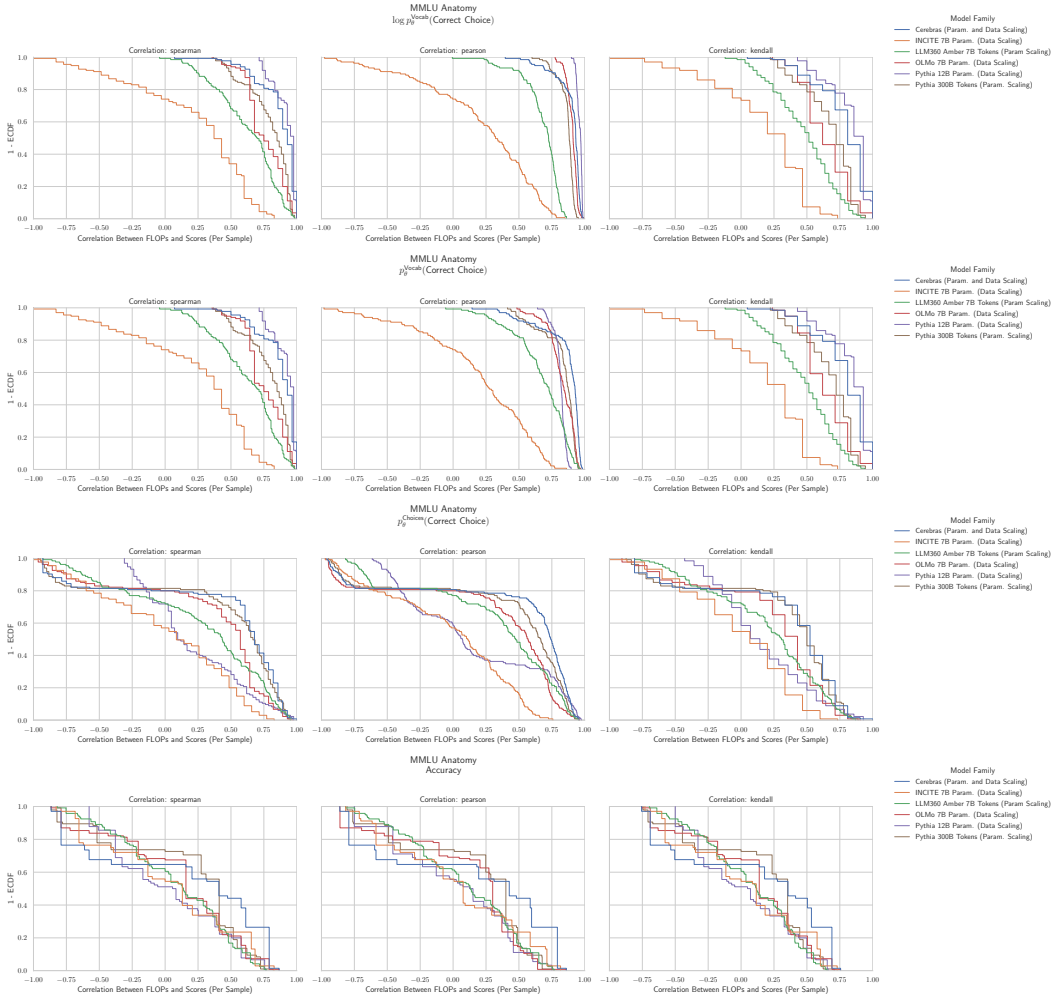

Figure 16: **MMLU Anatomy: Downstream performance is computed via a sequence of transformations that deteriorate correlations between scores and pretraining compute.**

G.8 NLP Benchmark: MMLU Astronomy [32]

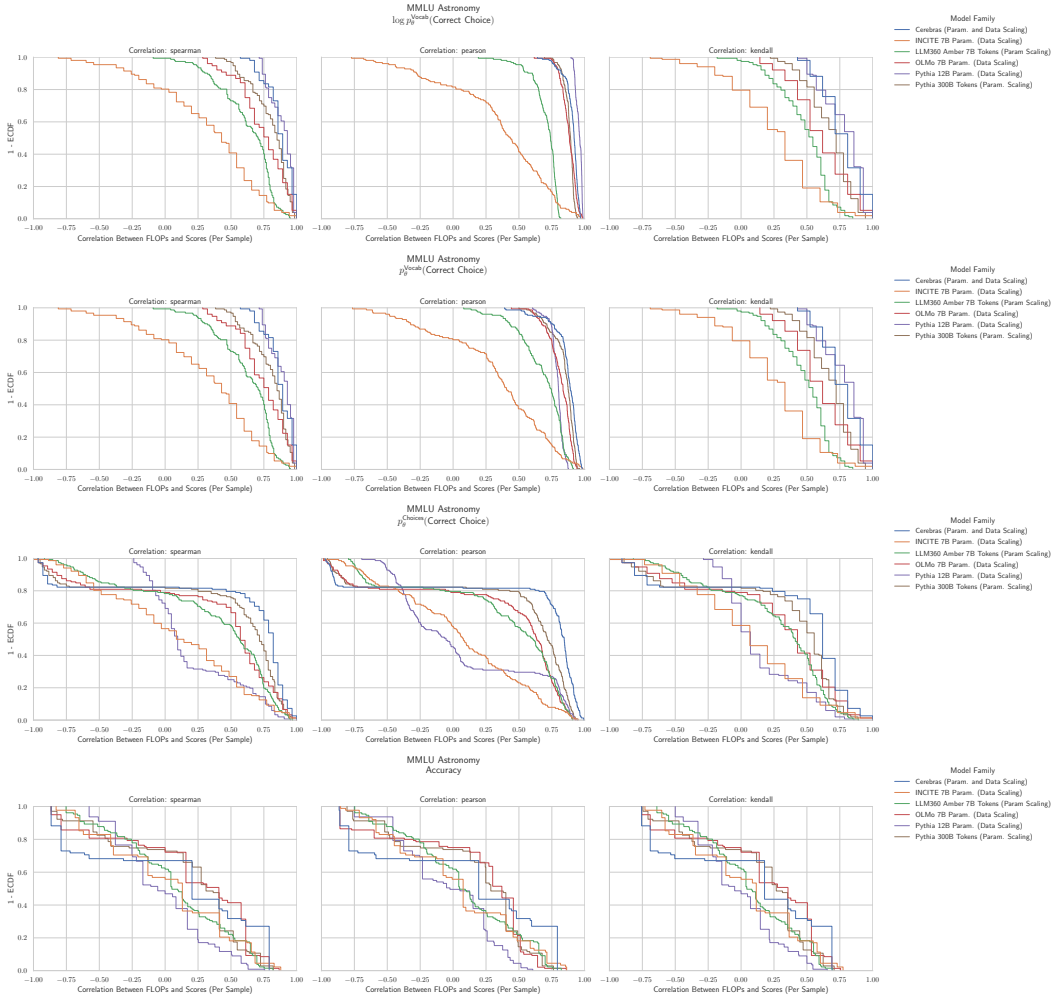

Figure 17: **MMLU Astronomy: Downstream performance is computed via a sequence of transformations that deteriorate correlations between scores and pretraining compute.**

G.9 NLP Benchmark: MMLU Business Ethics [32]

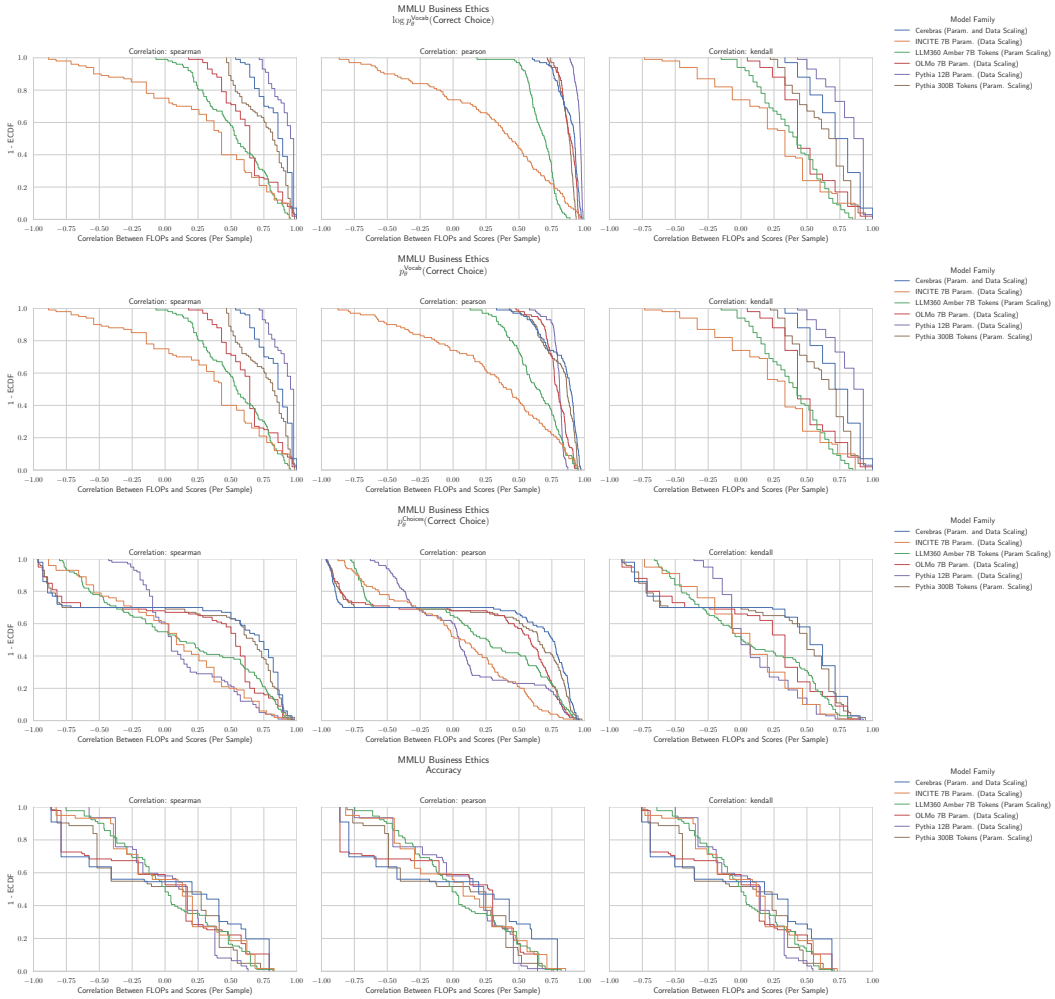

Figure 18: **MMLU Business Ethics: Downstream performance is computed via a sequence of transformations that deteriorate correlations between scores and pretraining compute.**

G.10 NLP Benchmark: MMLU Clinical Knowledge [32]

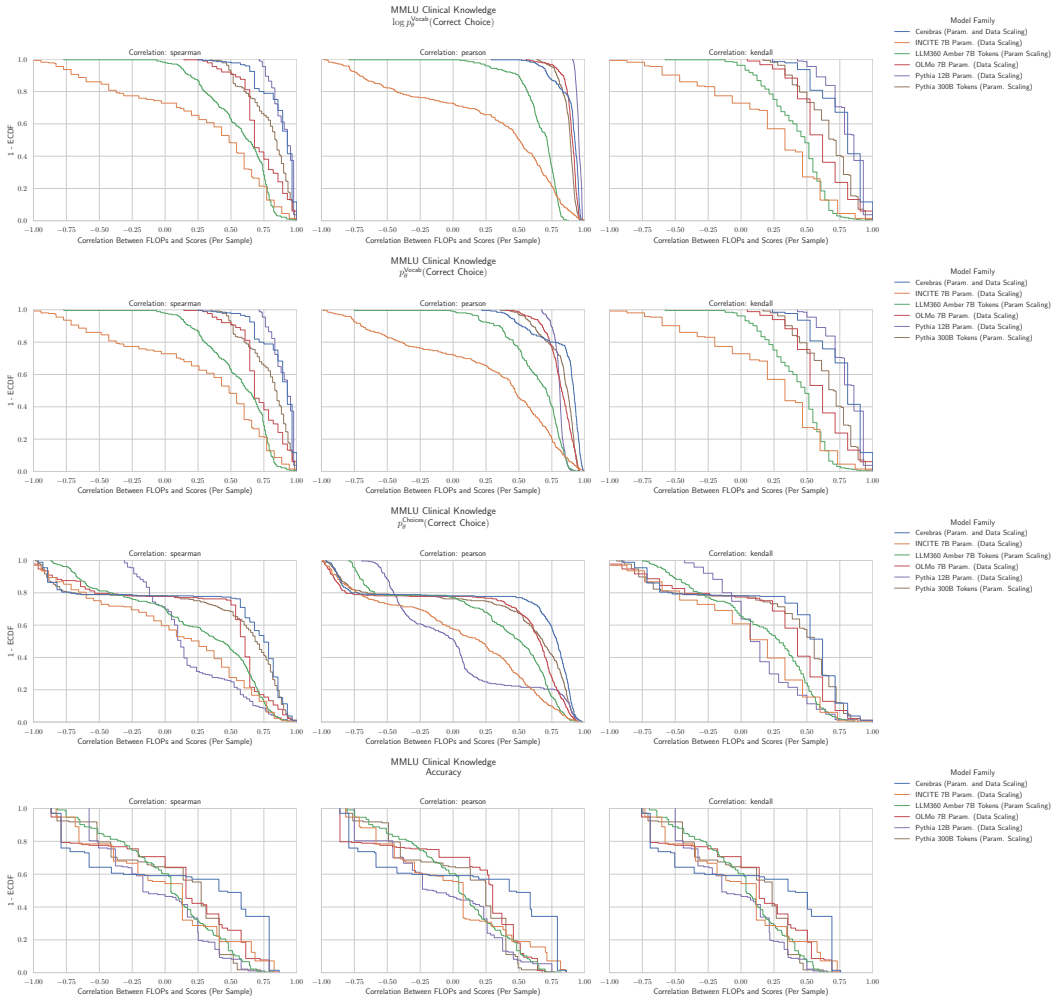

Figure 19: **MMLU Clinical Knowledge: Downstream performance is computed via a sequence of transformations that deteriorate correlations between scores and pretraining compute.**

G.11 NLP Benchmark: MMLU College Biology [32]

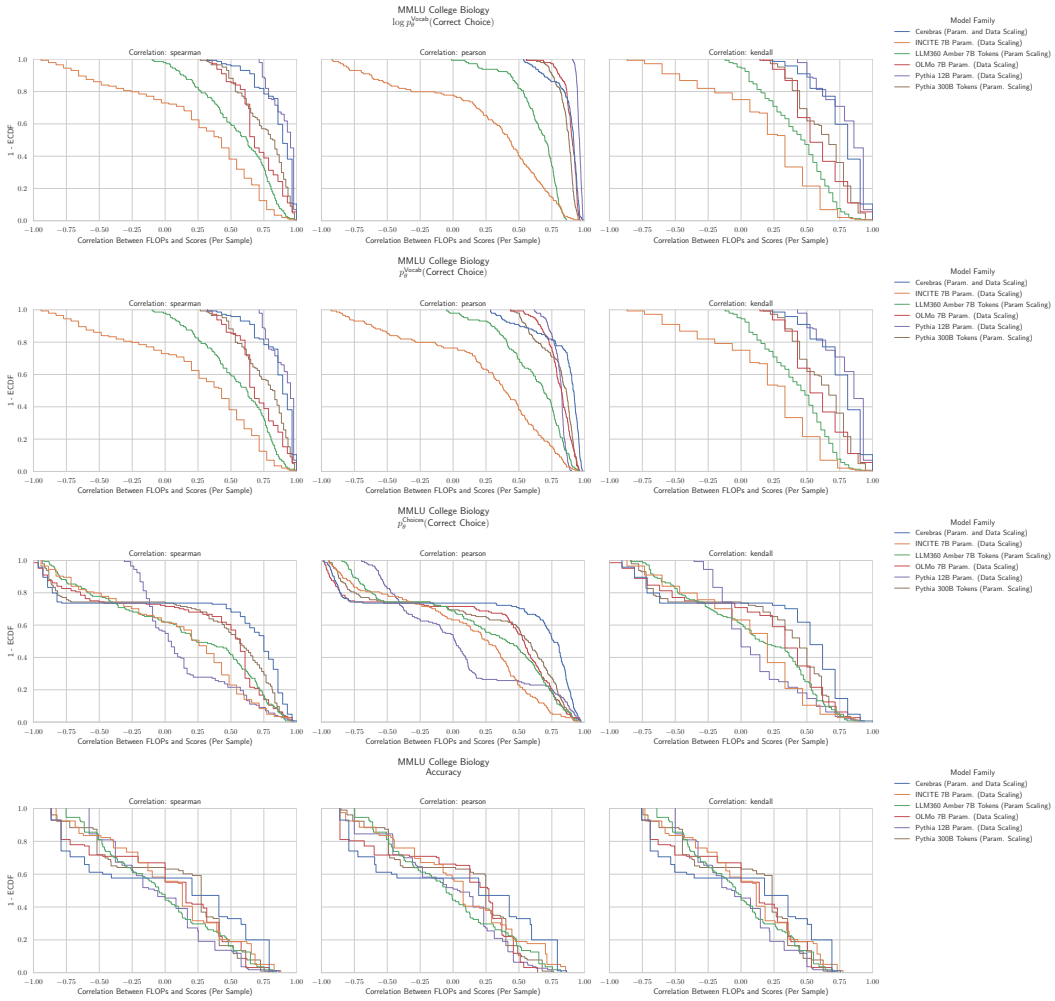

Figure 20: **MMLU College Biology: Downstream performance is computed via a sequence of transformations that deteriorate correlations between scores and pretraining compute.**

G.12 NLP Benchmark: MMLU College Chemistry [32]

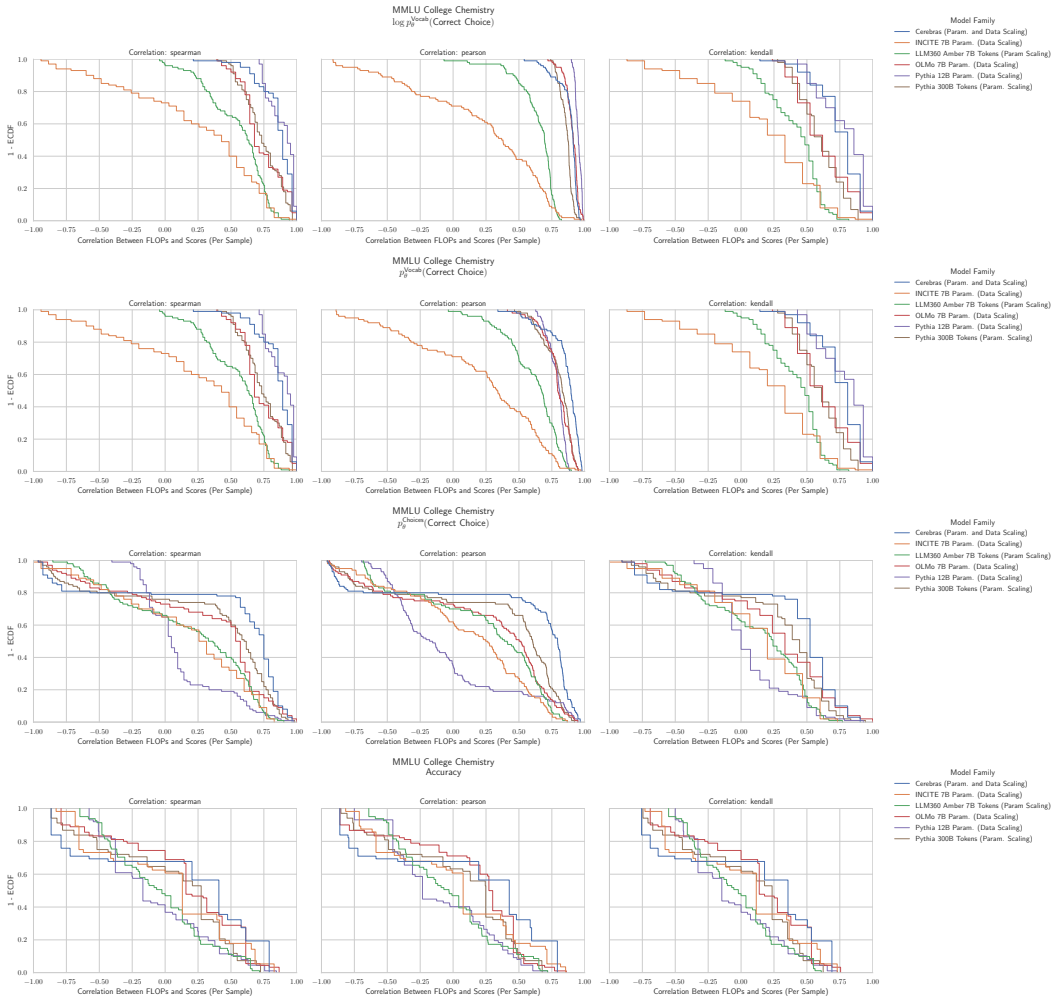

Figure 21: **MMLU College Chemistry: Downstream performance is computed via a sequence of transformations that deteriorate correlations between scores and pretraining compute.**

G.13 NLP Benchmark: MMLU College Computer Science [32]

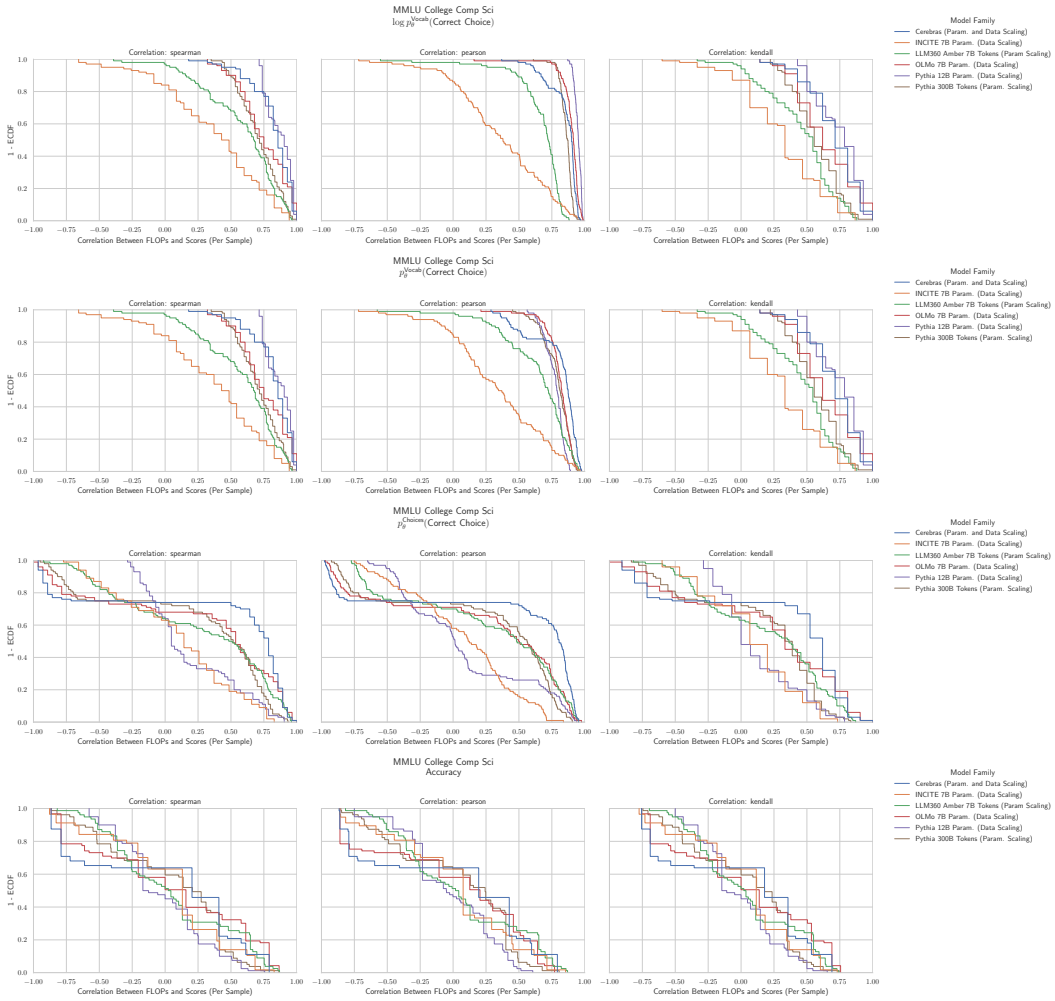

Figure 22: **MMLU College Computer Science: Downstream performance is computed via a sequence of transformations that deteriorate correlations between scores and pretraining compute.**

G.14 NLP Benchmark: MMLU College Mathematics [32]

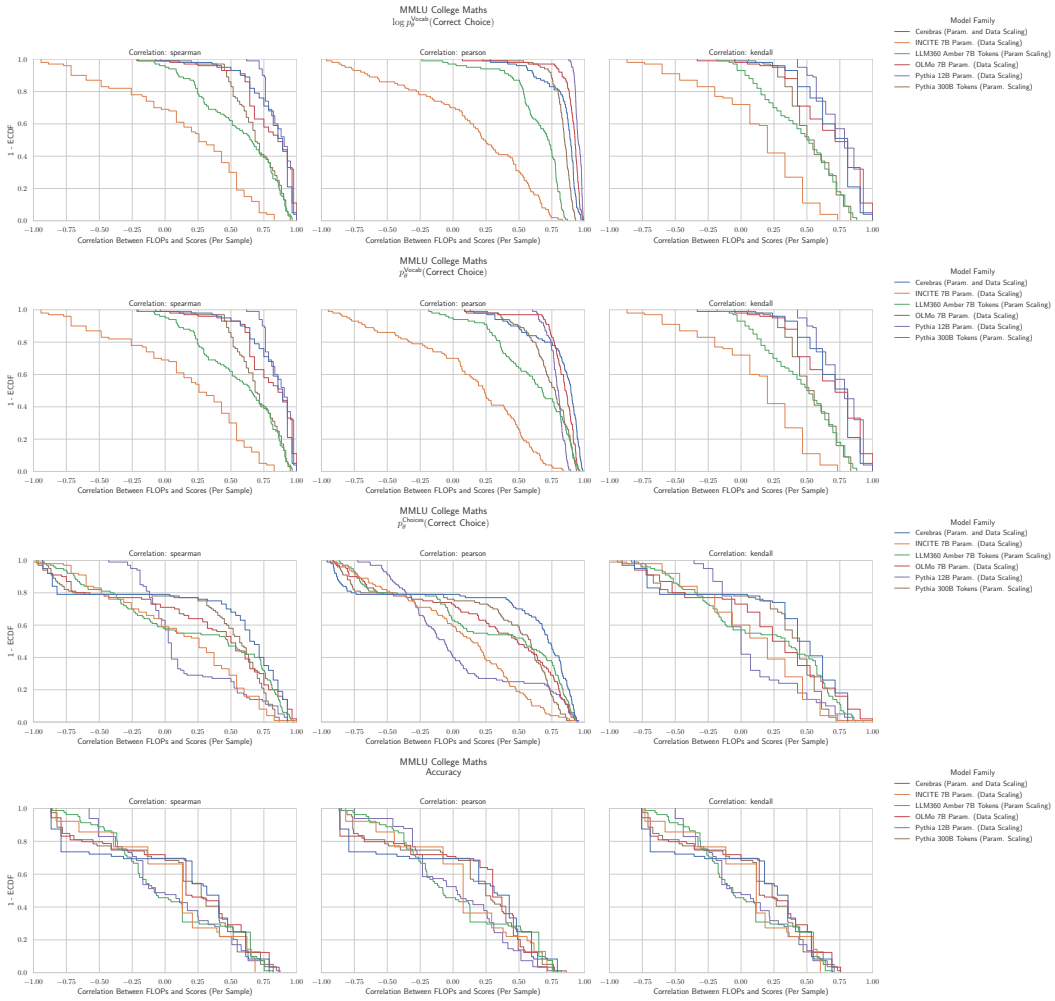

Figure 23: **MMLU College Mathematics: Downstream performance is computed via a sequence of transformations that deteriorate correlations between scores and pretraining compute.**

G.15 NLP Benchmark: MMLU College Medicine [32]

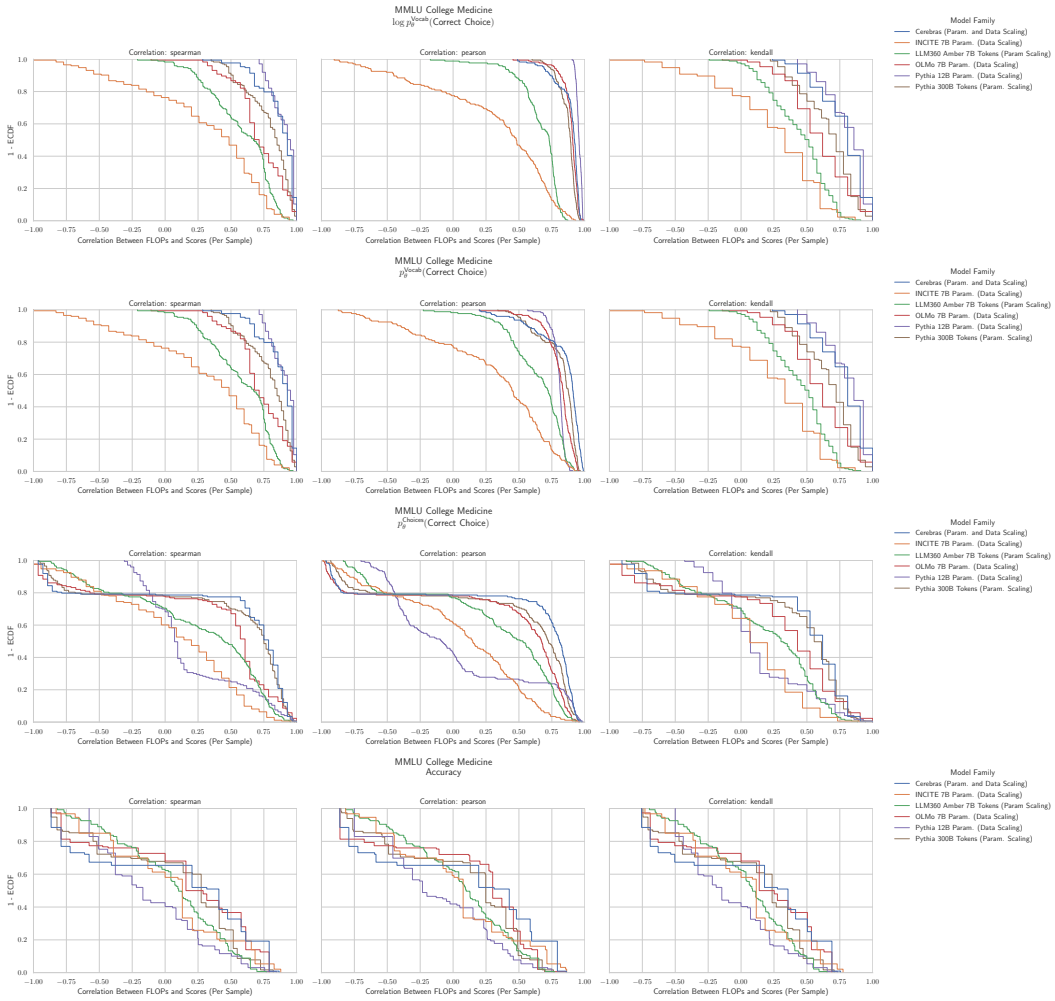

Figure 24: **MMLU College Medicine: Downstream performance is computed via a sequence of transformations that deteriorate correlations between scores and pretraining compute.**

G.16 NLP Benchmark: MMLU College Physics [32]

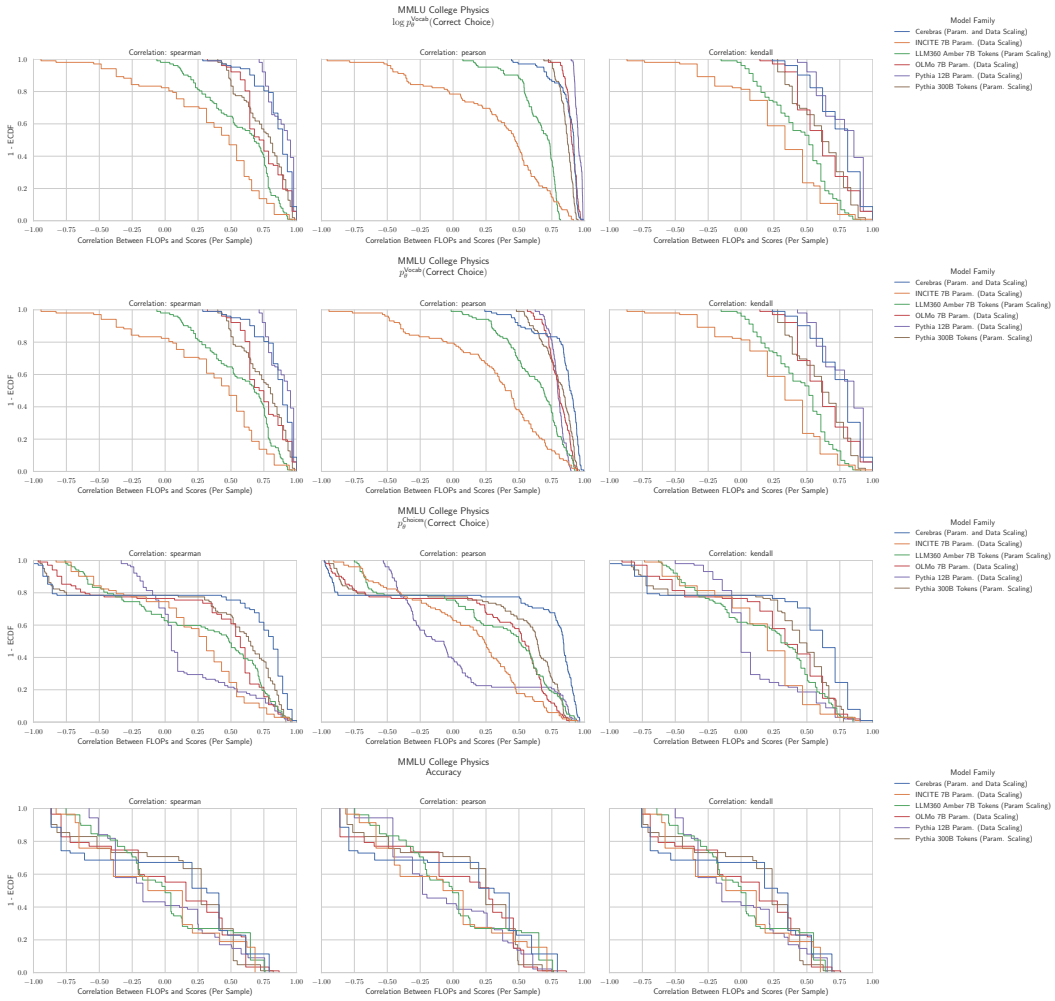

Figure 25: **MMLU College Physics: Downstream performance is computed via a sequence of transformations that deteriorate correlations between scores and pretraining compute.**

G.17 NLP Benchmark: MMLU Computer Security [32]

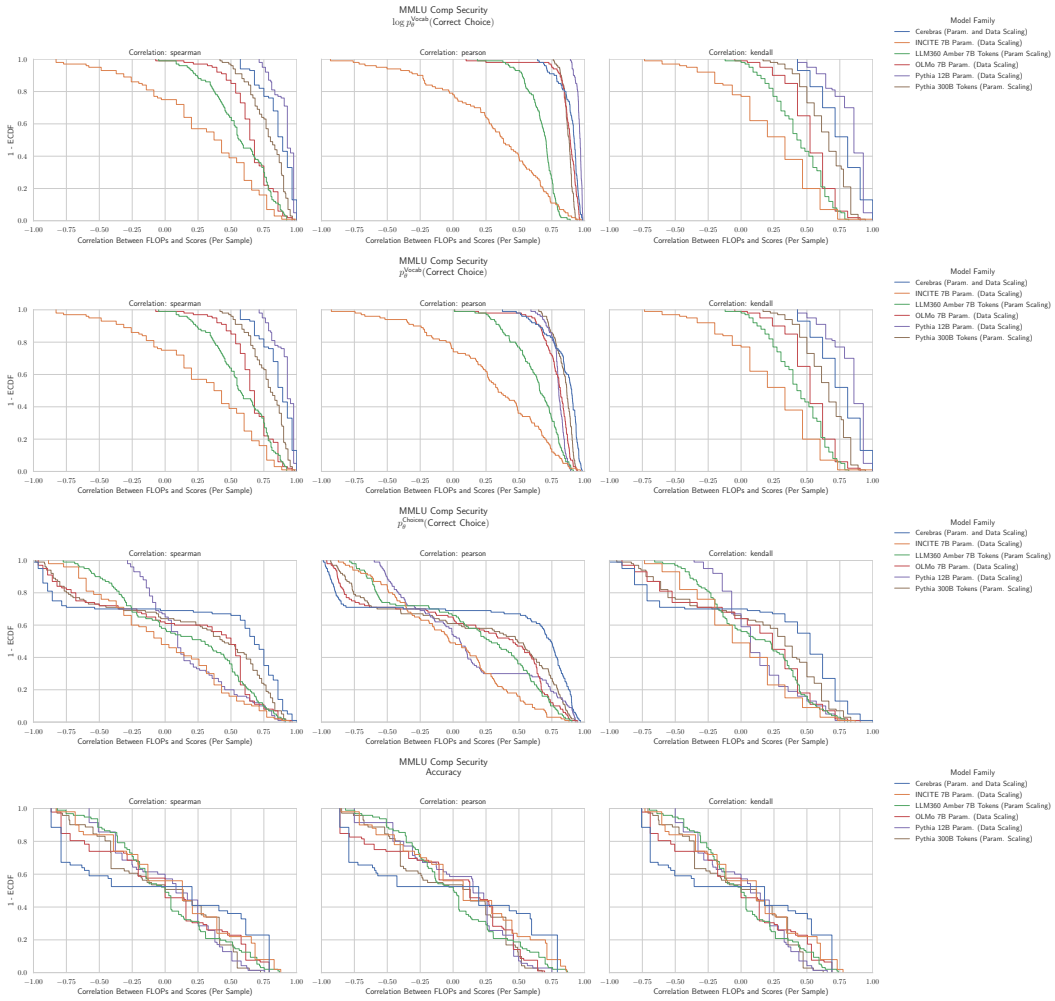

Figure 26: **MMLU Computer Security: Downstream performance is computed via a sequence of transformations that deteriorate correlations between scores and pretraining compute.**

G.18 NLP Benchmark: MMLU Conceptual Physics [32]

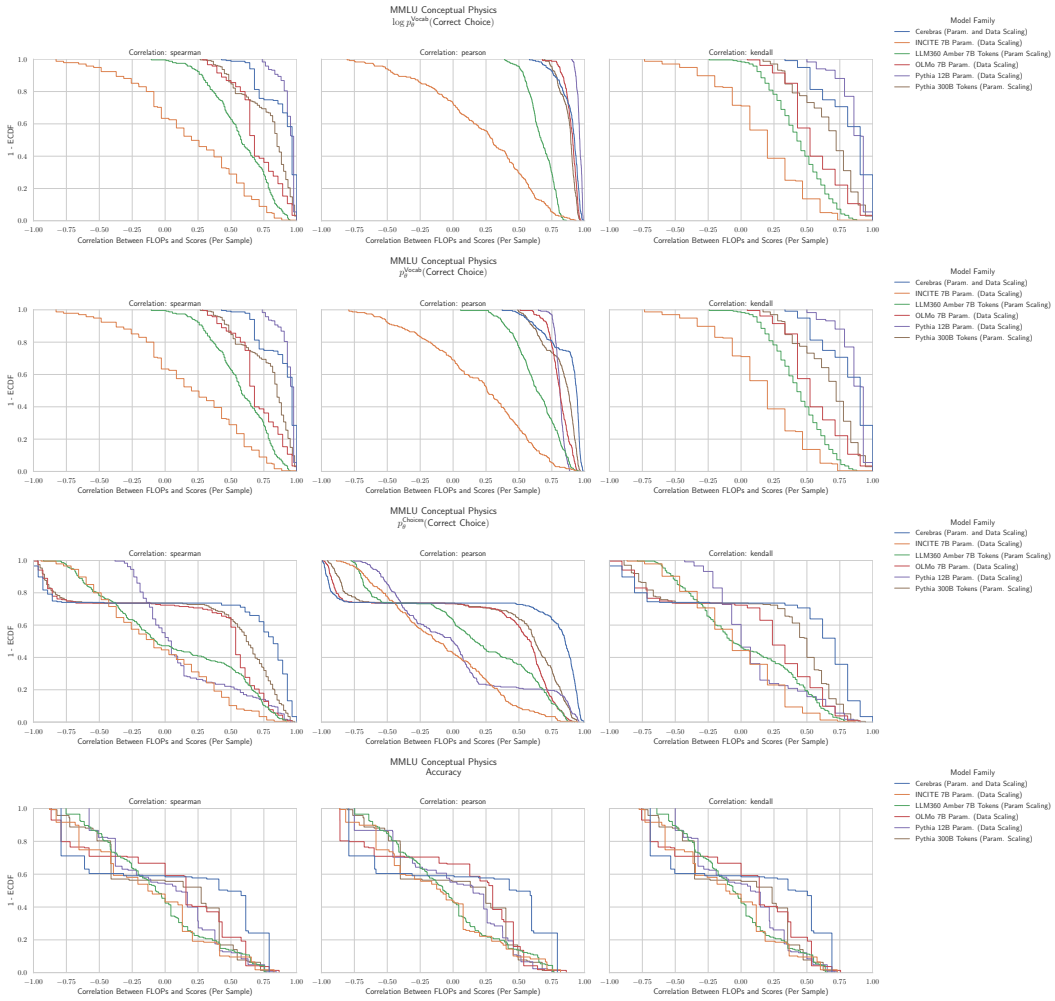

Figure 27: **MMLU Conceptual Physics: Downstream performance is computed via a sequence of transformations that deteriorate correlations between scores and pretraining compute.**

G.19 NLP Benchmark: MMLU Econometrics [32]

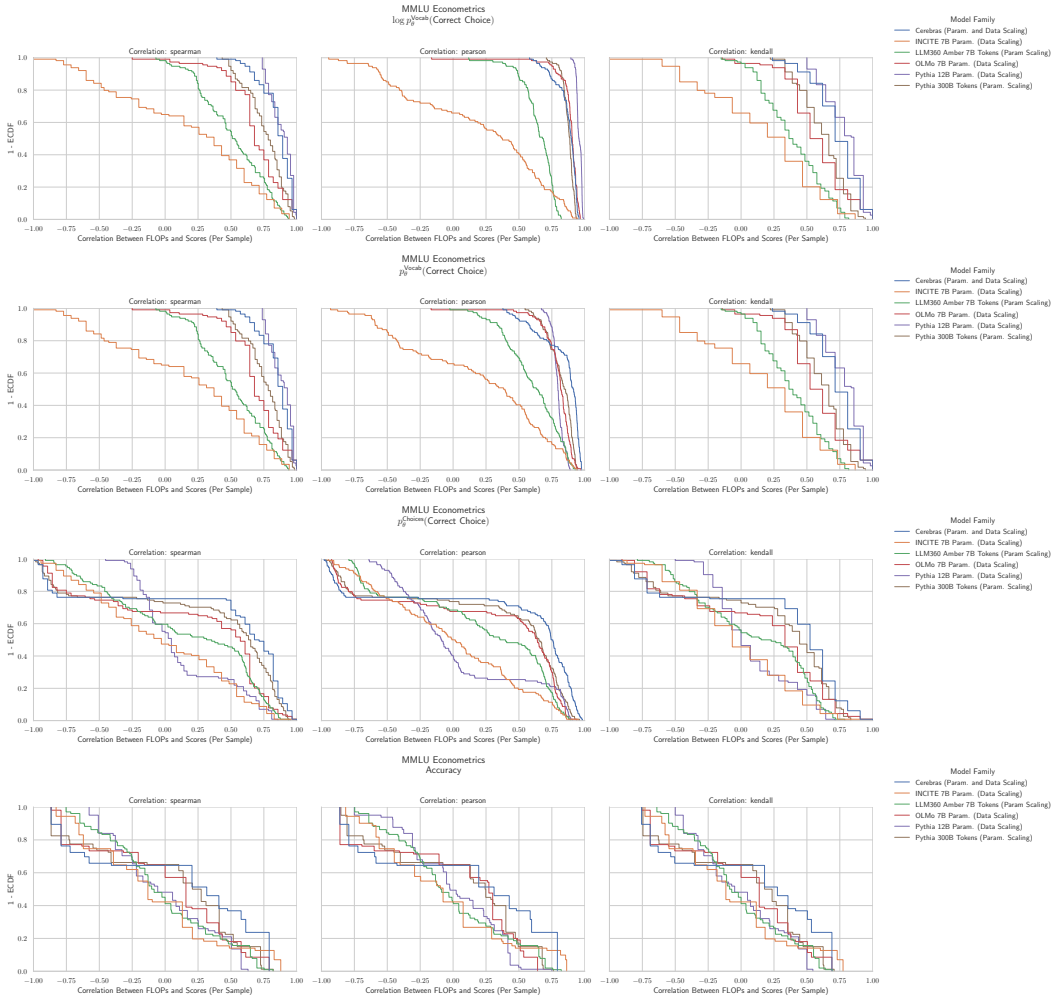

Figure 28: **MMLU Econometrics: Downstream performance is computed via a sequence of transformations that deteriorate correlations between scores and pretraining compute.**

G.20 NLP Benchmark: MMLU Electrical Engineering [32]

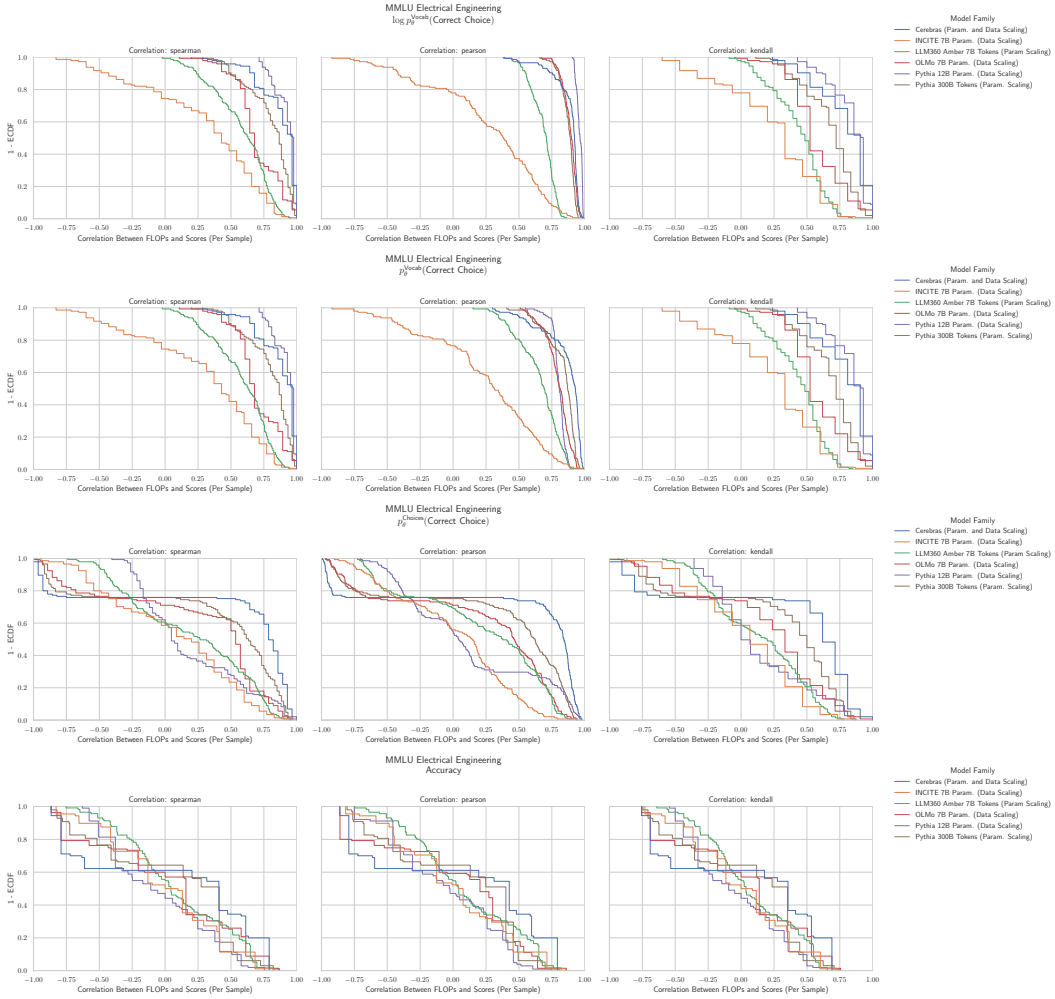

Figure 29: **MMLU Electrical Engineering: Downstream performance is computed via a sequence of transformations that deteriorate correlations between scores and pretraining compute.**

G.21 NLP Benchmark: MMLU Elementary Mathematics [32]

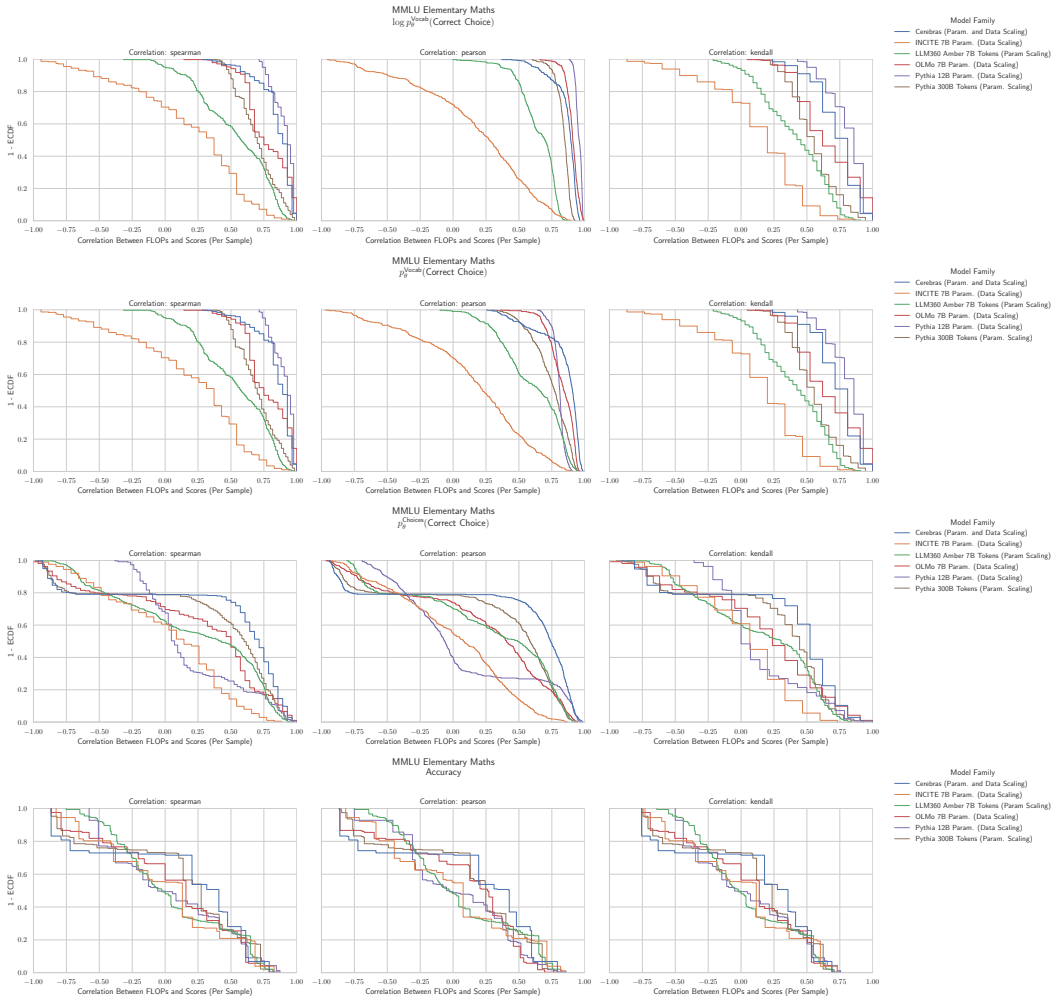

Figure 30: **MMLU Elementary Mathematics: Downstream performance is computed via a sequence of transformations that deteriorate correlations between scores and pretraining compute.**

G.22 NLP Benchmark: MMLU Formal Logic [32]

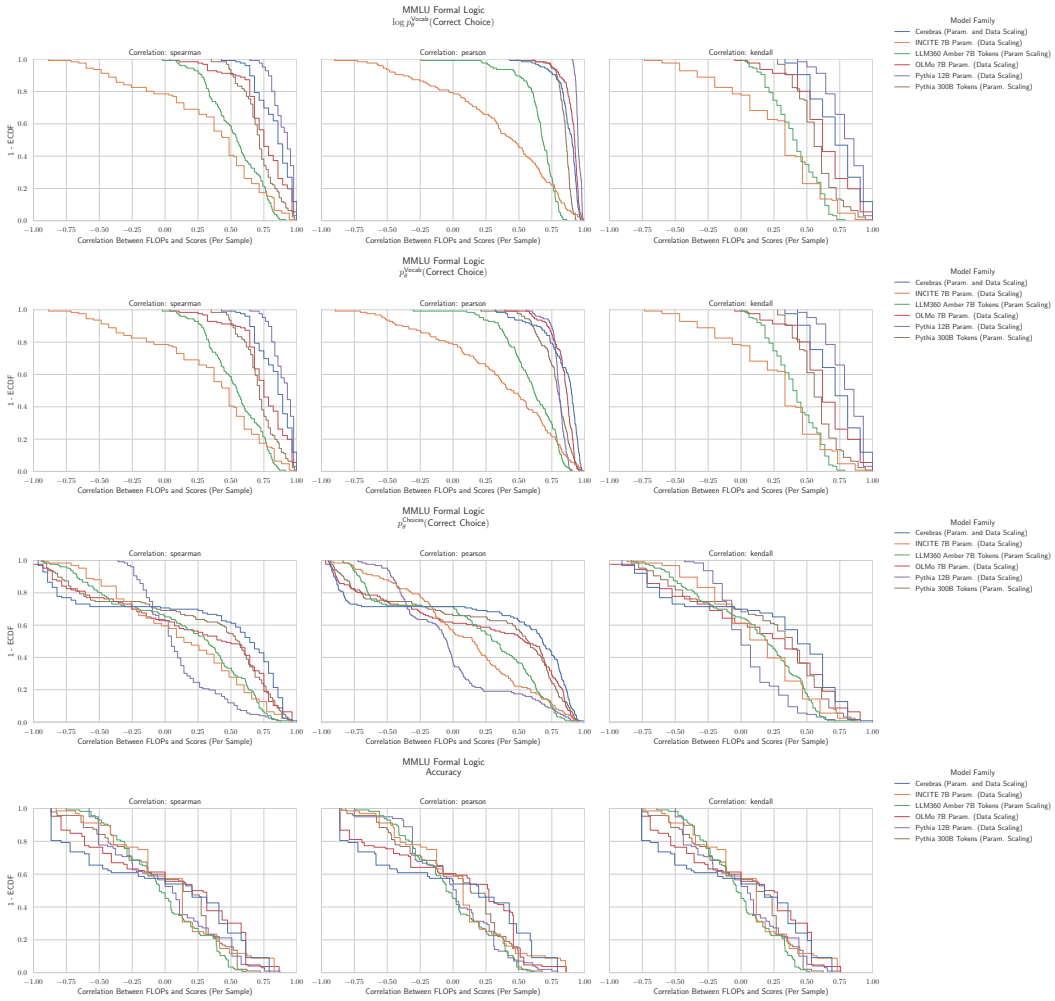

Figure 31: **MMLU Formal Logic: Downstream performance is computed via a sequence of transformations that deteriorate correlations between scores and pretraining compute.**

G.23 NLP Benchmark: MMLU Global Facts [32]

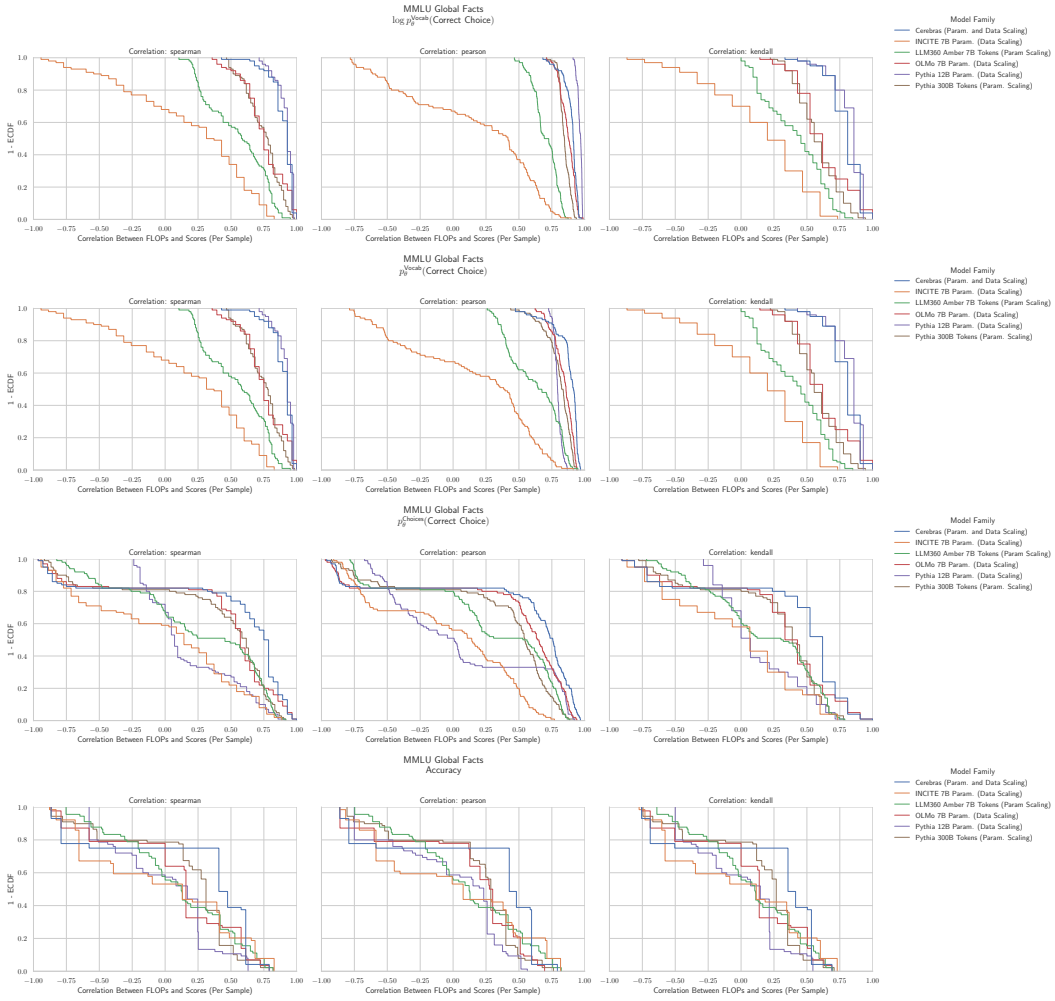

Figure 32: **MMLU Global Facts: Downstream performance is computed via a sequence of transformations that deteriorate correlations between scores and pretraining compute.**

G.24 NLP Benchmark: MMLU High School Biology [32]

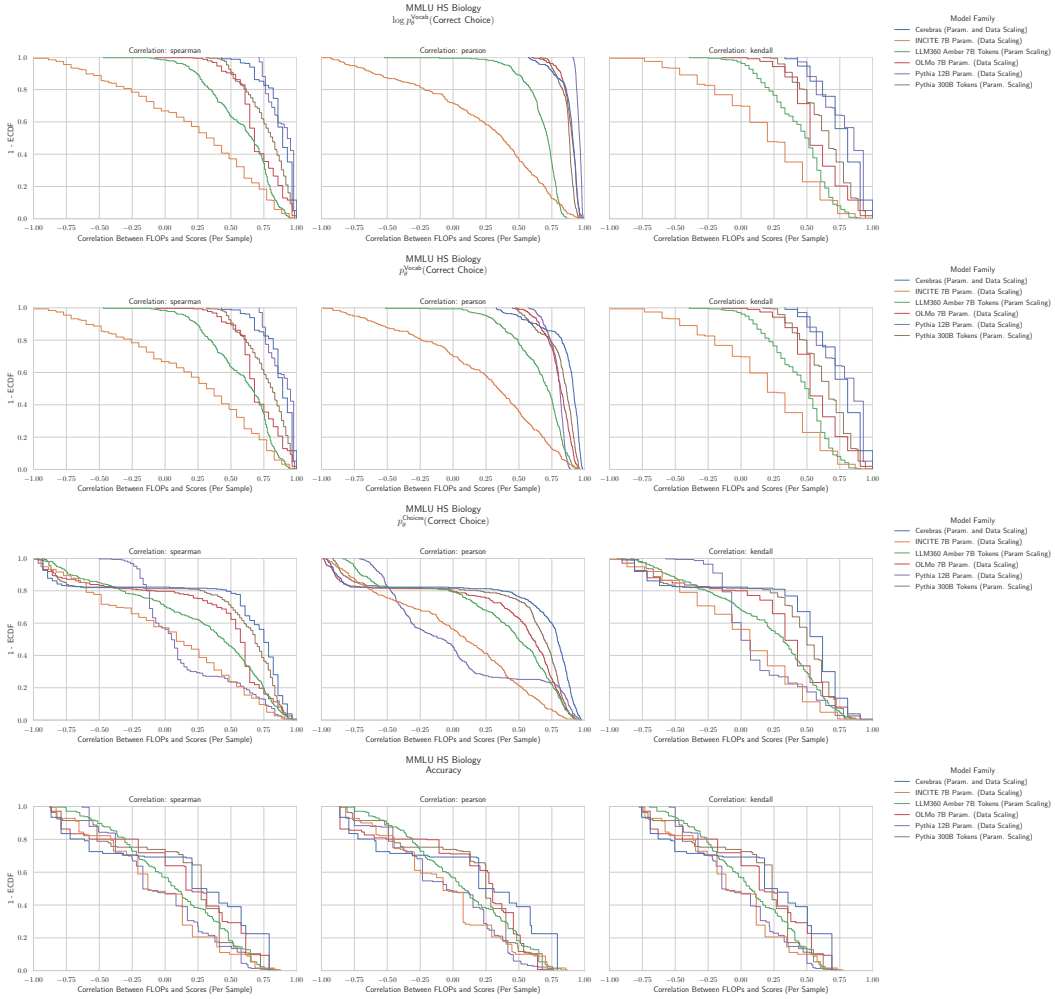

Figure 33: **MMLU High School Biology: Downstream performance is computed via a sequence of transformations that deteriorate correlations between scores and pretraining compute.**

G.25 NLP Benchmark: MMLU High School Chemistry [32]

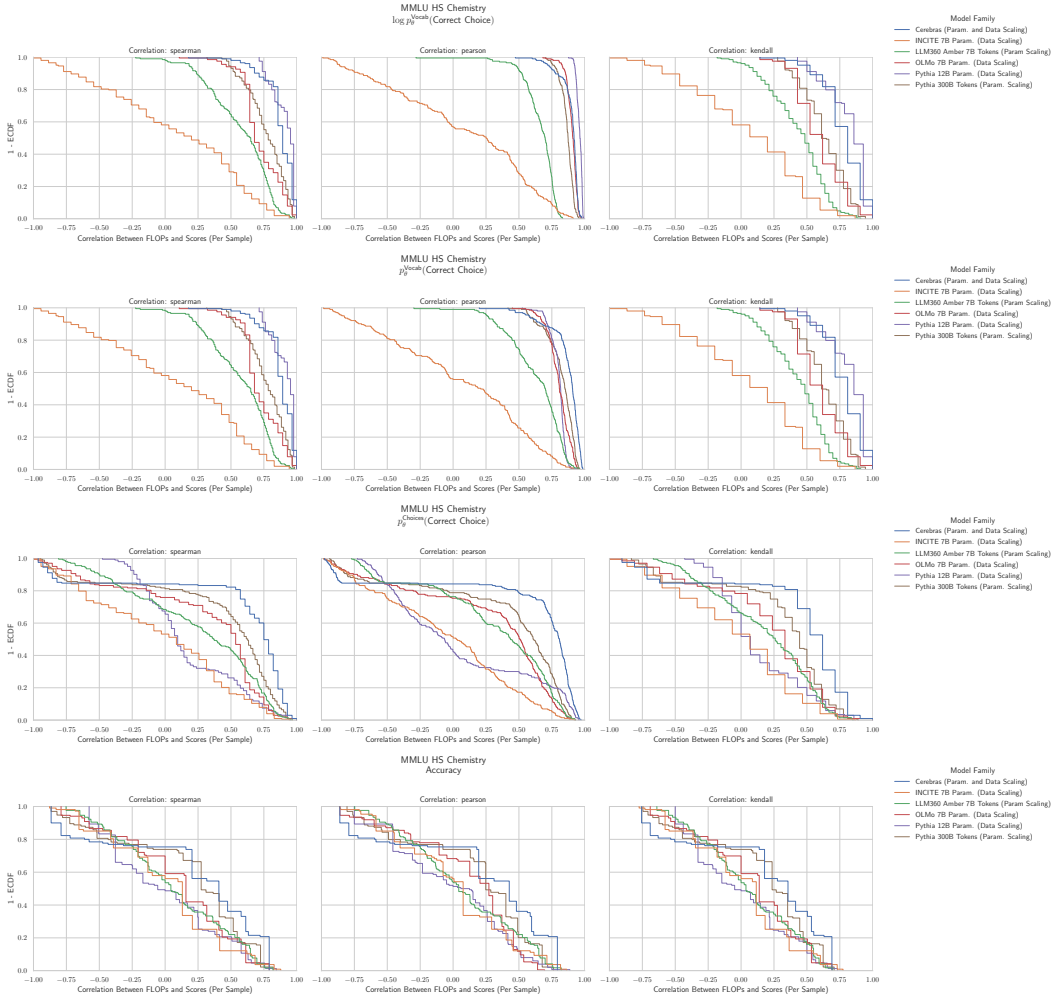

Figure 34: **MMLU High School Chemistry: Downstream performance is computed via a sequence of transformations that deteriorate correlations between scores and pretraining compute.**

G.26 NLP Benchmark: MMLU High School Computer Science [32]

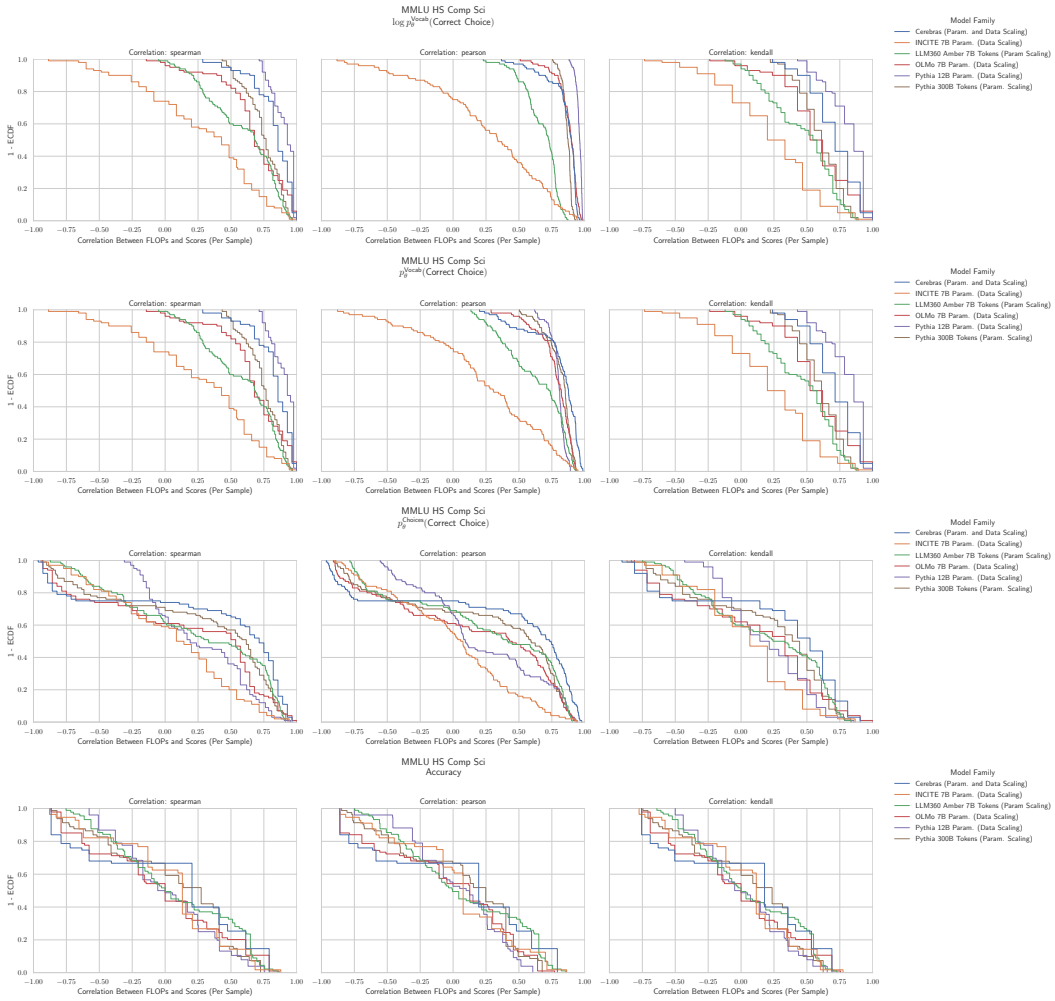

Figure 35: **MMLU High School Computer Science: Downstream performance is computed via a sequence of transformations that deteriorate correlations between scores and pretraining compute.**

G.27 NLP Benchmark: MMLU High School Chemistry [32]

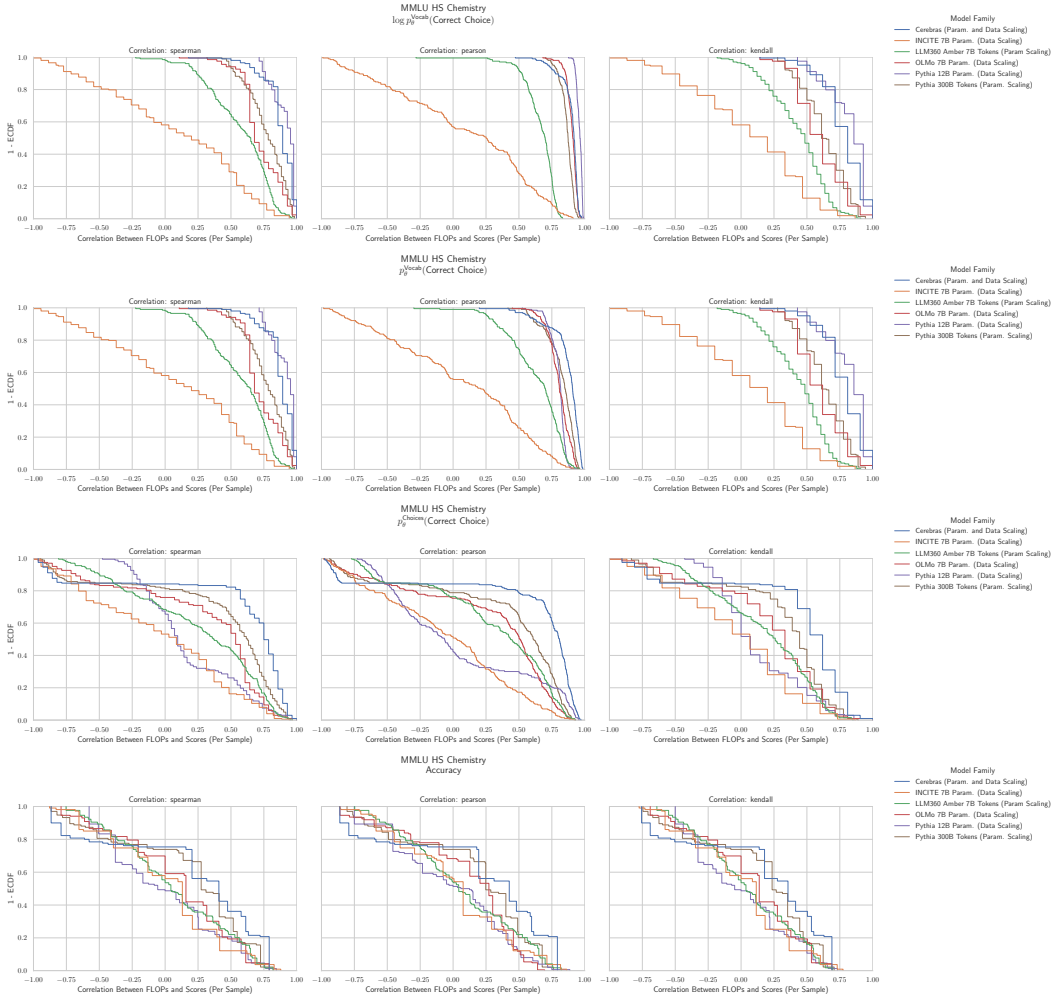

Figure 36: **MMLU High School Chemistry: Downstream performance is computed via a sequence of transformations that deteriorate correlations between scores and pretraining compute.**

G.28 NLP Benchmark: MMLU High School European History [32]

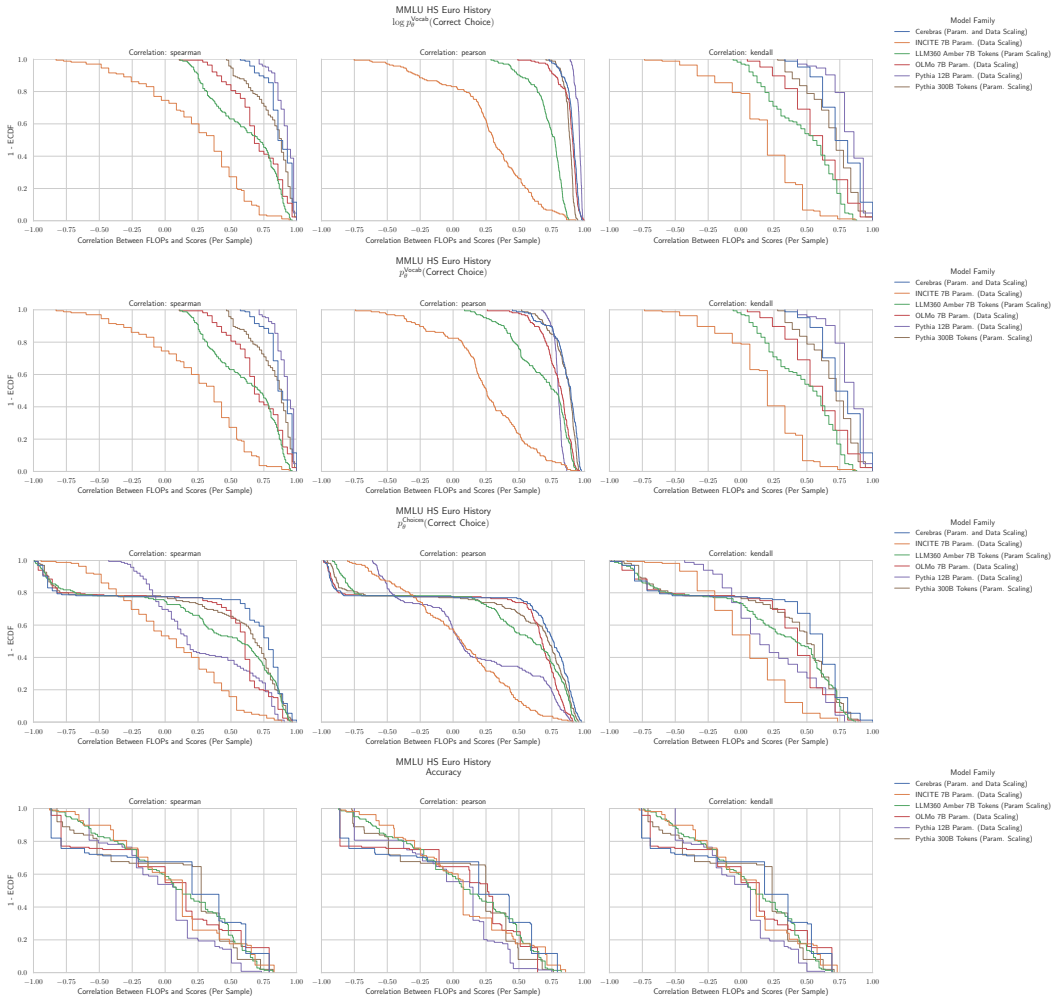

Figure 37: **MMLU High School European History: Downstream performance is computed via a sequence of transformations that deteriorate correlations between scores and pretraining compute.**

G.29 NLP Benchmark: MMLU High School Geography [32]

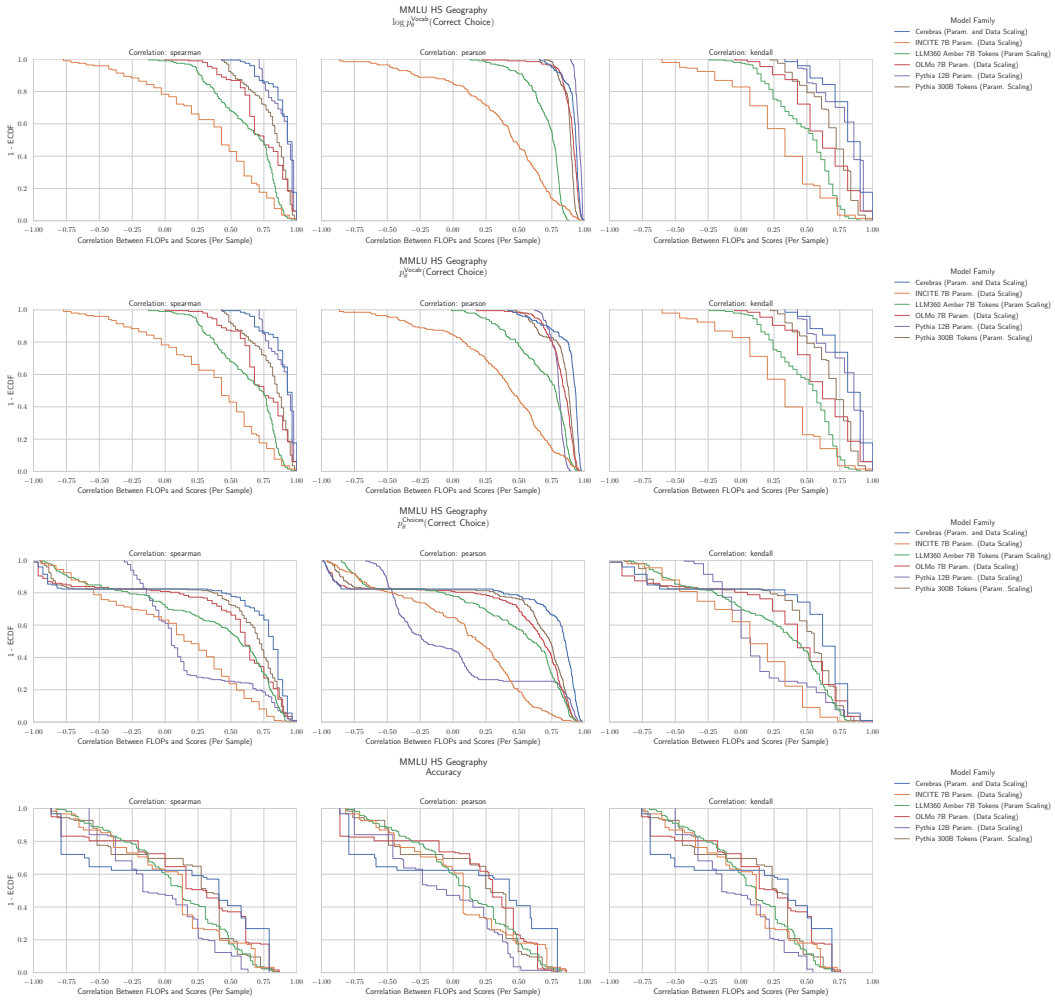

Figure 38: **MMLU High School Geography: Downstream performance is computed via a sequence of transformations that deteriorate correlations between scores and pretraining compute.**

G.30 NLP Benchmark: MMLU High School Government & Politics [32]

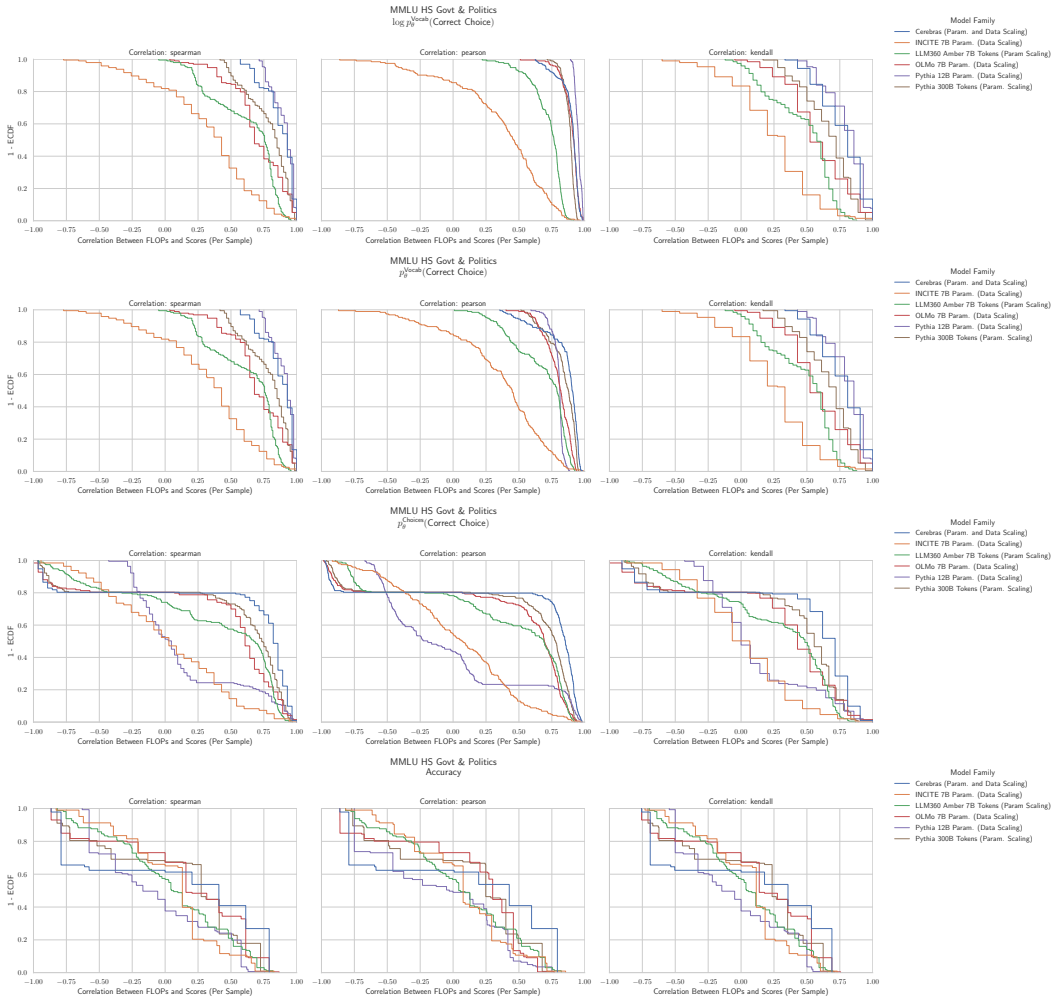

Figure 39: **MMLU High School Government & Politics: Downstream performance is computed via a sequence of transformations that deteriorate correlations between scores and pretraining compute.**

G.31 NLP Benchmark: MMLU High School Macroeconomics [32]

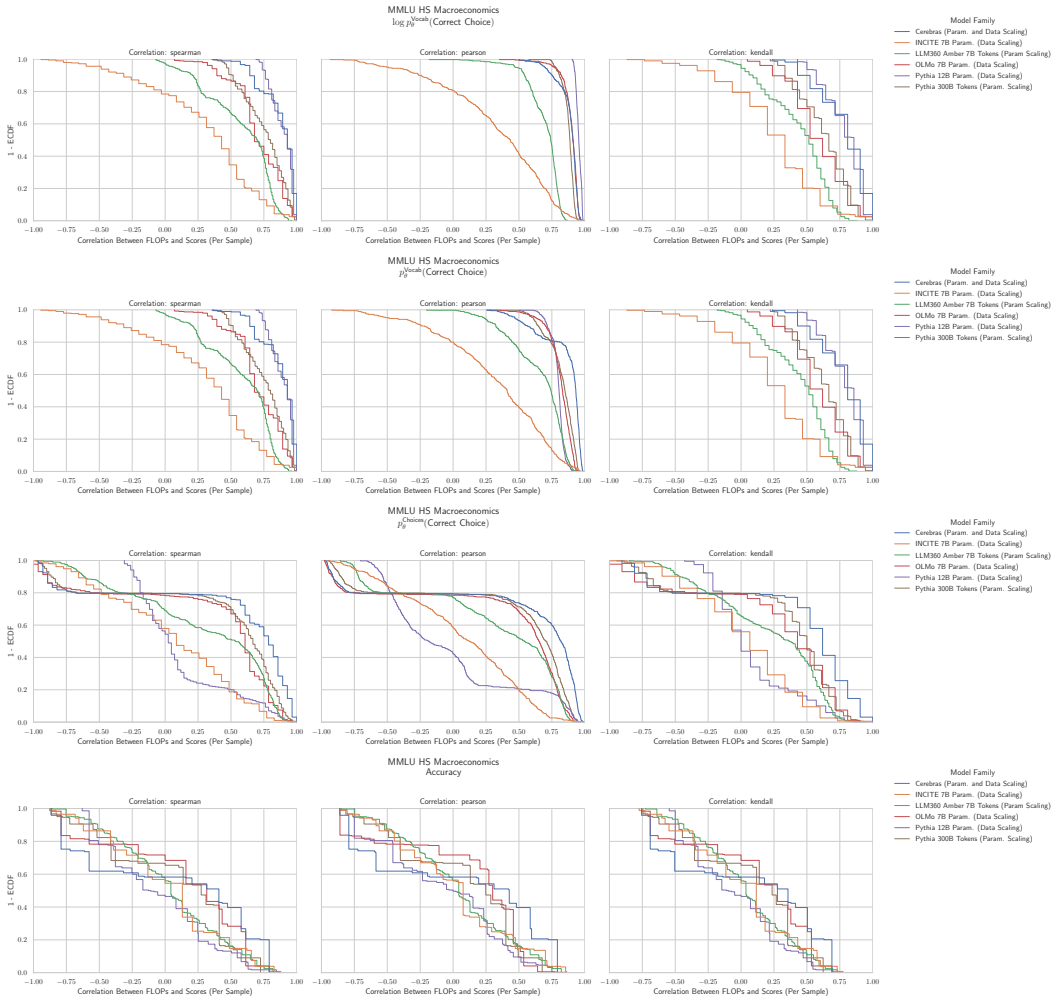

Figure 40: **MMLU High School Macroeconomics: Downstream performance is computed via a sequence of transformations that deteriorate correlations between scores and pretraining compute.**

G.32 NLP Benchmark: MMLU High School Mathematics [32]

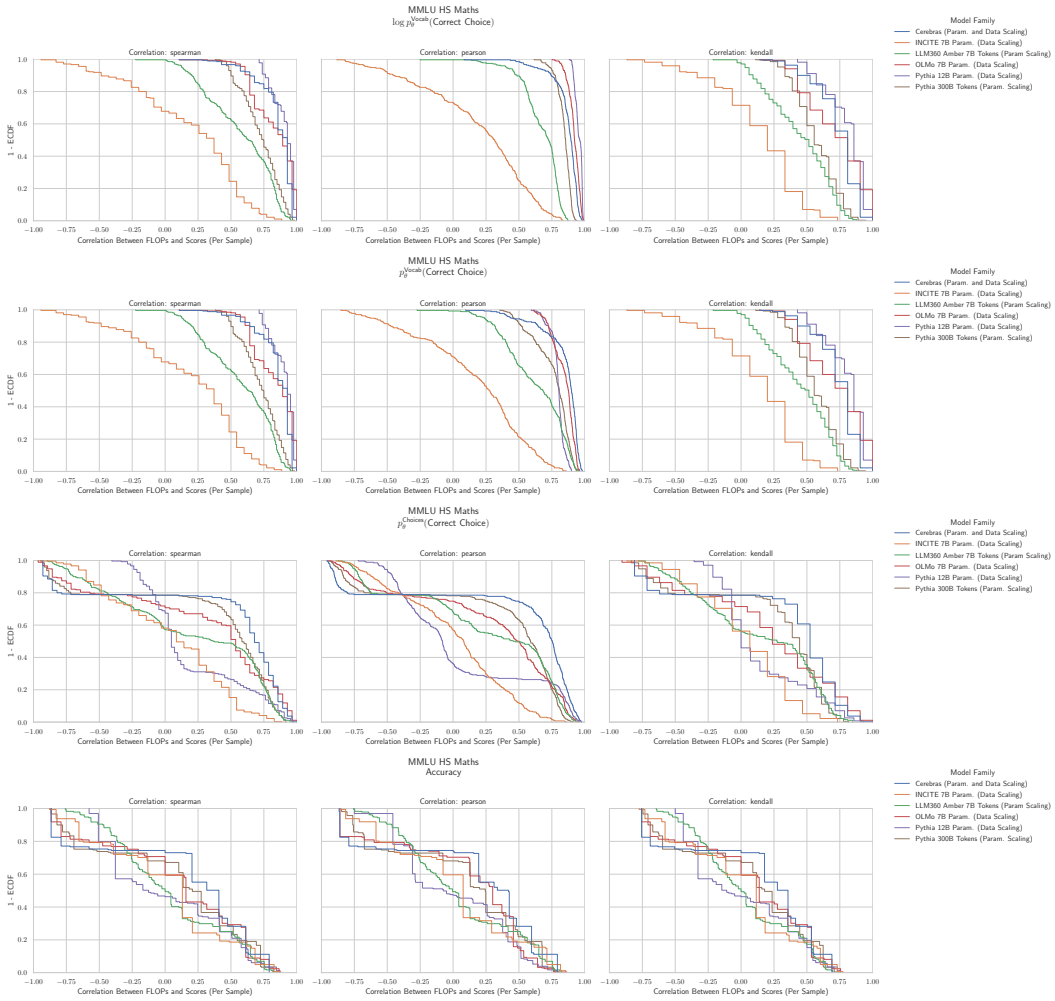

Figure 41: **MMLU High School Mathematics: Downstream performance is computed via a sequence of transformations that deteriorate correlations between scores and pretraining compute.**

G.33 NLP Benchmark: MMLU High School Microeconomics [32]

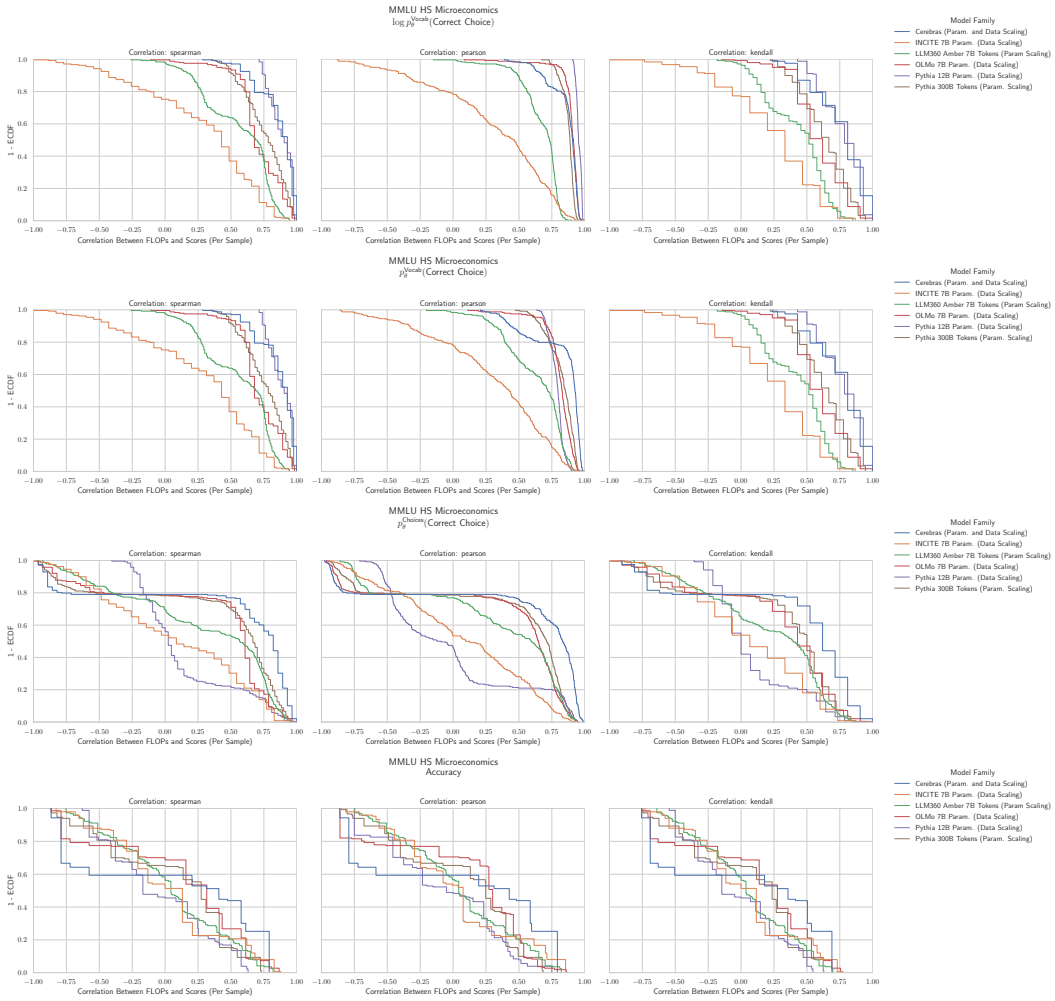

Figure 42: **MMLU High School Microeconomics: Downstream performance is computed via a sequence of transformations that deteriorate correlations between scores and pretraining compute.**

G.34 NLP Benchmark: MMLU High School Physics [32]

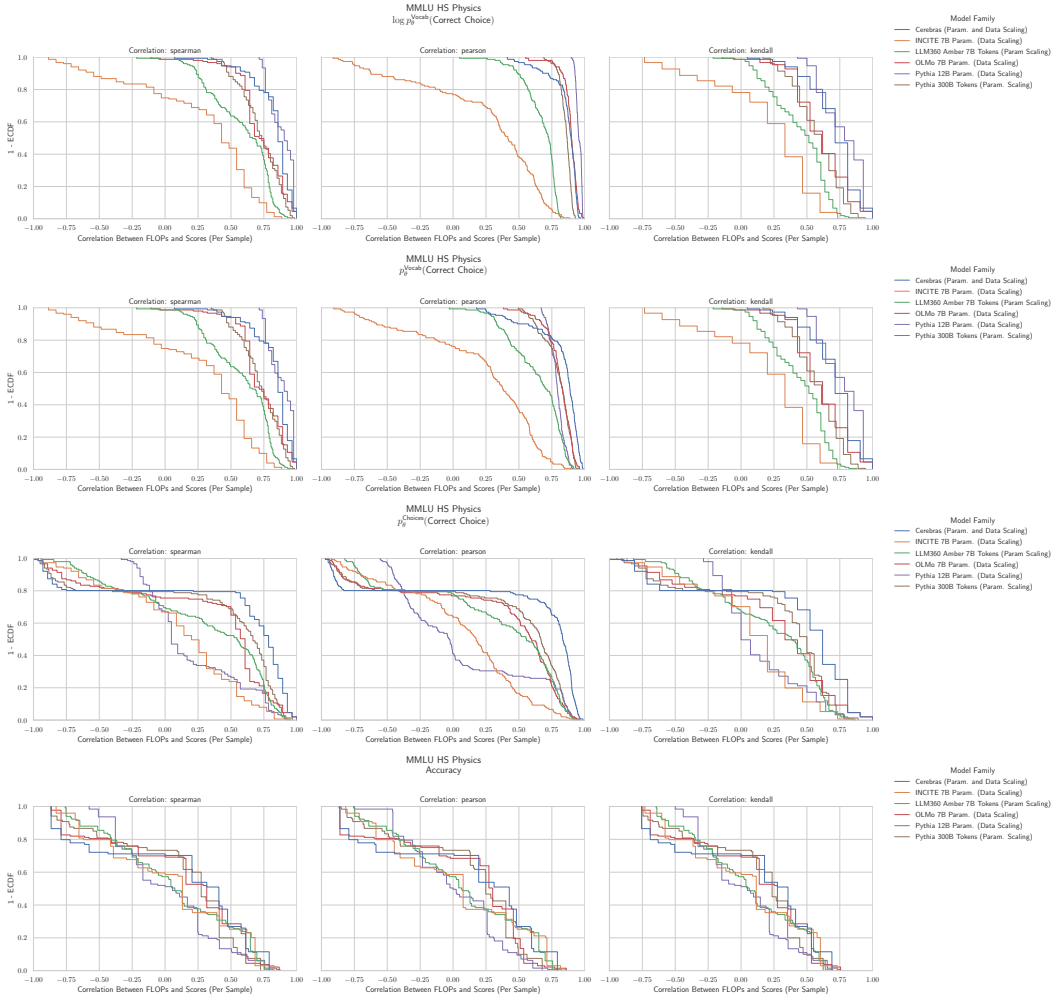

Figure 43: **MMLU High School Physics: Downstream performance is computed via a sequence of transformations that deteriorate correlations between scores and pretraining compute.**

G.35 NLP Benchmark: MMLU High School Psychology [32]

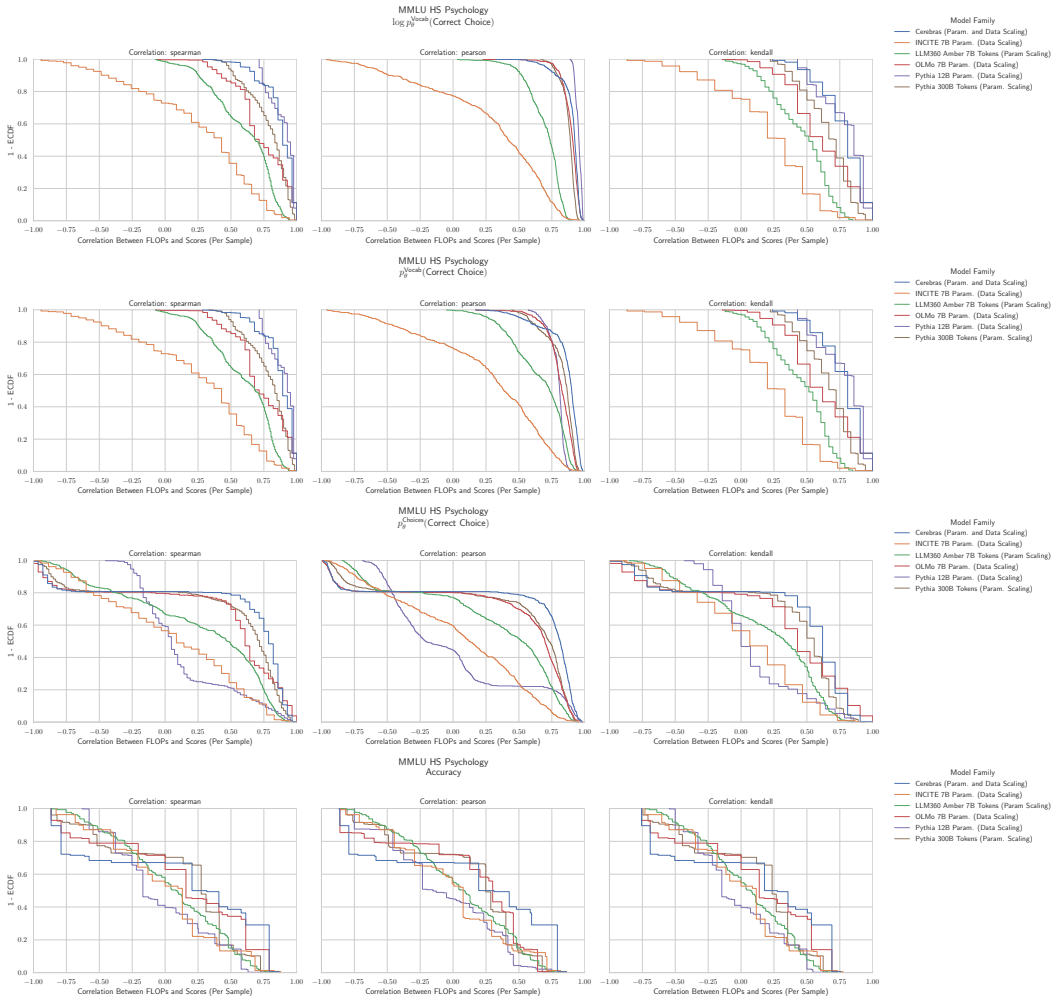

Figure 44: **MMLU High School Psychology: Downstream performance is computed via a sequence of transformations that deteriorate correlations between scores and pretraining compute.**

G.36 NLP Benchmark: MMLU High School Statistics [32]

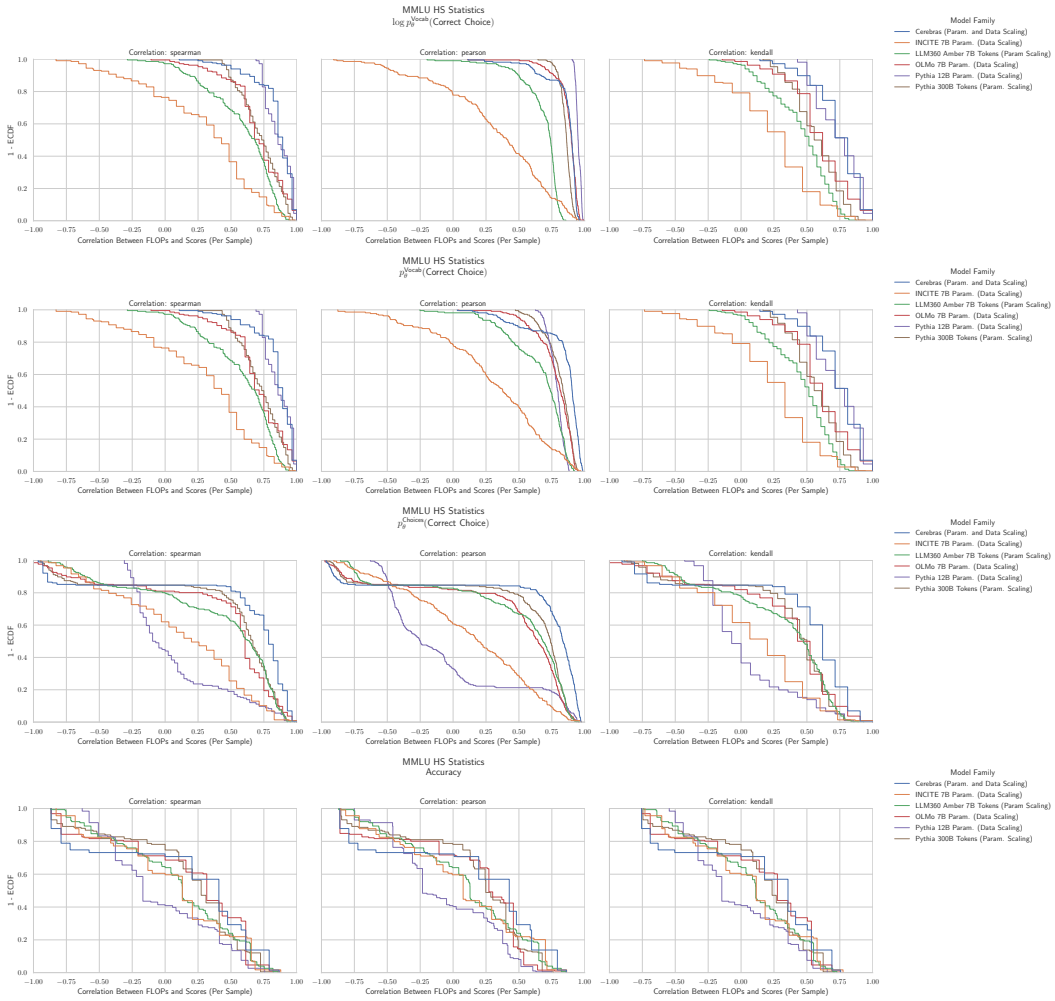

Figure 45: **MMLU High School Statistics: Downstream performance is computed via a sequence of transformations that deteriorate correlations between scores and pretraining compute.**

G.37 NLP Benchmark: MMLU High School US History [32]

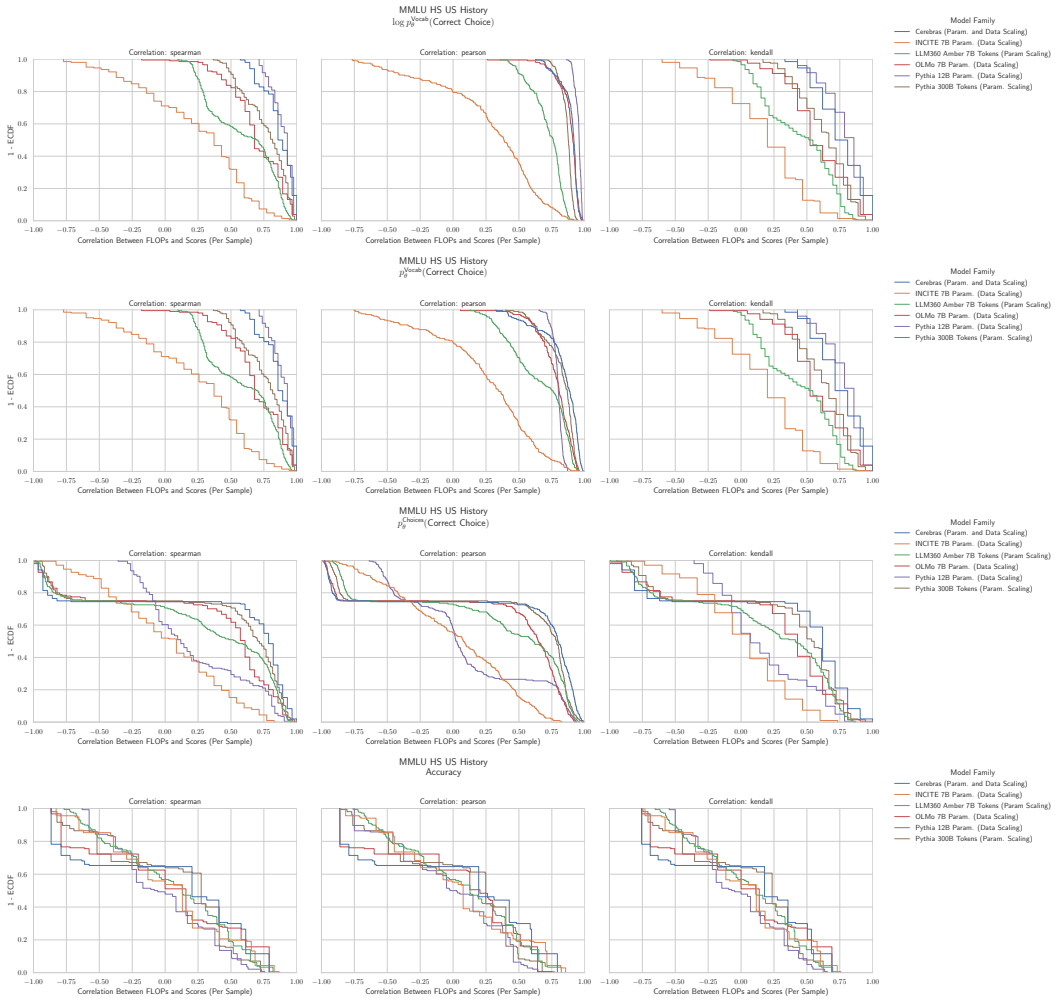

Figure 46: **MMLU High School US History: Downstream performance is computed via a sequence of transformations that deteriorate correlations between scores and pretraining compute.**

G.38 NLP Benchmark: MMLU High School World History [32]

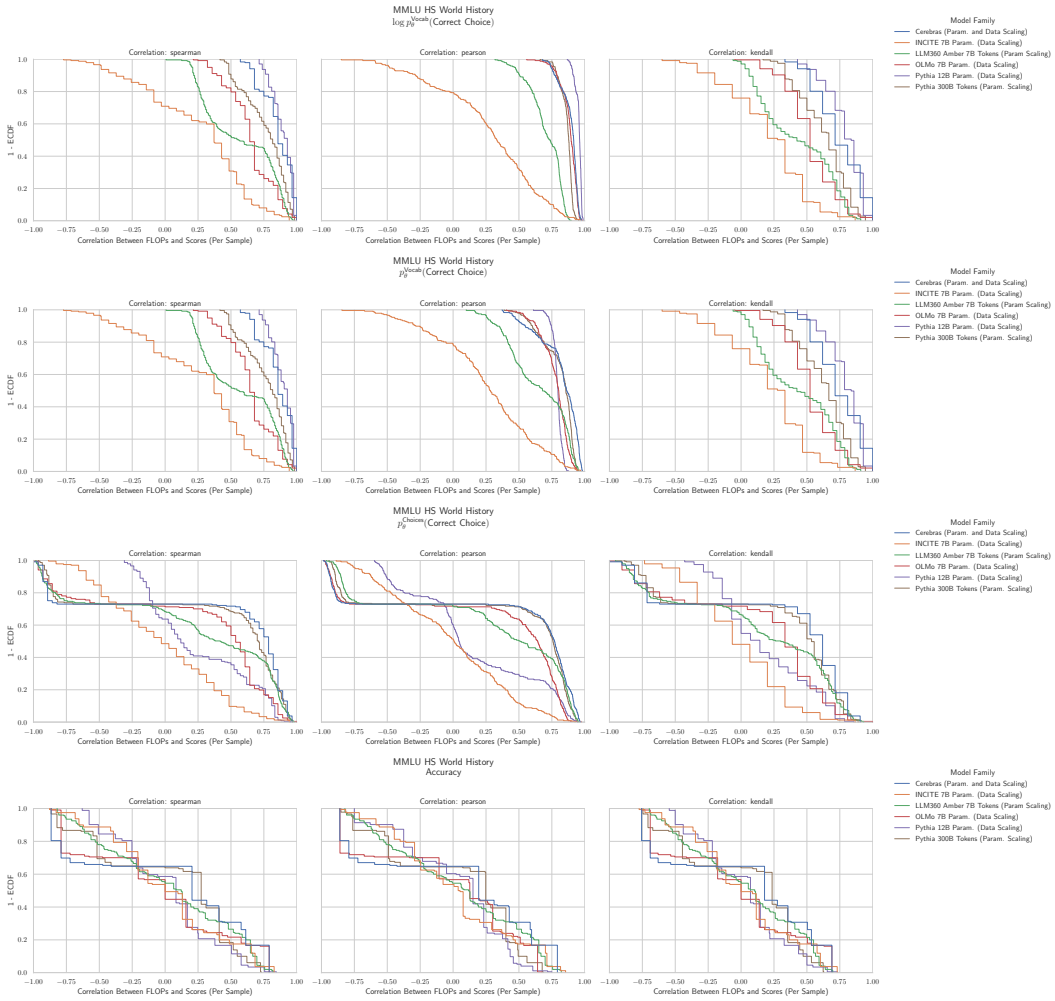

Figure 47: **MMLU High School World History: Downstream performance is computed via a sequence of transformations that deteriorate correlations between scores and pretraining compute.**

G.39 NLP Benchmark: MMLU Human Aging [32]

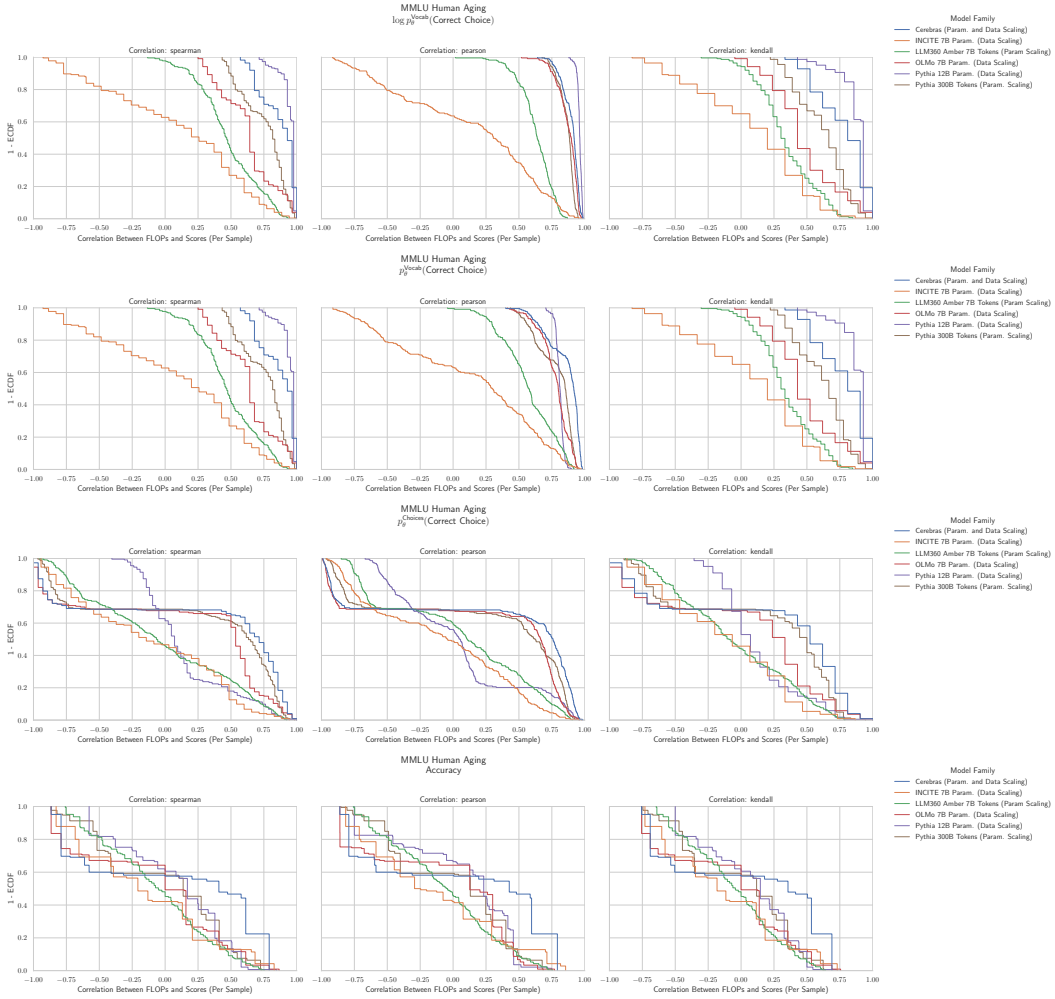

Figure 48: **MMLU Human Aging: Downstream performance is computed via a sequence of transformations that deteriorate correlations between scores and pretraining compute.**

G.40 NLP Benchmark: MMLU Human Sexuality [32]

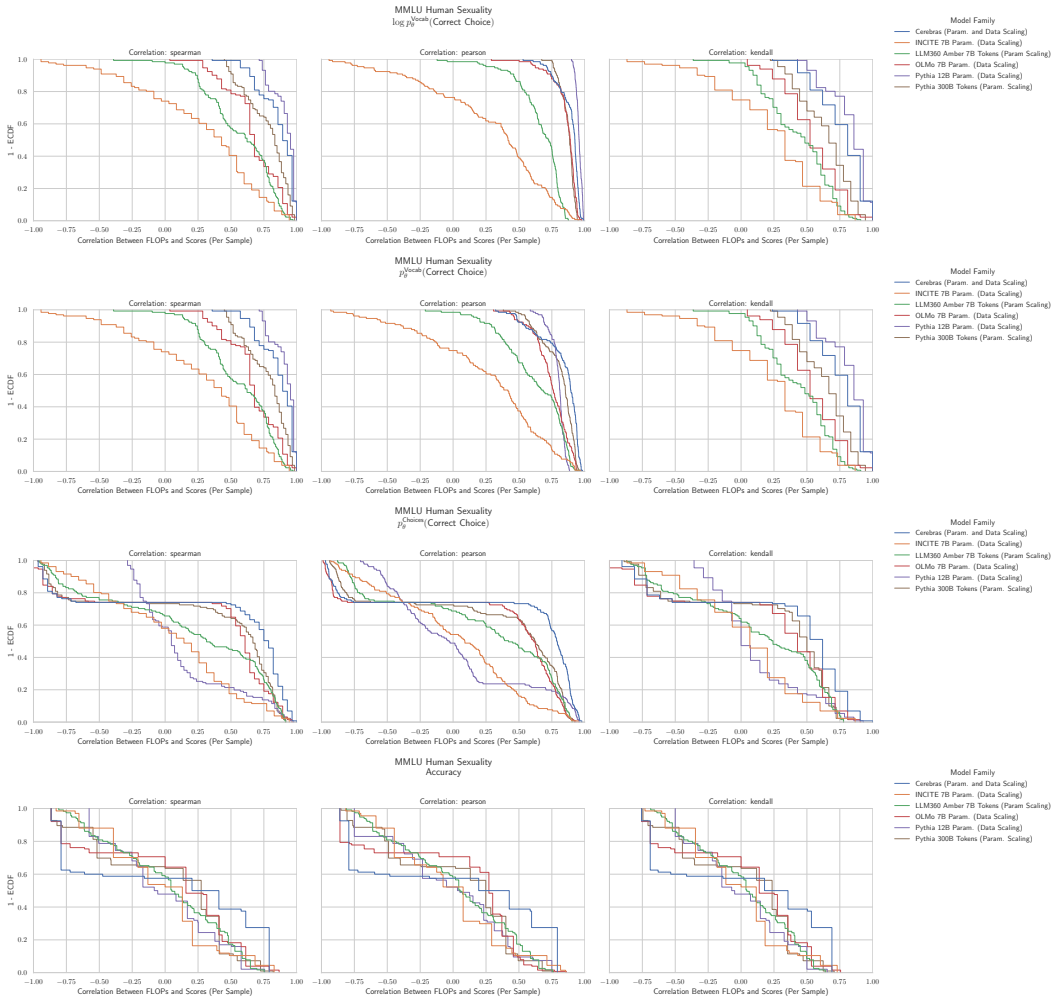

Figure 49: **MMLU Human Sexuality: Downstream performance is computed via a sequence of transformations that deteriorate correlations between scores and pretraining compute.**

G.41 NLP Benchmark: MMLU International Law [32]

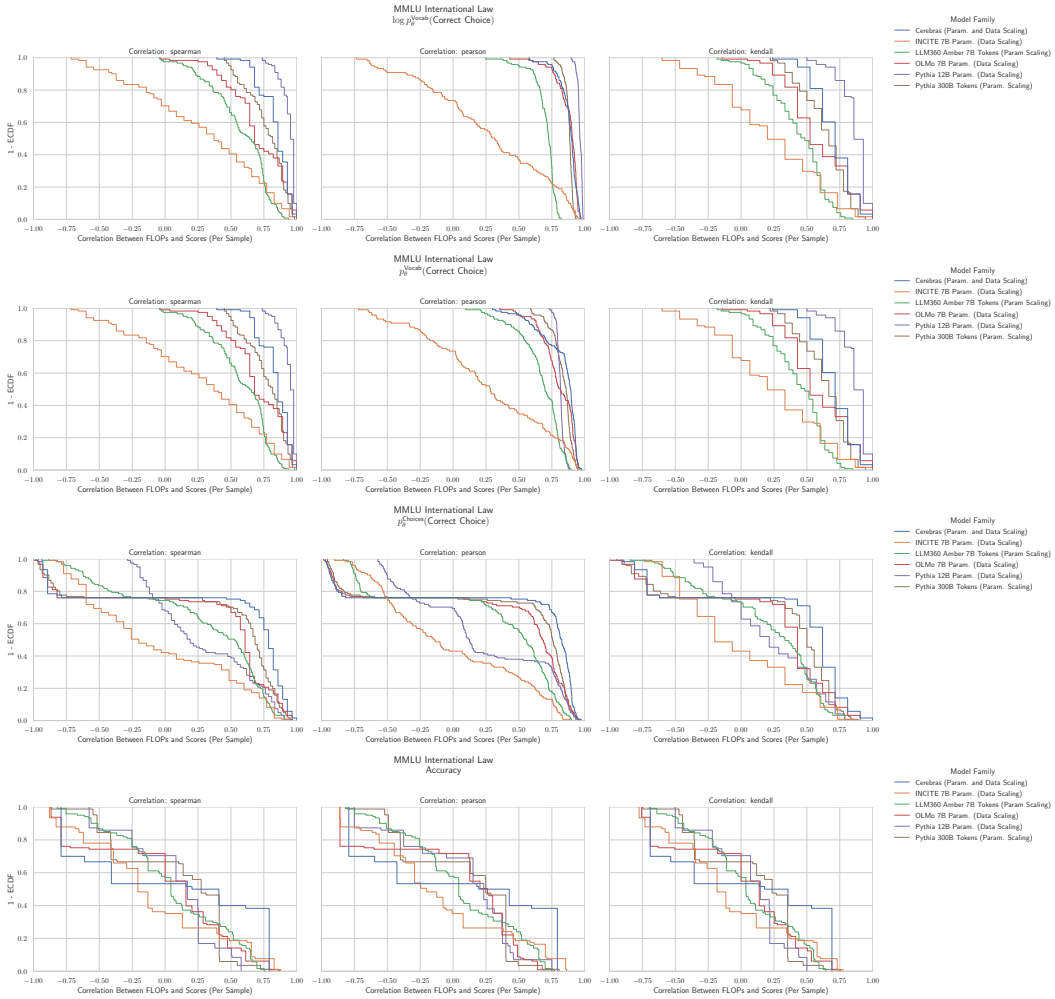

Figure 50: **MMLU International Law: Downstream performance is computed via a sequence of transformations that deteriorate correlations between scores and pretraining compute.**

G.42 NLP Benchmark: MMLU Jurisprudence [32]

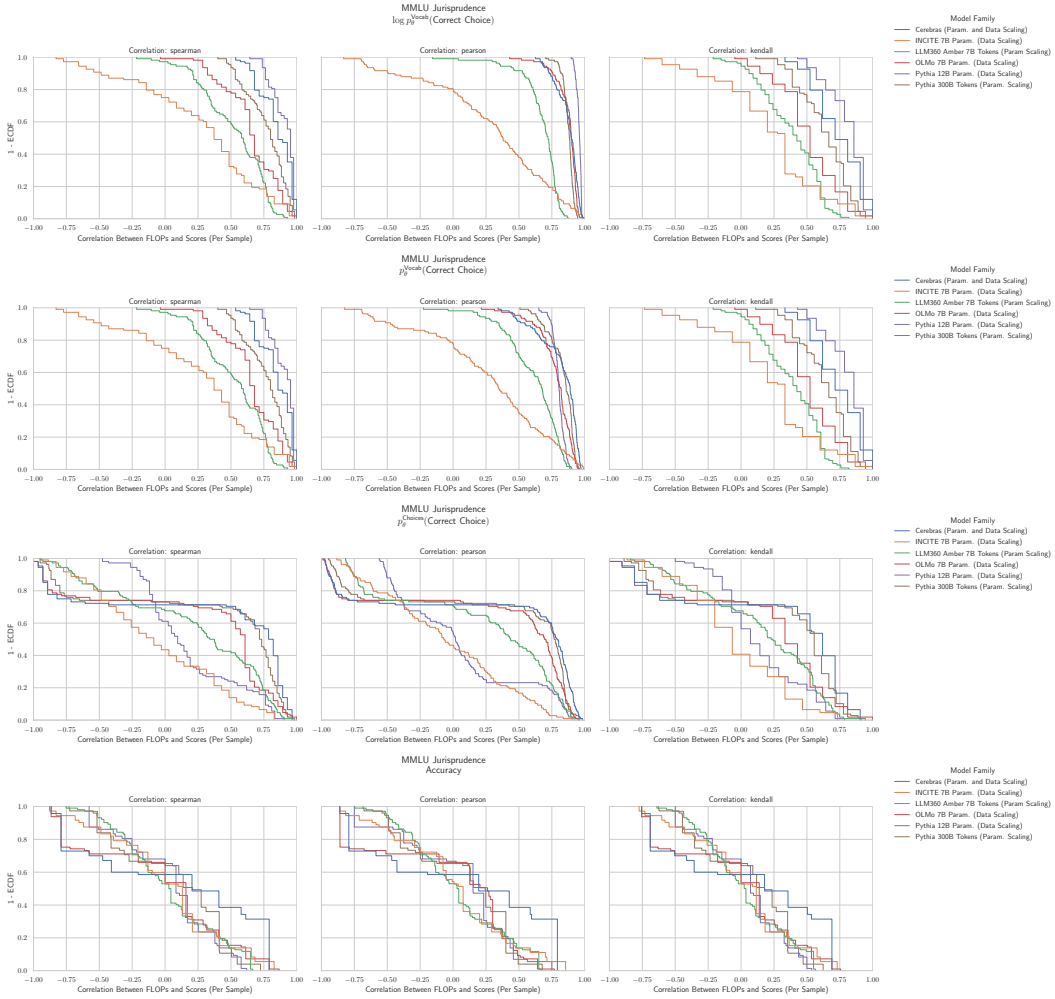

Figure 51: **MMLU Jurisprudence: Downstream performance is computed via a sequence of transformations that deteriorate correlations between scores and pretraining compute.**

G.43 NLP Benchmark: MMLU Logical Fallacies [32]

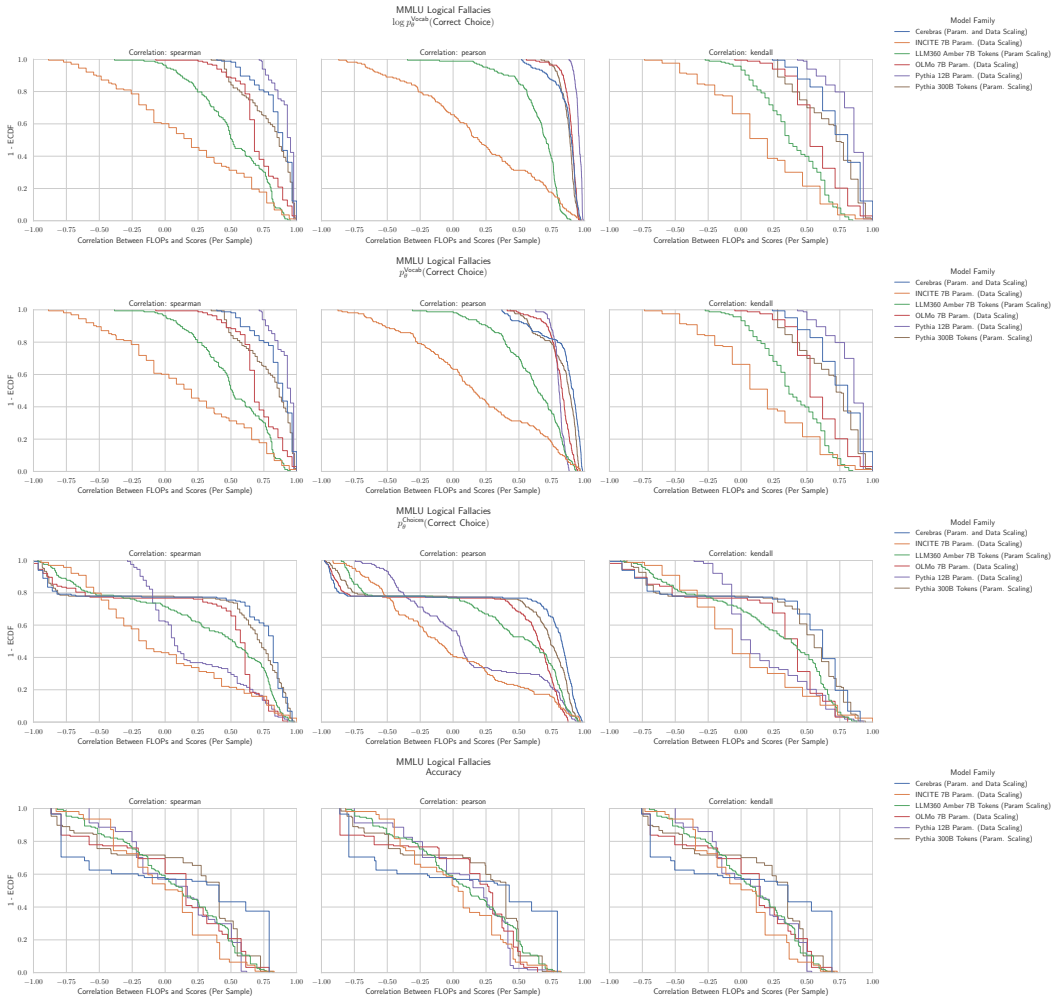

Figure 52: **MMLU Logical Fallacies: Downstream performance is computed via a sequence of transformations that deteriorate correlations between scores and pretraining compute.**

G.44 NLP Benchmark: MMLU Machine Learning [32]

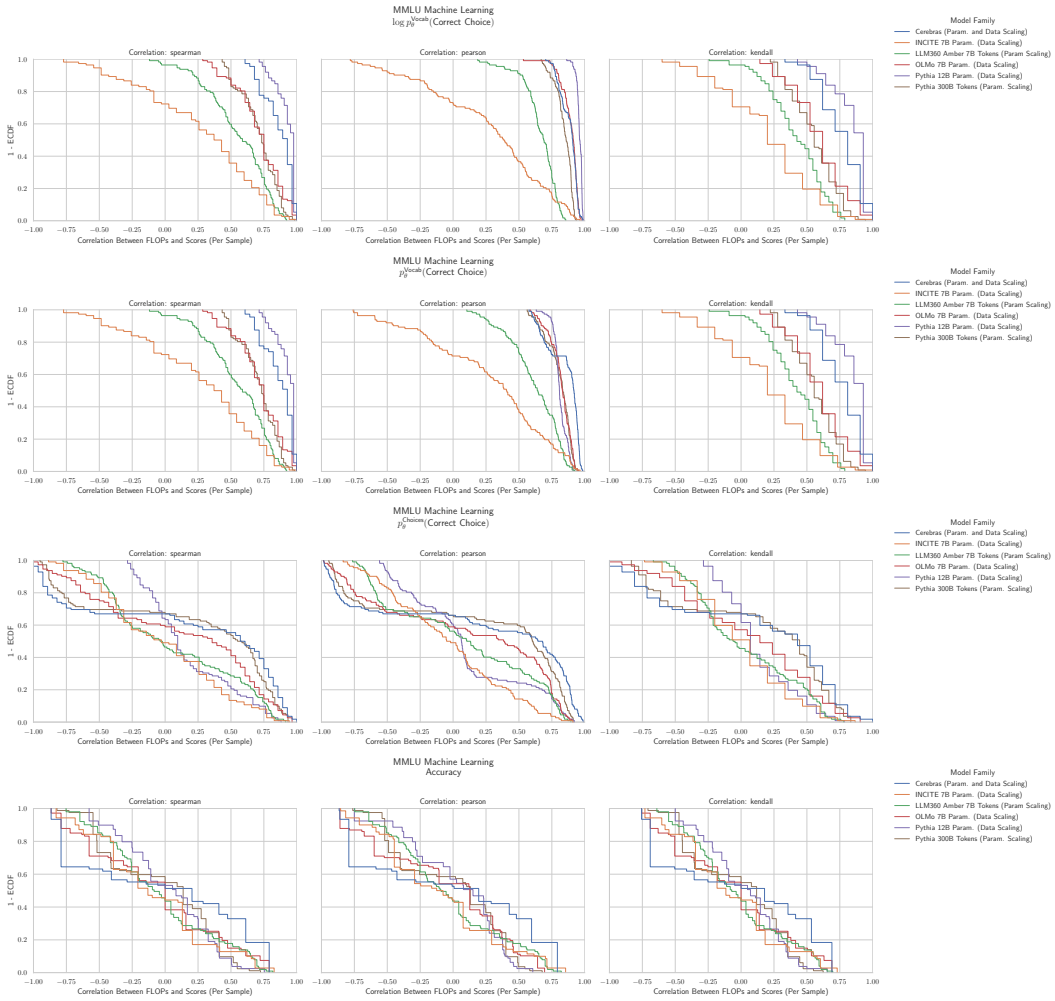

Figure 53: **MMLU Machine Learning: Downstream performance is computed via a sequence of transformations that deteriorate correlations between scores and pretraining compute.**

G.45 NLP Benchmark: MMLU Management [32]

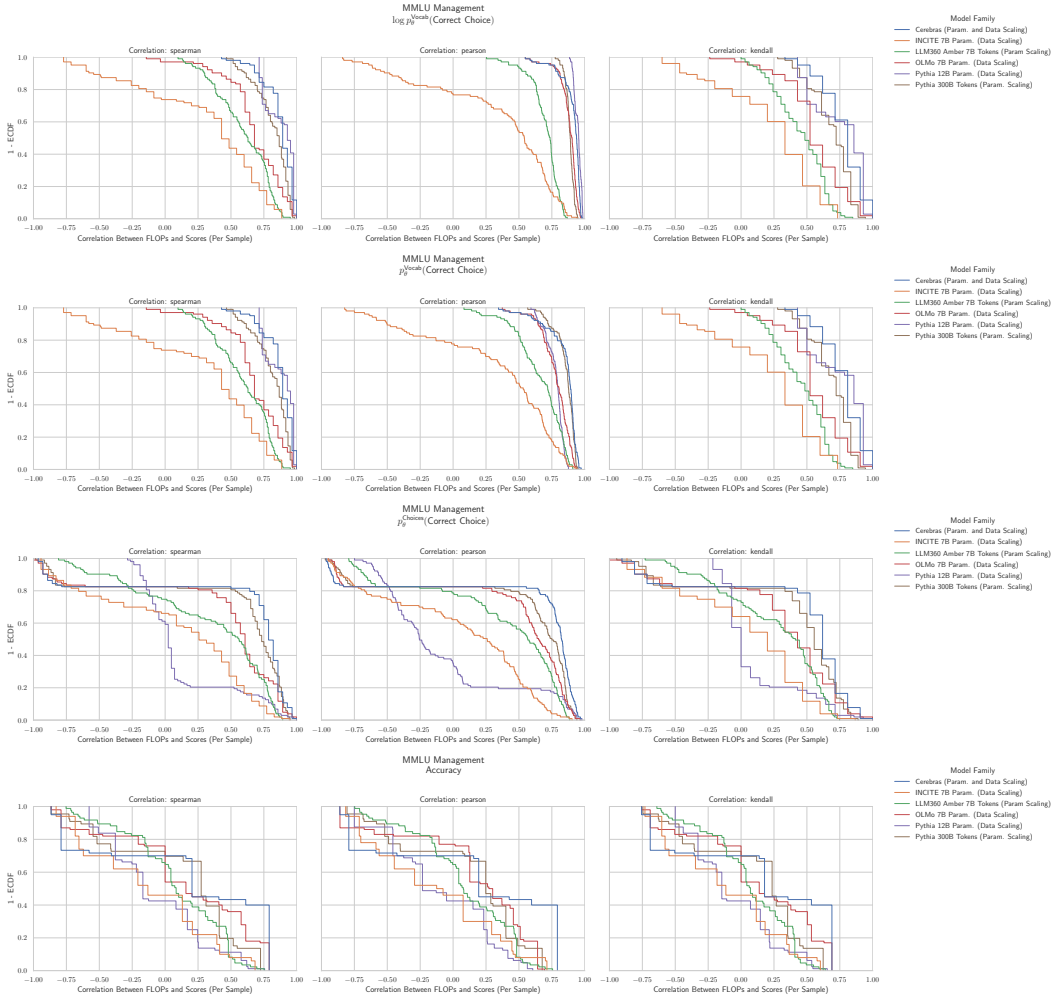

Figure 54: **MMLU Management: Downstream performance is computed via a sequence of transformations that deteriorate correlations between scores and pretraining compute.**

G.46 NLP Benchmark: MMLU Marketing [32]

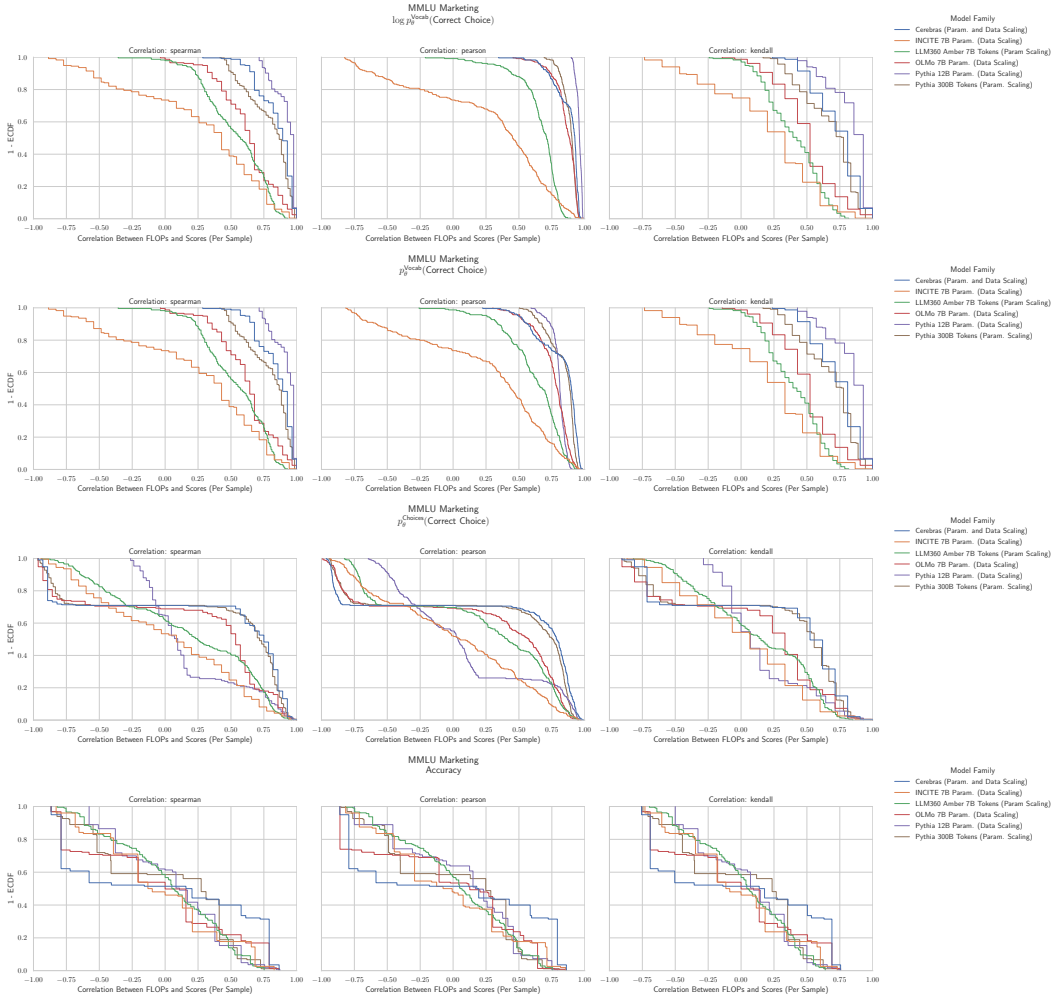

Figure 55: **MMLU Marketing: Downstream performance is computed via a sequence of transformations that deteriorate correlations between scores and pretraining compute.**

G.47 NLP Benchmark: MMLU Medical Genetics [32]

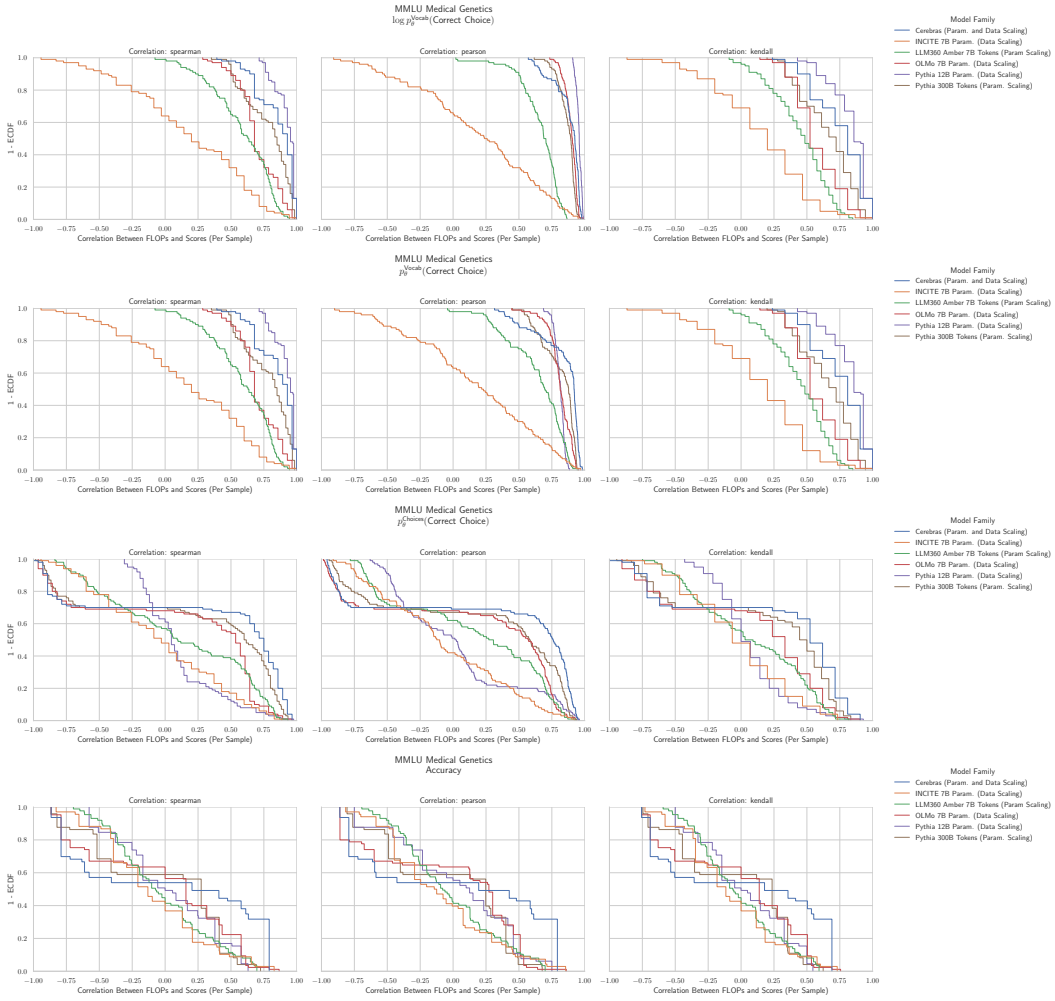

Figure 56: **MMLU Medical Genetics: Downstream performance is computed via a sequence of transformations that deteriorate correlations between scores and pretraining compute.**

G.48 NLP Benchmark: MMLU Miscellaneous [32]

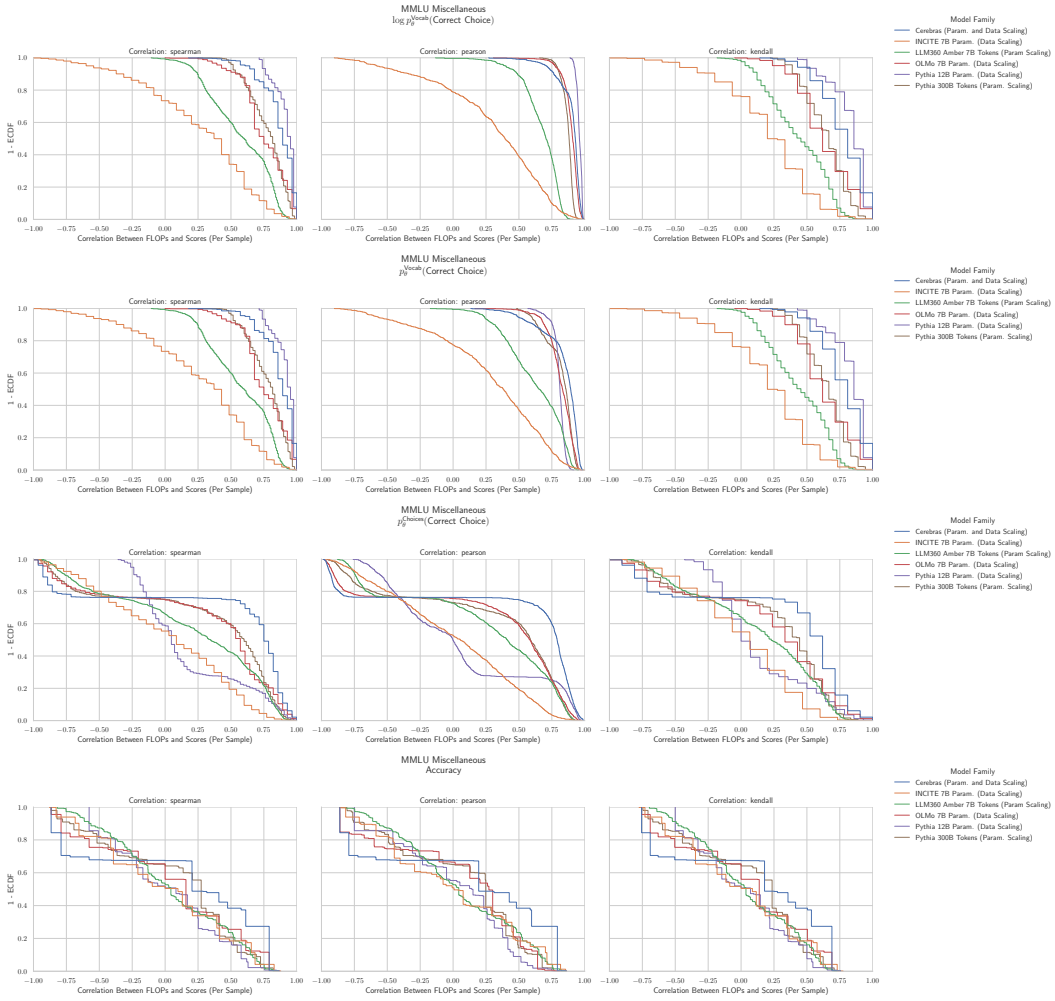

Figure 57: **MMLU Miscellaneous: Downstream performance is computed via a sequence of transformations that deteriorate correlations between scores and pretraining compute.**

G.49 NLP Benchmark: MMLU Moral Disputes [32]

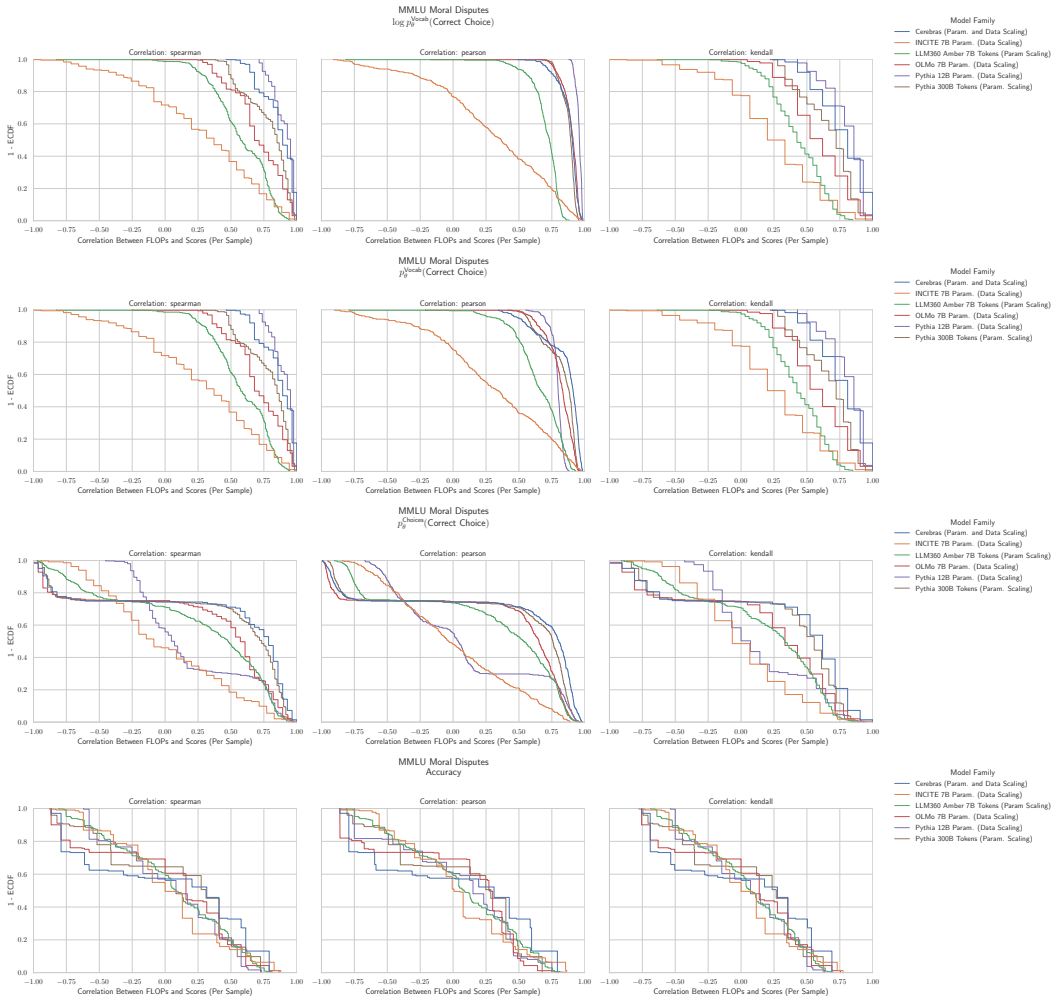

Figure 58: **MMLU Moral Disputes: Downstream performance is computed via a sequence of transformations that deteriorate correlations between scores and pretraining compute.**

G.50 NLP Benchmark: MMLU Moral Scenarios [32]

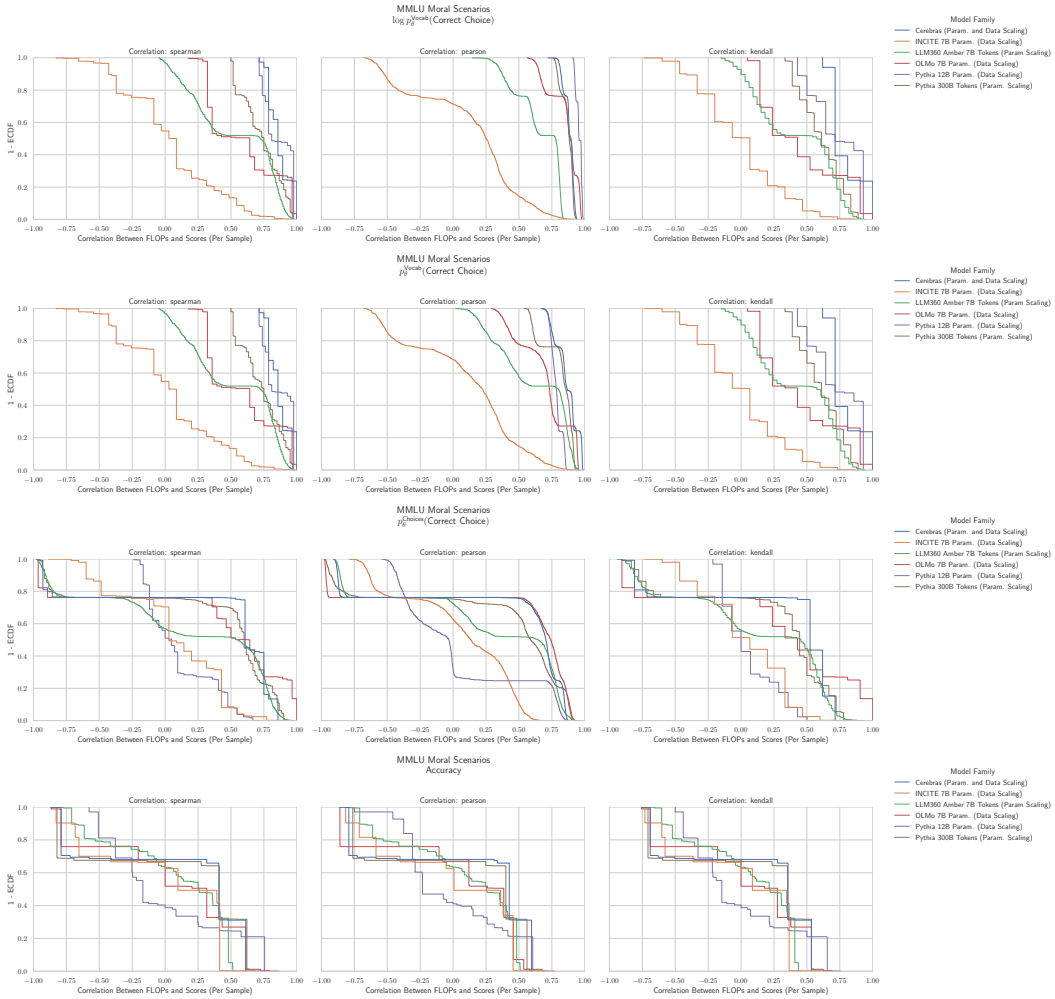

Figure 59: **MMLU Moral Scenarios: Downstream performance is computed via a sequence of transformations that deteriorate correlations between scores and pretraining compute.**

G.51 NLP Benchmark: MMLU Nutrition [32]

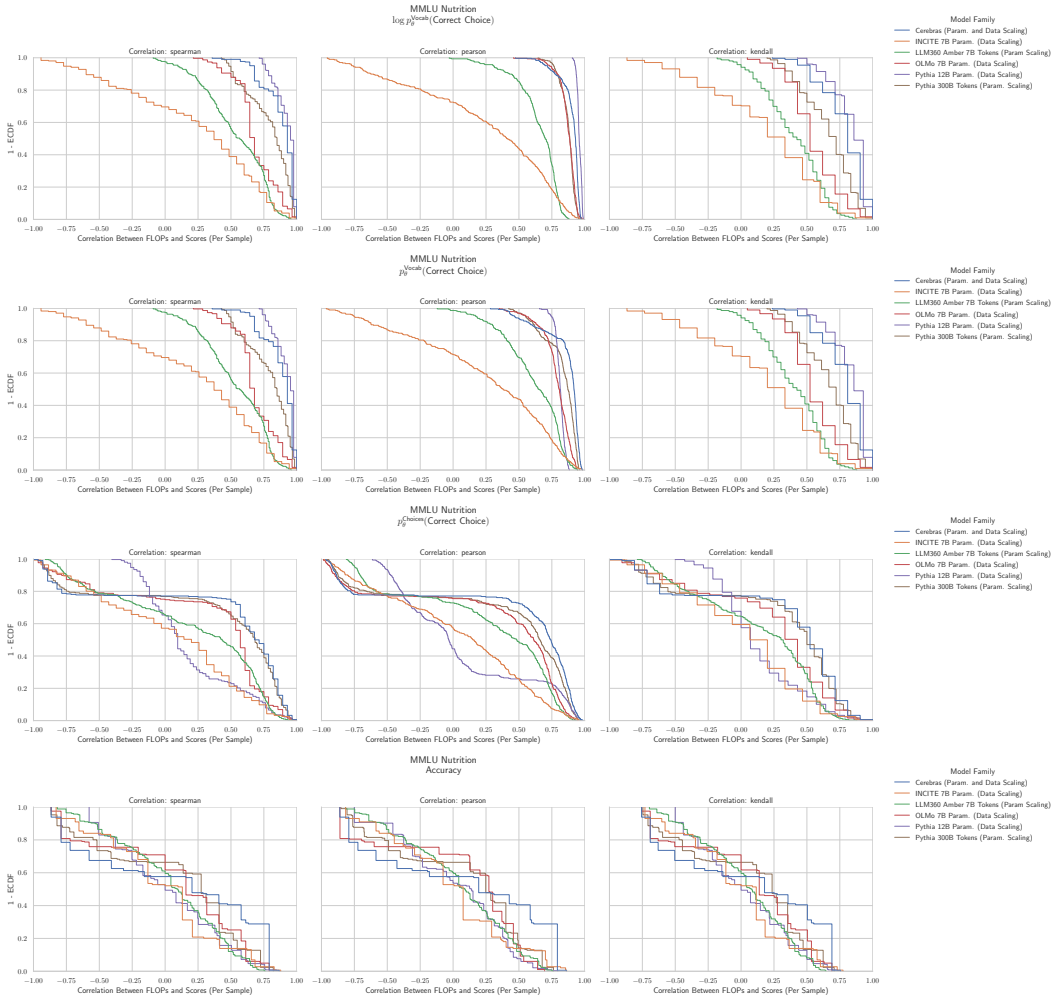

Figure 60: **MMLU Nutrition: Downstream performance is computed via a sequence of transformations that deteriorate correlations between scores and pretraining compute.**

G.52 NLP Benchmark: MMLU Philosophy [32]

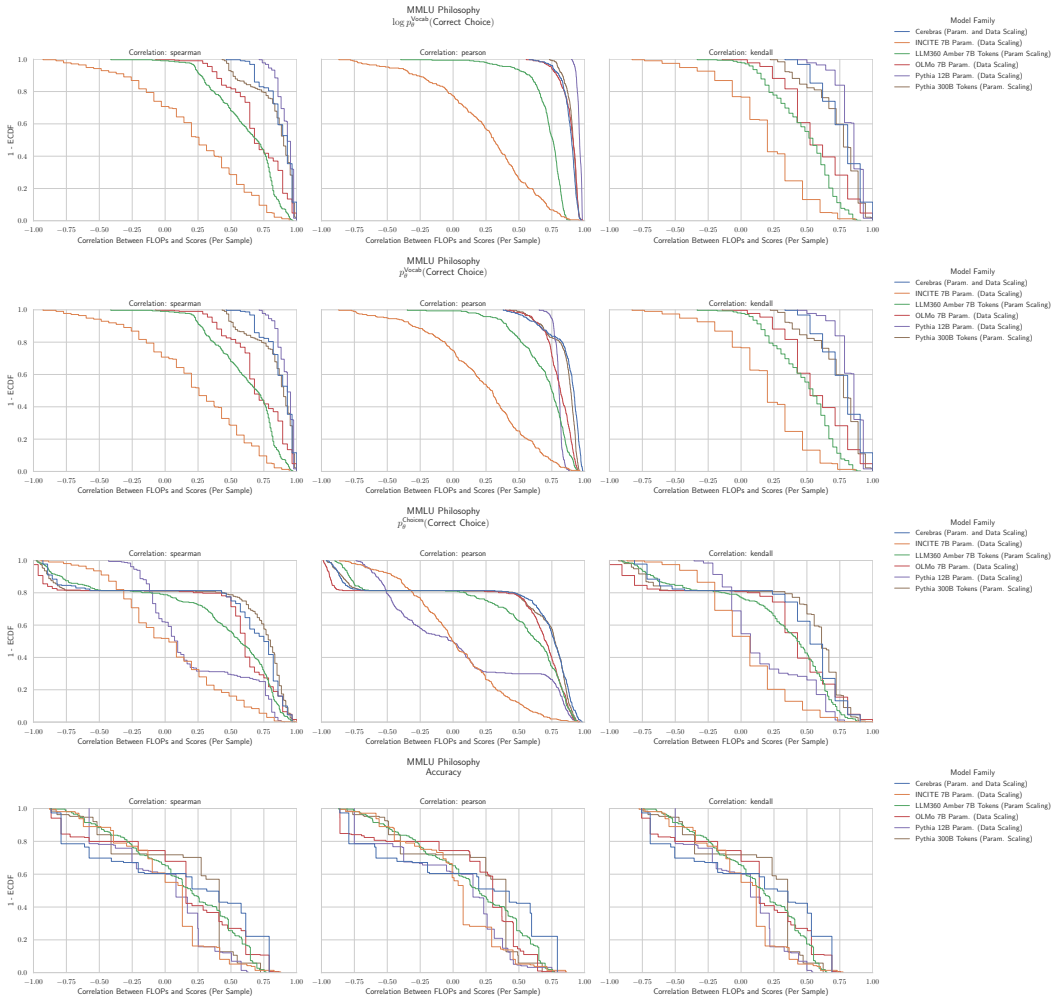

Figure 61: **MMLU Philosophy: Downstream performance is computed via a sequence of transformations that deteriorate correlations between scores and pretraining compute.**

G.53 NLP Benchmark: MMLU Prehistory [32]

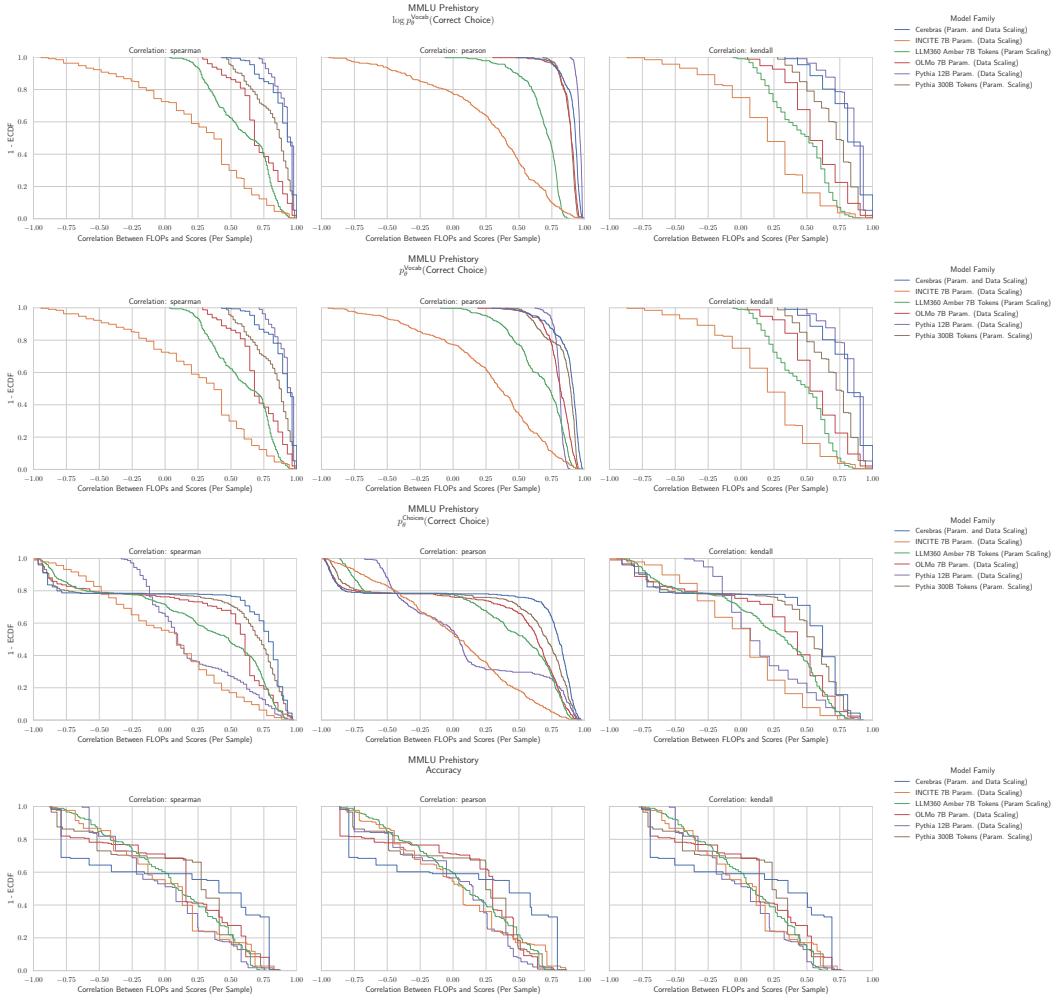

Figure 62: **MMLU Prehistory: Downstream performance is computed via a sequence of transformations that deteriorate correlations between scores and pretraining compute.**

G.54 NLP Benchmark: MMLU Professional Accounting [32]

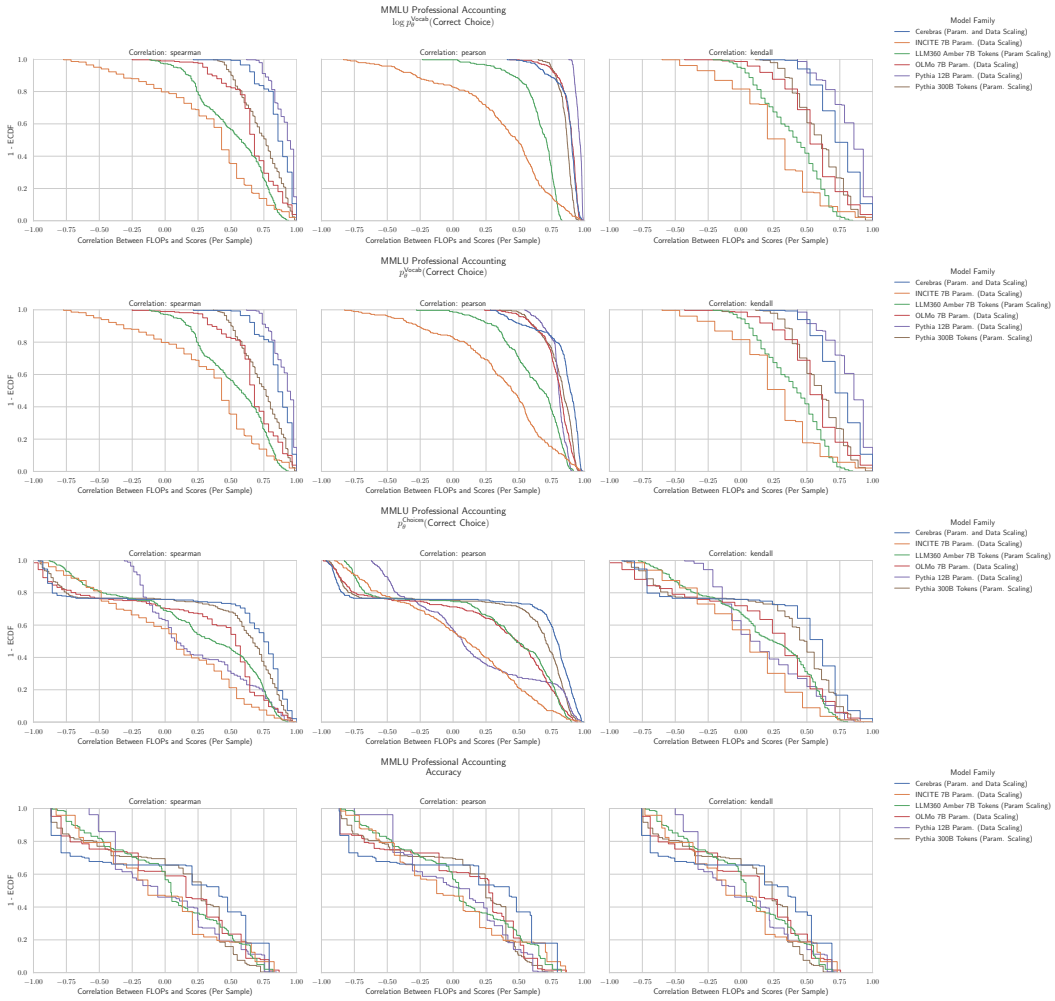

Figure 63: **MMLU Professional Accounting: Downstream performance is computed via a sequence of transformations that deteriorate correlations between scores and pretraining compute.**

G.55 NLP Benchmark: MMLU Professional Law [32]

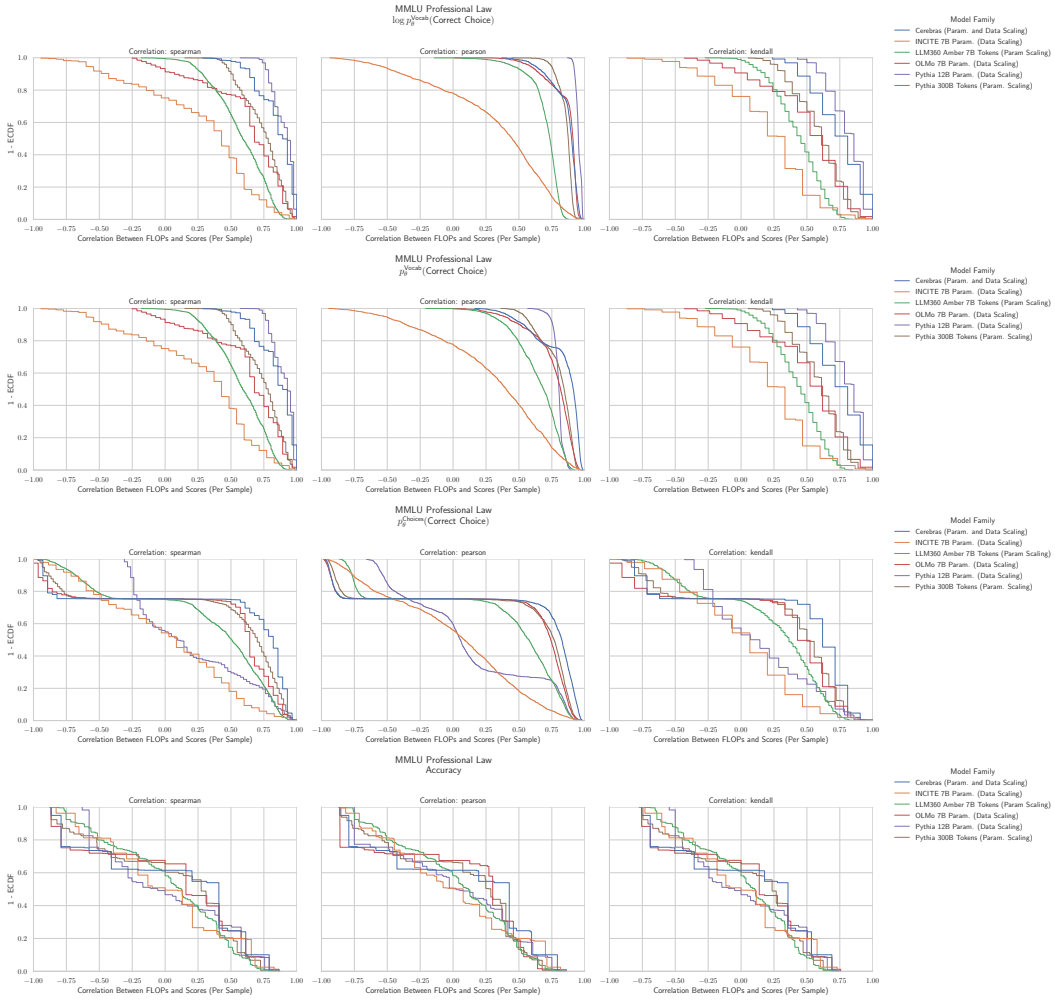

Figure 64: **MMLU Professional Law: Downstream performance is computed via a sequence of transformations that deteriorate correlations between scores and pretraining compute.**

G.56 NLP Benchmark: MMLU Professional Medicine [32]

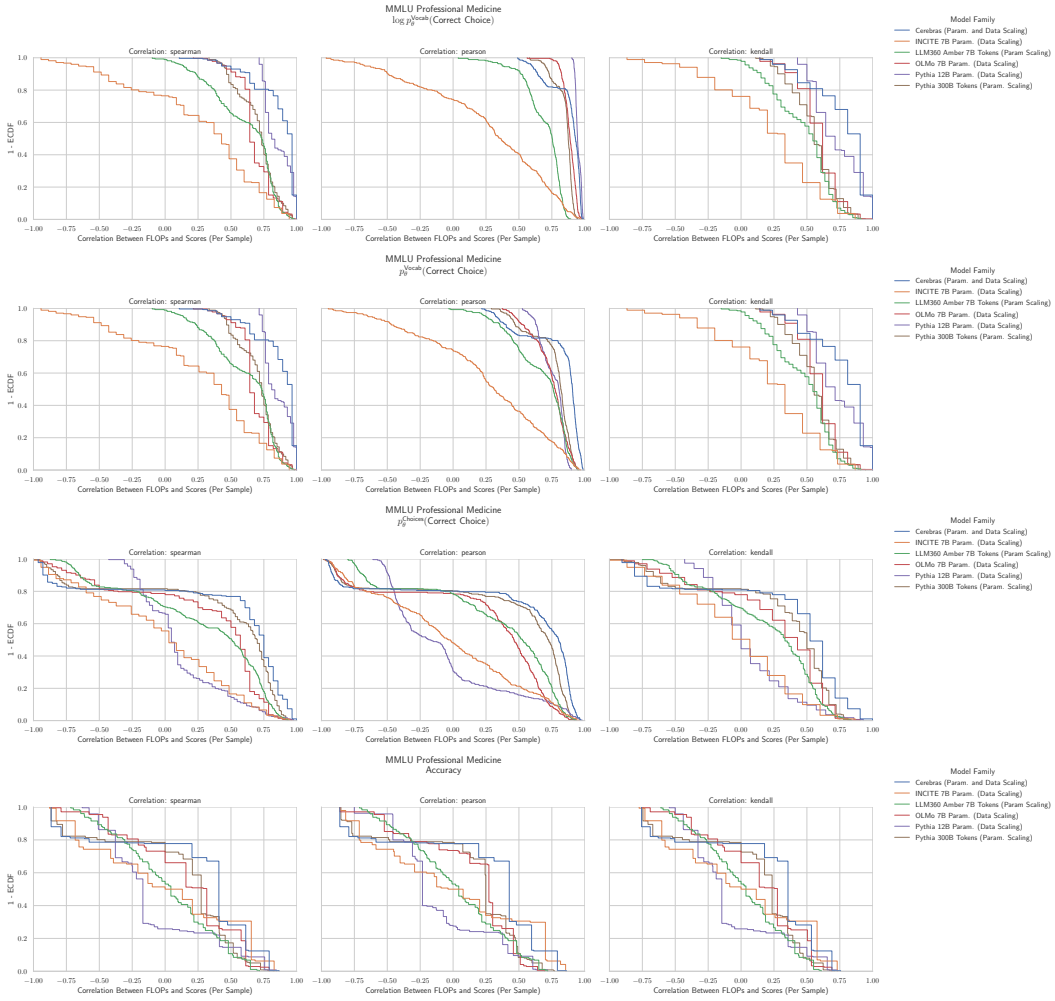

Figure 65: **MMLU Professional Medicine: Downstream performance is computed via a sequence of transformations that deteriorate correlations between scores and pretraining compute.**

G.57 NLP Benchmark: MMLU Professional Psychology [32]

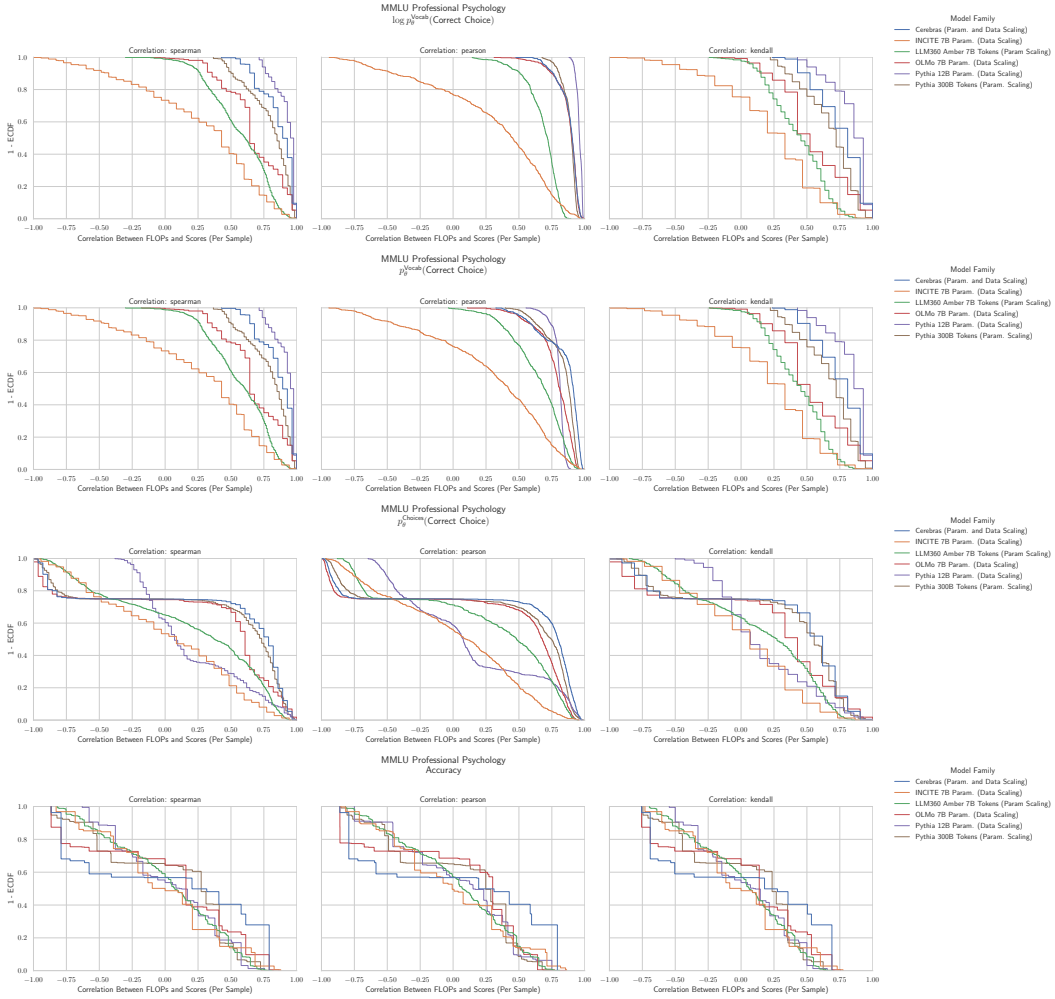

Figure 66: **MMLU Professional Psychology: Downstream performance is computed via a sequence of transformations that deteriorate correlations between scores and pretraining compute.**

G.58 NLP Benchmark: MMLU Public Relations [32]

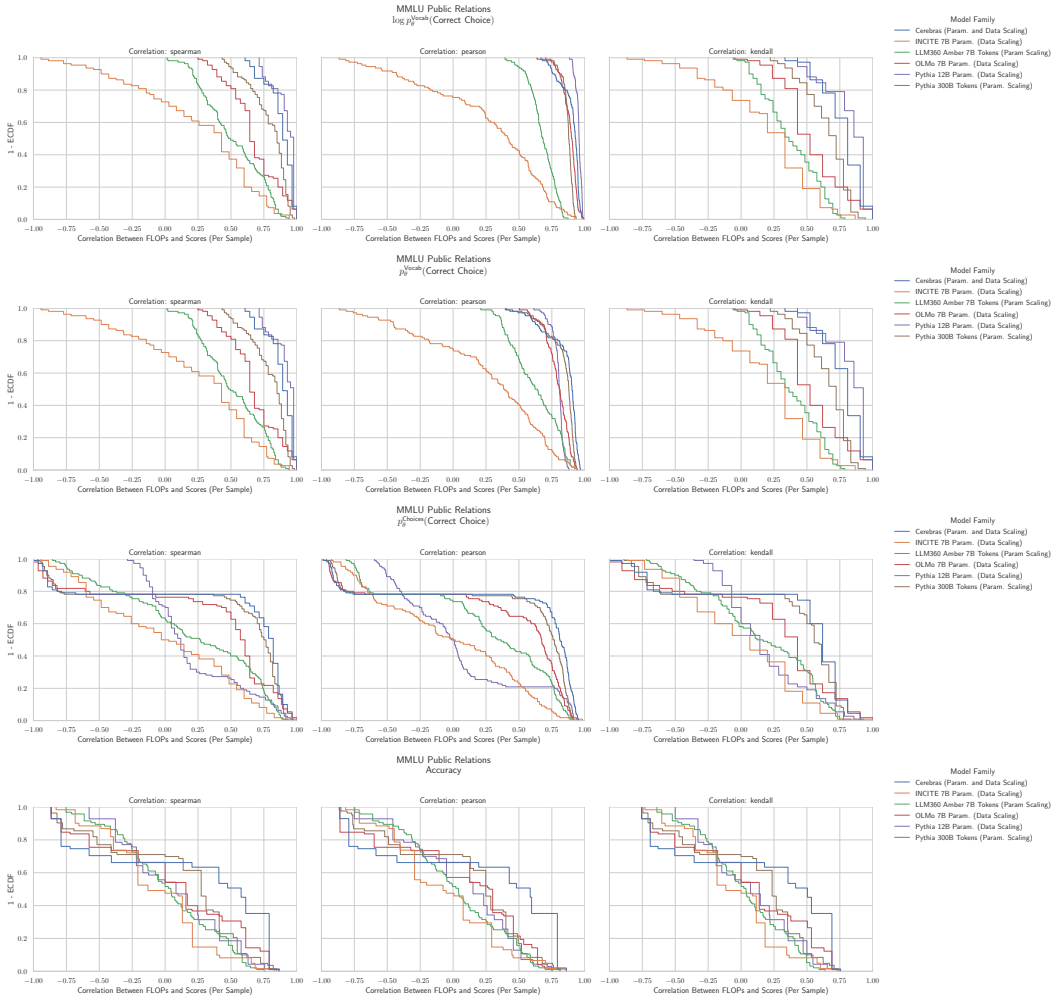

Figure 67: **MMLU Public Relations: Downstream performance is computed via a sequence of transformations that deteriorate correlations between scores and pretraining compute.**

G.59 NLP Benchmark: MMLU Security Studies [32]

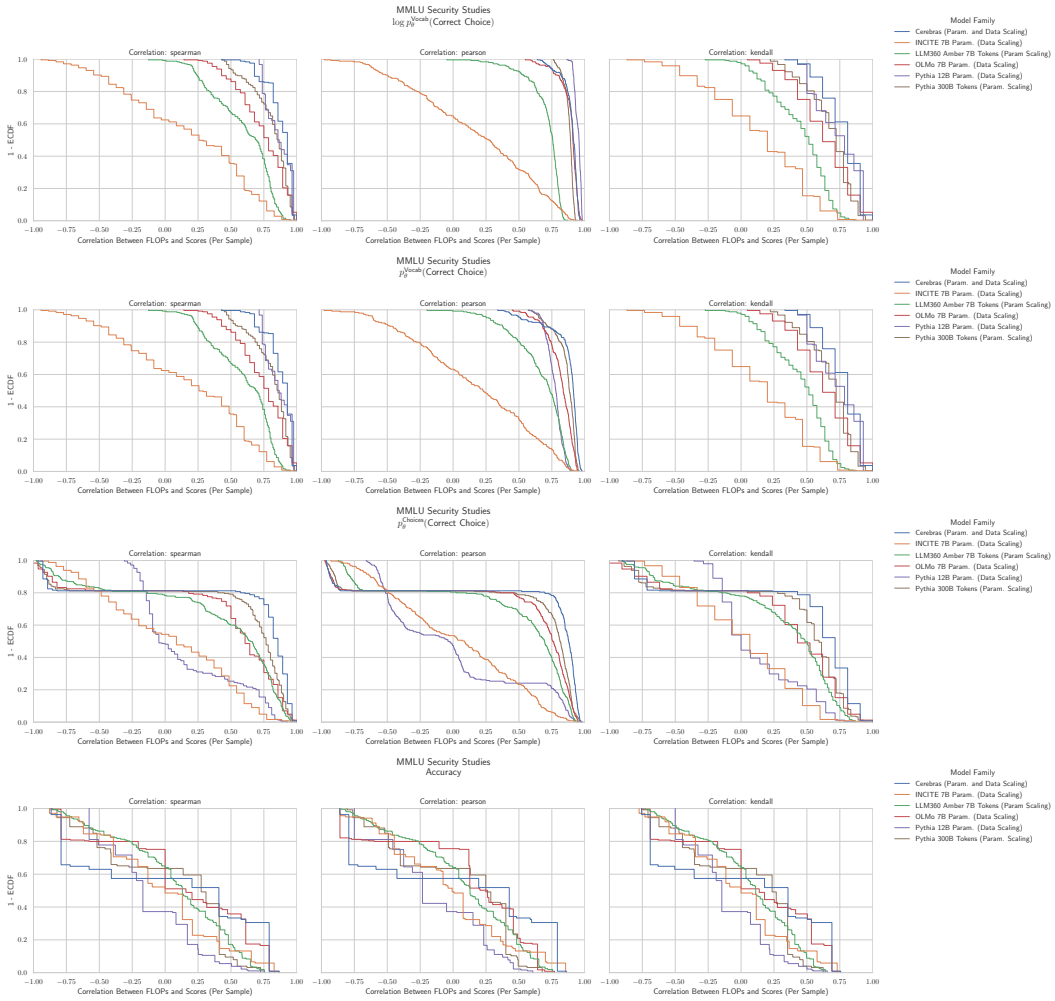

Figure 68: **MMLU Security Studies: Downstream performance is computed via a sequence of transformations that deteriorate correlations between scores and pretraining compute.**

G.60 NLP Benchmark: MMLU Sociology [32]

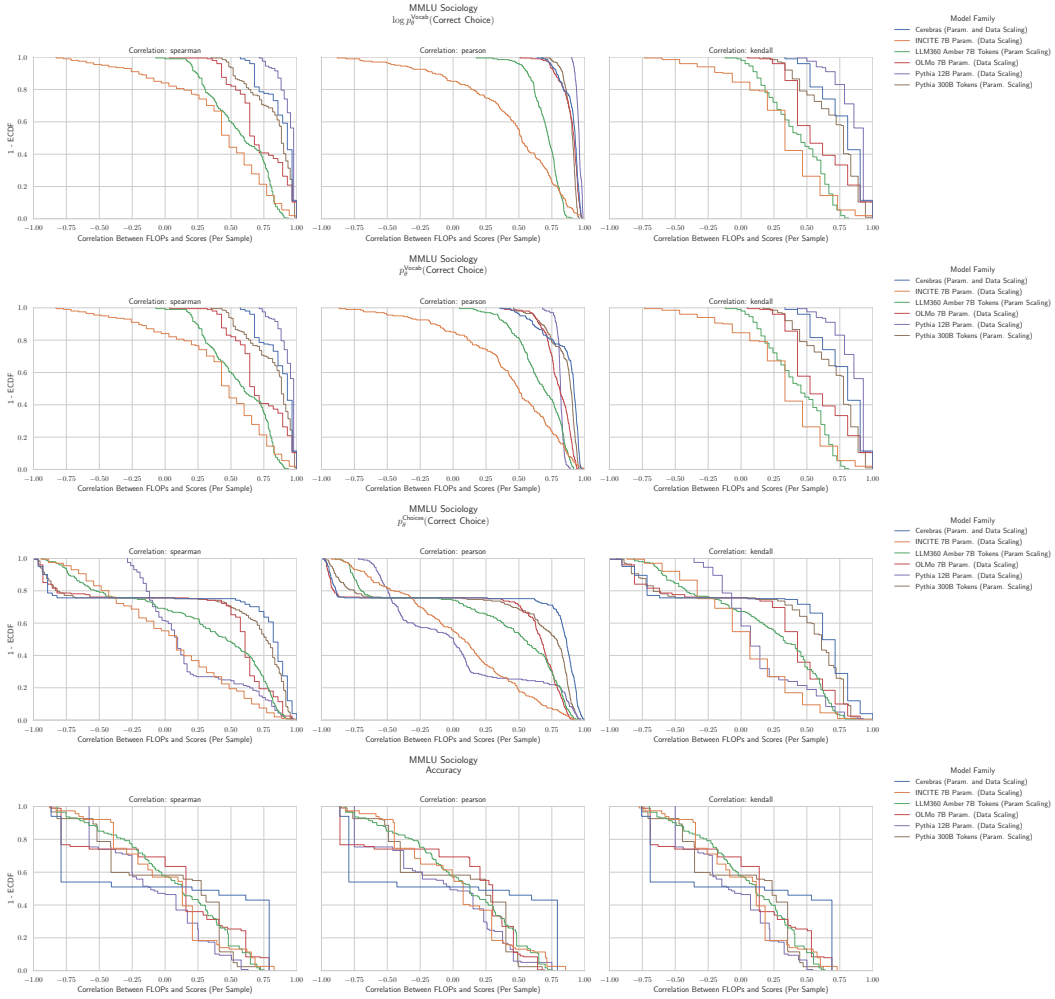

Figure 69: **MMLU Sociology: Downstream performance is computed via a sequence of transformations that deteriorate correlations between scores and pretraining compute.**

G.61 NLP Benchmark: MMLU US Foreign Policy [32]

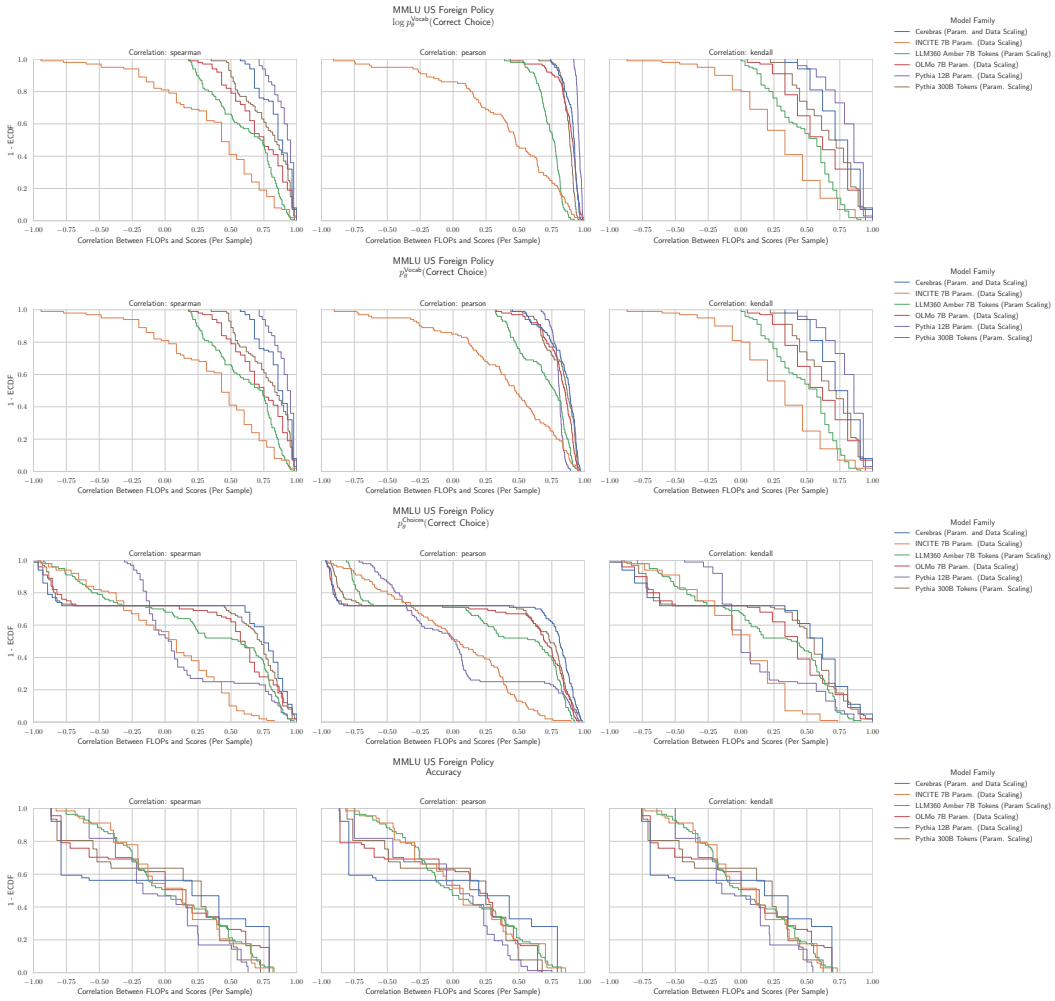

Figure 70: **MMLU US Foreign Policy: Downstream performance is computed via a sequence of transformations that deteriorate correlations between scores and pretraining compute.**

G.62 NLP Benchmark: MMLU Virology [32]

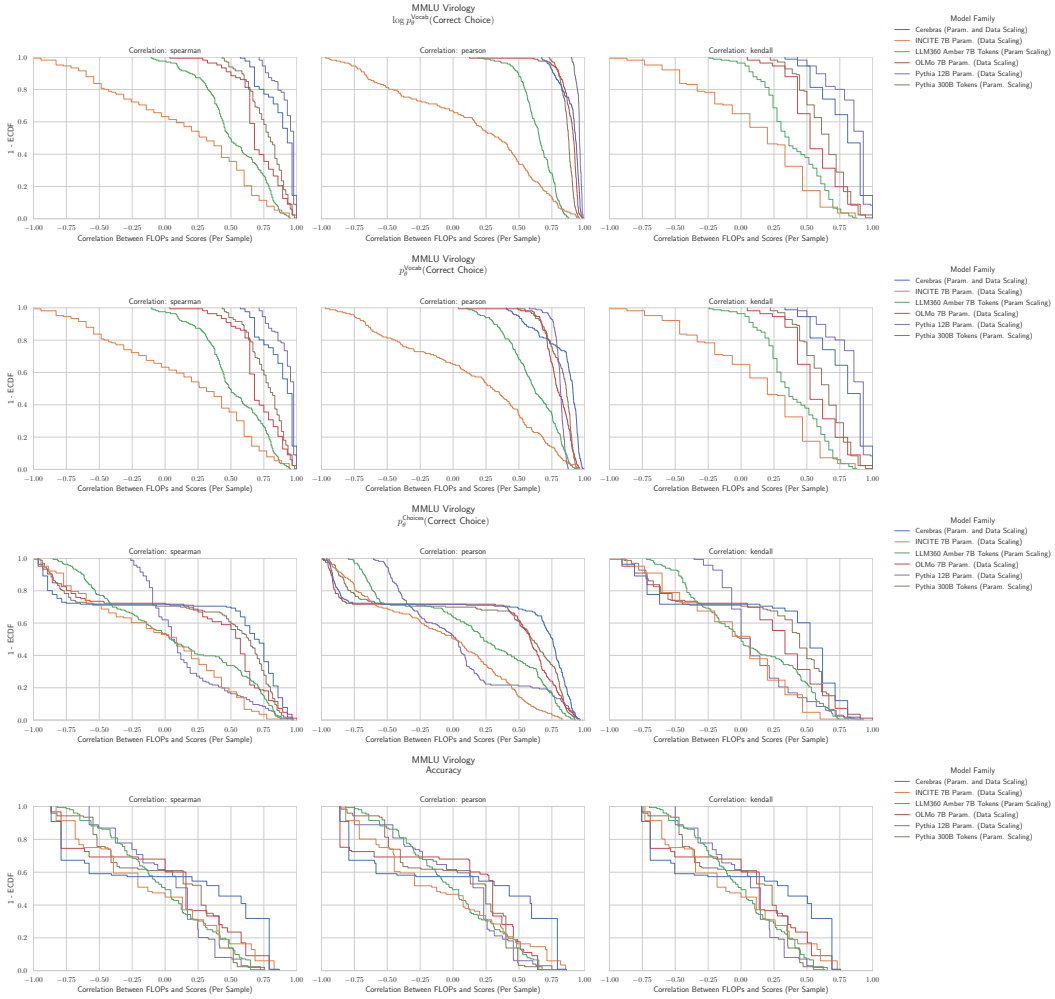

Figure 71: **MMLU Virology: Downstream performance is computed via a sequence of transformations that deteriorate correlations between scores and pretraining compute.**

G.63 NLP Benchmark: MMLU World Religions [32]

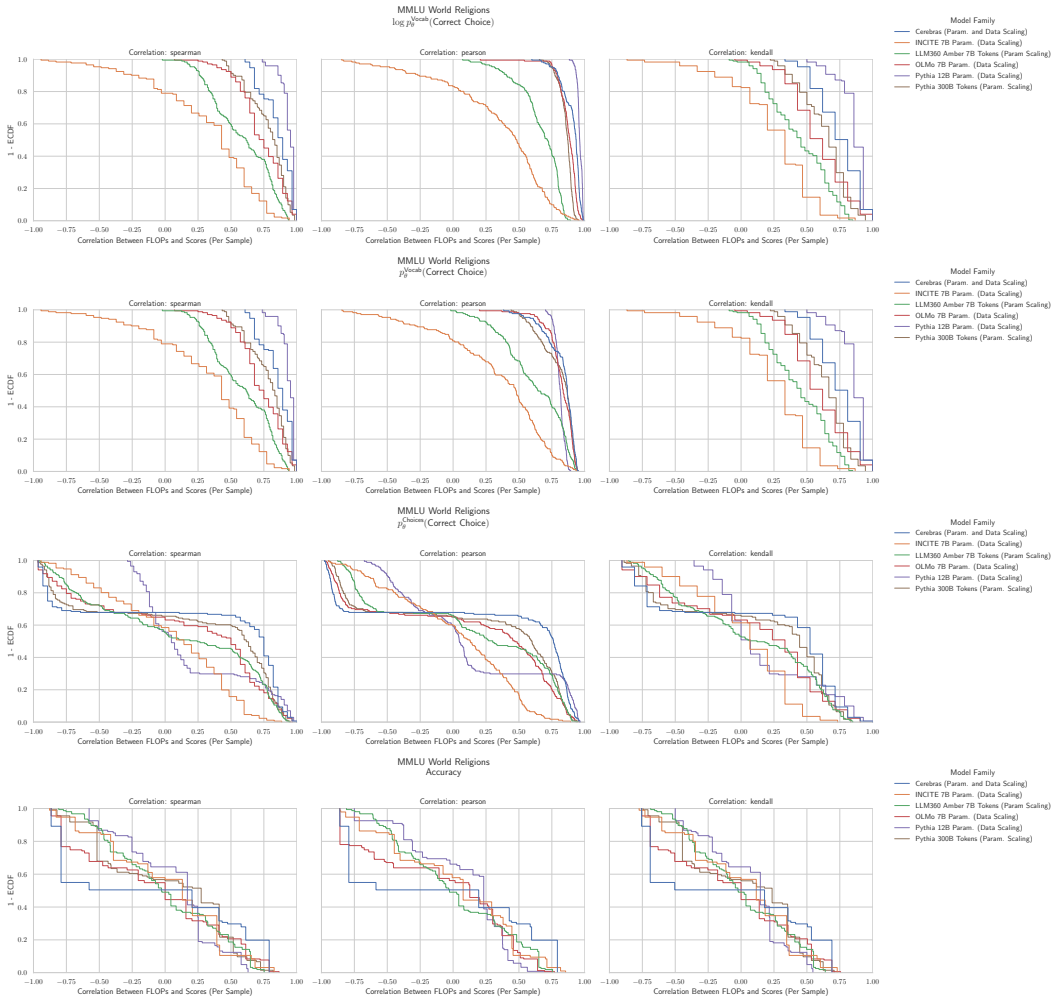

Figure 72: **MMLU World Religions: Downstream performance is computed via a sequence of transformations that deteriorate correlations between scores and pretraining compute.**

G.64 NLP Benchmark: OpenBookQA [55]

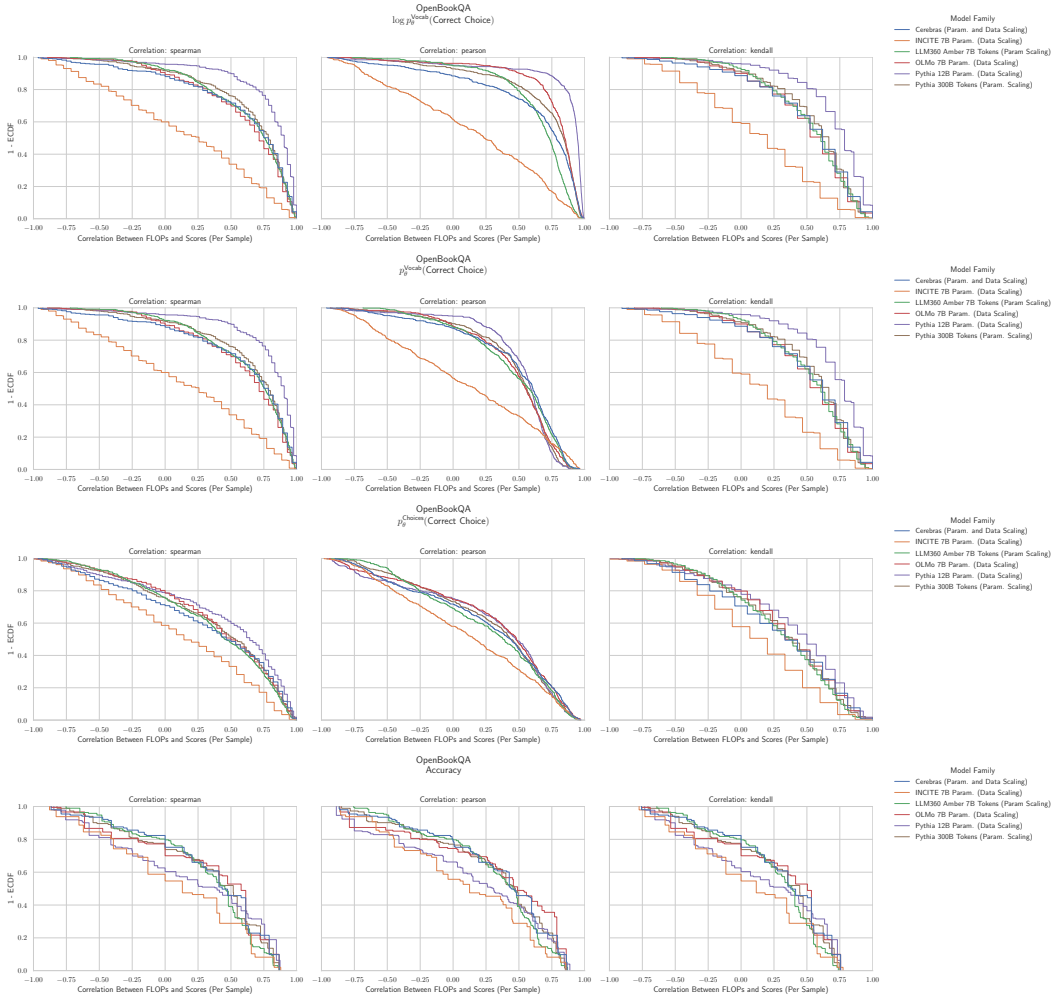

Figure 73: **OpenBookQA: Downstream performance is computed via a sequence of transformations that deteriorate correlations between scores and pretraining compute.**

G.65 NLP Benchmark: PIQA [11]

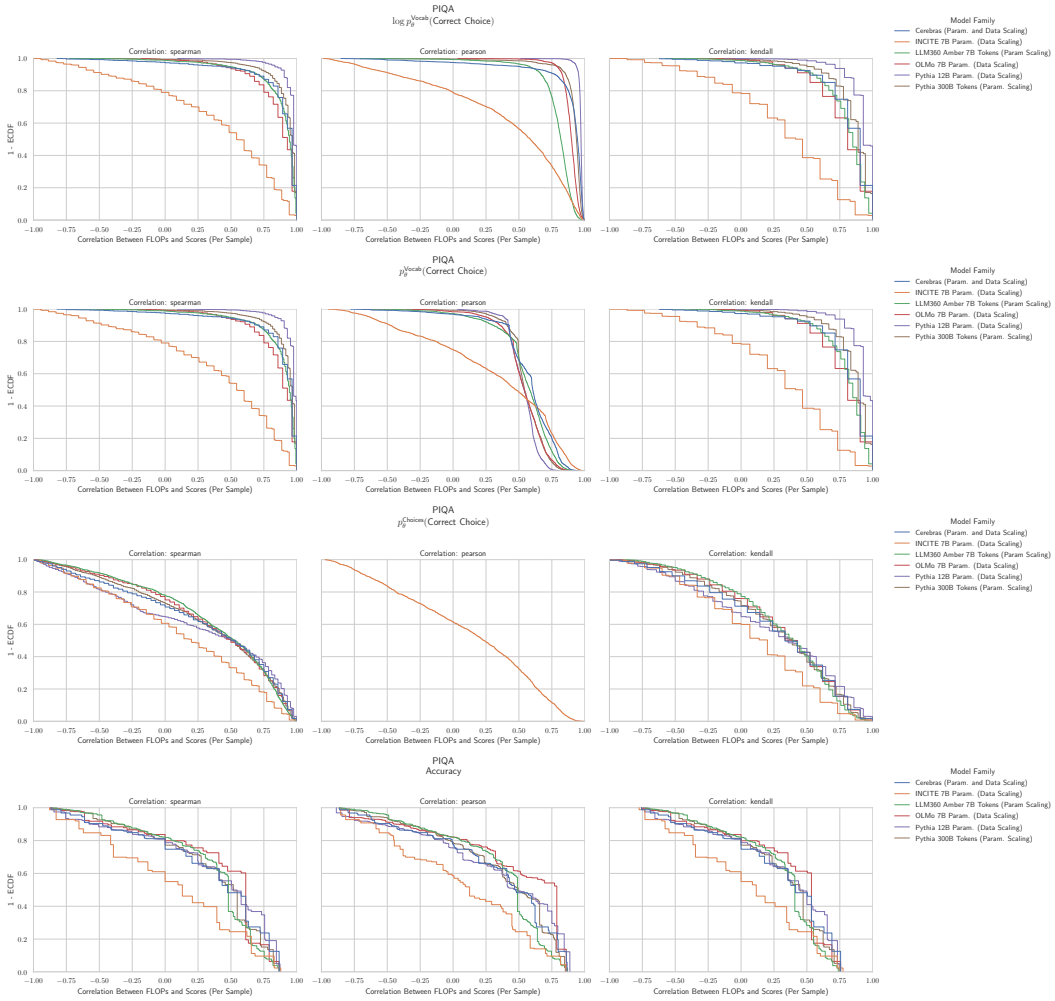

Figure 74: **PIQA: Downstream performance is computed via a sequence of transformations that deteriorate correlations between scores and pretraining compute.**

G.66 NLP Benchmark: RACE [49]

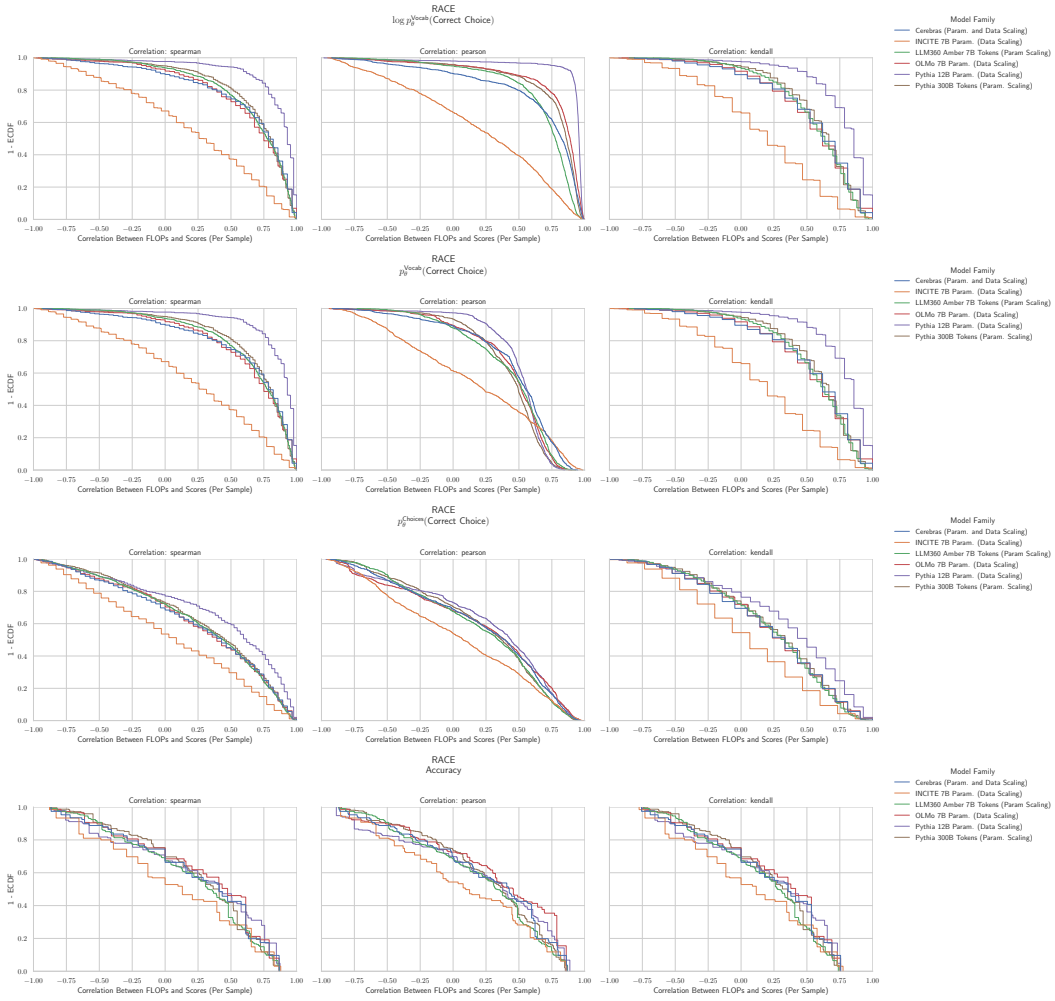

Figure 75: **RACE: Downstream performance is computed via a sequence of transformations that deteriorate correlations between scores and pretraining compute.**

G.67 NLP Benchmark: SciQ [75]

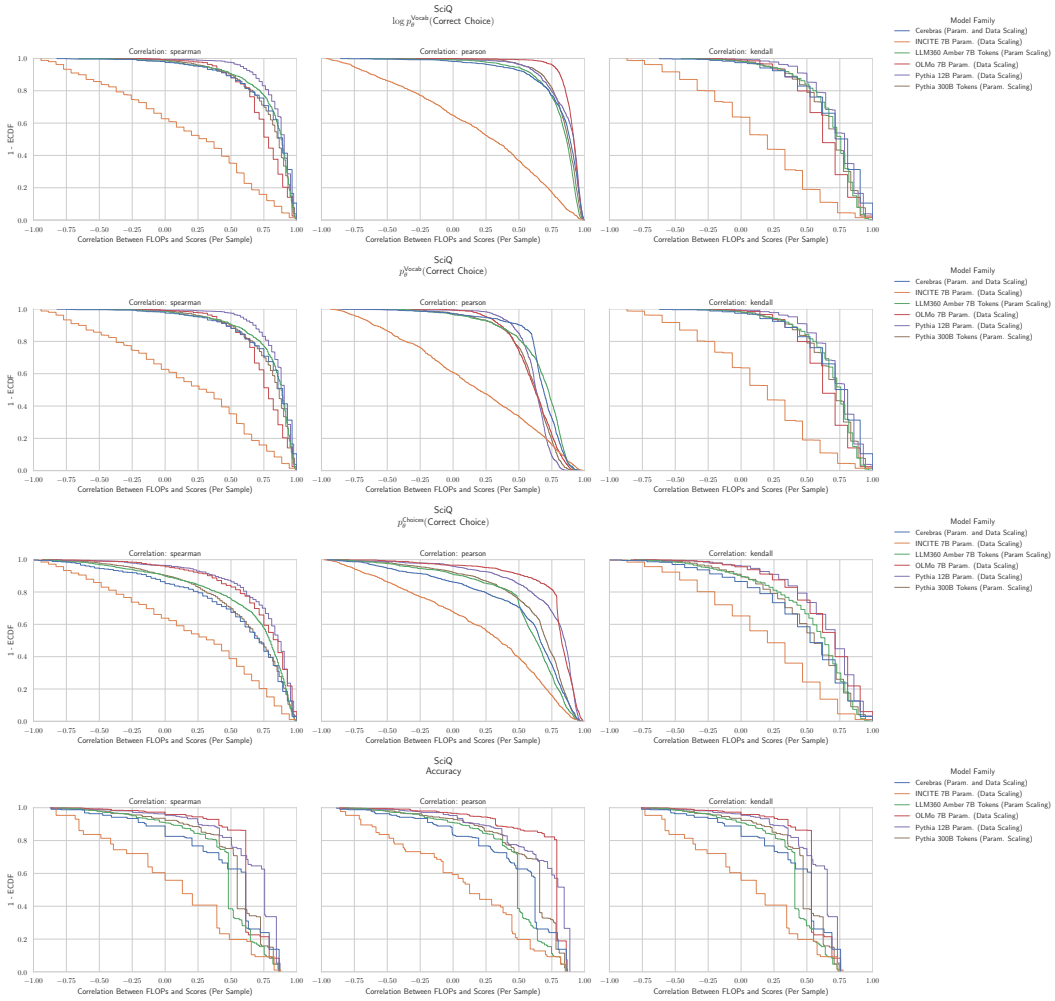

Figure 76: **SciQ: Downstream performance is computed via a sequence of transformations that deteriorate correlations between scores and pretraining compute.**

G.68 NLP Benchmark: Social IQA [68]

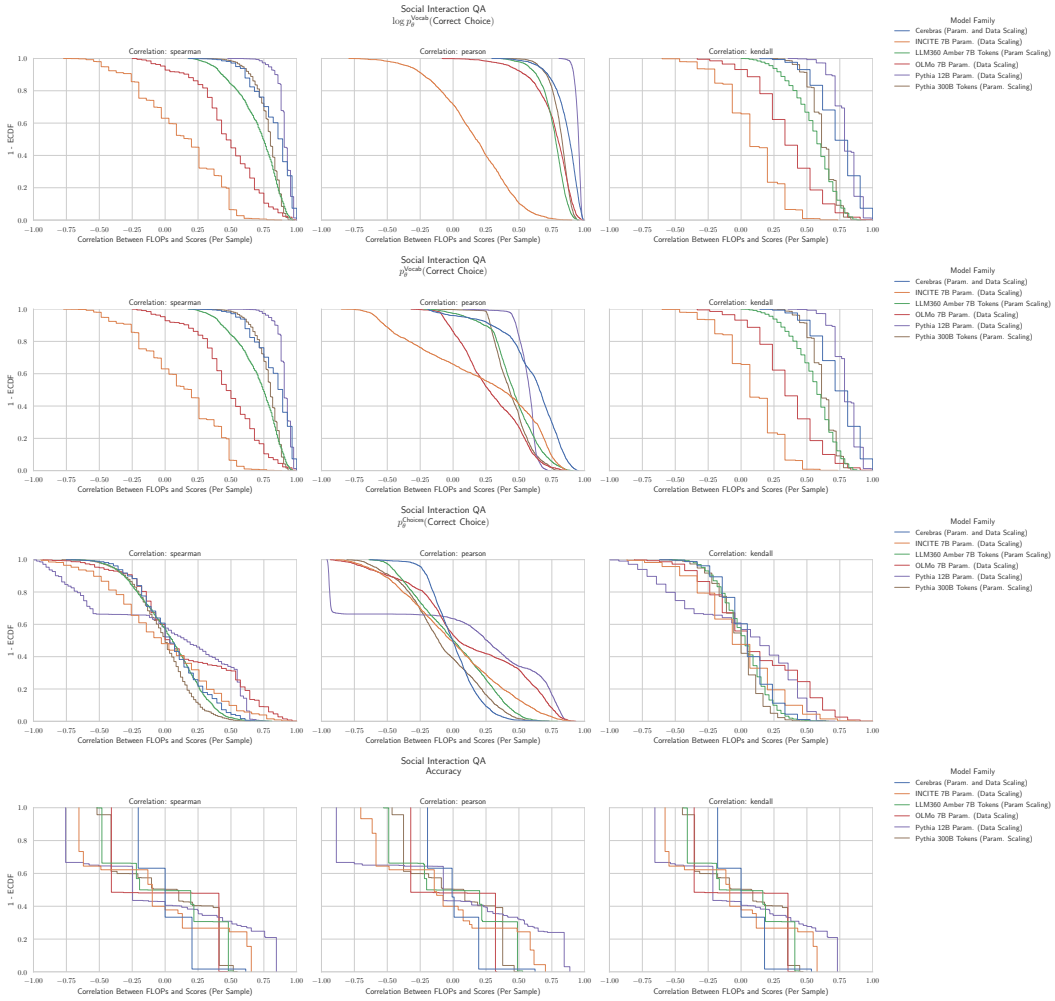

Figure 77: **Social IQA: Downstream performance is computed via a sequence of transformations that deteriorate correlations between scores and pretraining compute.**

G.69 NLP Benchmark: Winogrande [45]

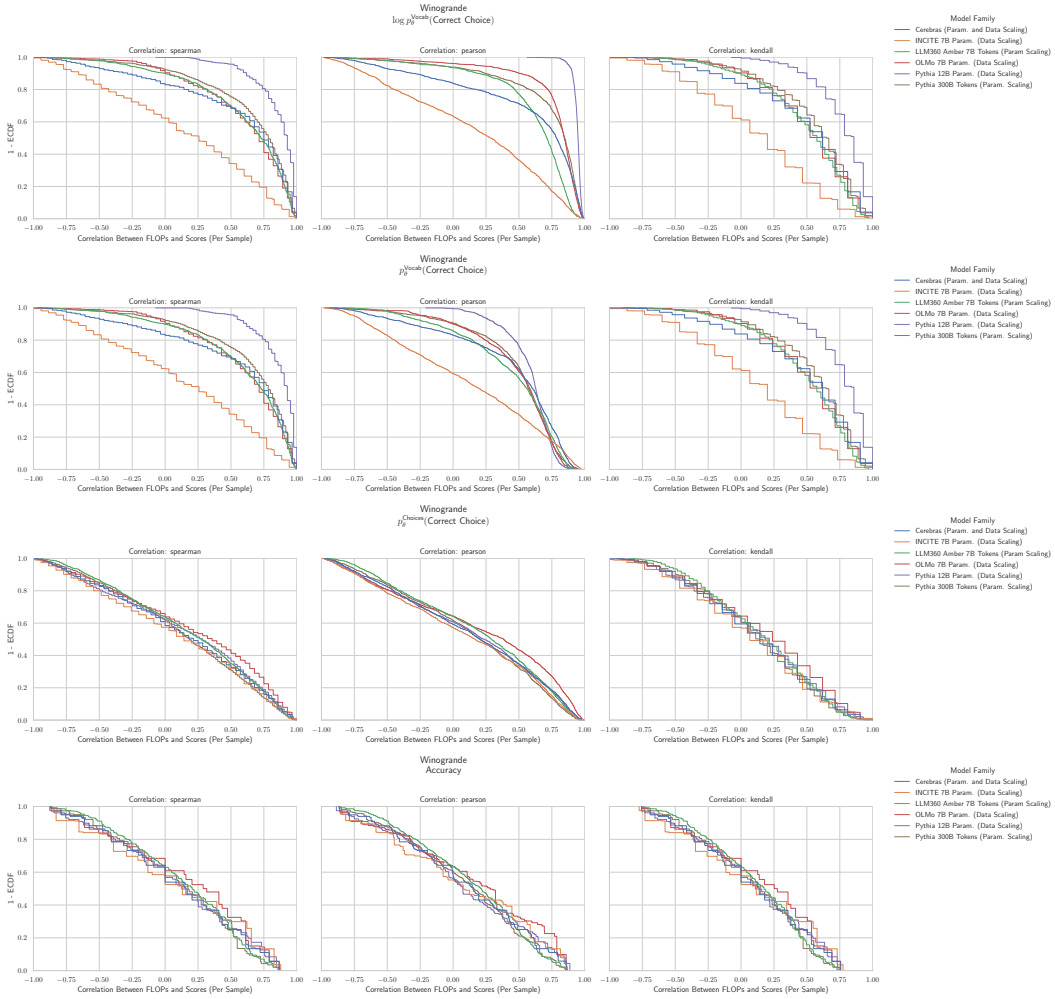

Figure 78: **Social IQA: Downstream performance is computed via a sequence of transformations that deteriorate correlations between scores and pretraining compute.**

G.70 NLP Benchmark: XWinograd English [57]

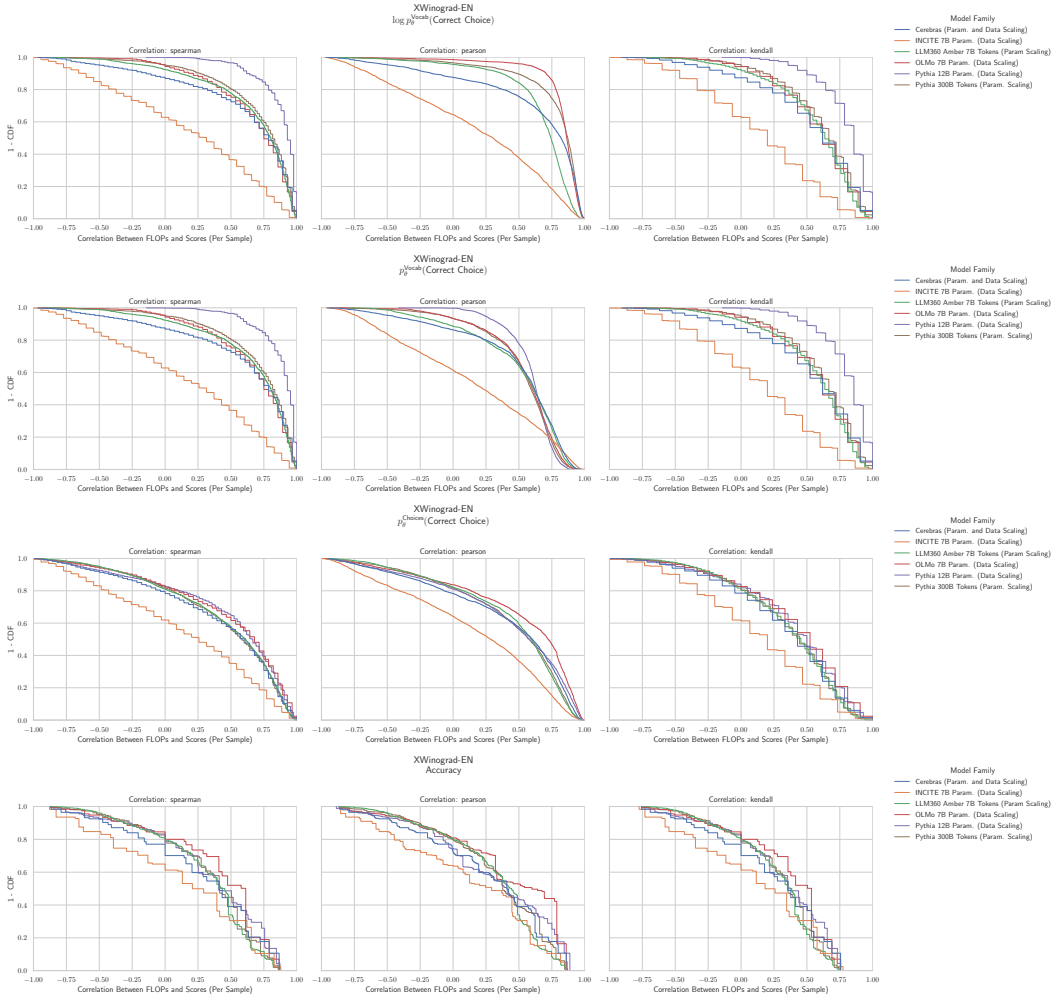

Figure 79: **XWinograd English: Downstream performance is computed via a sequence of transformations that deteriorate correlations between scores and pretraining compute.**